Tooling aspects of micro electrochemical machining (ECM) technology: Design, functionality, and fabrication routes

Guodong Liu[1], Md Radwanul Karim[1], Muhammad Hazak Arshad[2], Krishna Kumar Saxena[2], Wei Liang[3], Hao Tong[4], Yong Li[4], Yuxin Yang[5], Chaojiang Li[1,*], Dominiek Reynaerts[2,*]

[1]*School of Mechanical Engineering, Beijing Institute of Technology, Beijing 100081, China*
[2]*Micro-& Precision Engineering Group, Division Manufacturing Process, and Systems (MaPS), Department of Mechanical Engineering, KU Leuven, Leuven 3001, Belgium | Member Flanders Make (https://www.flandersmake.be/)*
[3]*AECC Beijing Institute of Aeronautical Materials, Beijing 100095, China*
[4]*Beijing Key Lab. of Precision/Ultra-Precision Manufacturing Equipments and Control, Department of Mechanical Engineering, Tsinghua University, Beijing 100084, China*
[5]*Department of Electronic and Computer Engineering, University of Alberta, 9120 116 St NW, Edmonton, Alberta T6G 2V4, Canada*

Corresponding author: Chaojiang Li. Address: School of Mechanical Engineering, Beijing Institute of Technology, Beijing 100081, China. E-mail: mecjli@bit.edu.cn.
Corresponding author: Dominiek Reynaerts. Address: Department of Mechanical Engineering, KU Leuven, Leuven 3001, Belgium. E-mail: dominiek.reynaerts@kuleuven.be.

Abstract

The era of advanced manufacturing involves the parallel development of sophisticated miniature products as well as novel materials which have necessitated research into electrochemical micromachining technology (micro-ECM) where the material removal is achieved in an athermal manner through the controlled anodic dissolution of the workpiece. High-quality micromachining is obtained through the controlled application of electric and flow fields. The development of micro-ECM is backed by several industries including aerospace, mold, space, automotive, microelectronics, consumer goods, and biomedical industries. In micro-ECM technology, the tool serves as one of the main factors influencing processing accuracy and capability. This aspect has not been covered in detail in existing review articles. Therefore, this review article focuses on tooling aspects of micro-ECM technology. It incorporates all the aspects of tooling from functional design, structures, and materials

to fabrication routes in a single manuscript. This article also attempts to highlight the development of composite micro-tools to deliver multiple process energies, ECM tools fabricated through additive manufacturing routes, proposes future research directions and the associated challenges involved with the use of micro- and nano-tools in ECM technology. This review article seeks to address both the academic and industrial audience thereby leading to further tooling innovations for micro-ECM technology.

Keywords: Electrochemical micromachining; micro-tool; multifunctional tool; tool fabrication routes; micro-ECM.

1. Introduction

The trend toward the miniaturization of products/devices (Ceylan1 et al., 2021; Dabbagh et al., 2022; Sharstnioua et al., 2018) with multiple functionalities and the associated trend towards higher accuracy still continues as predicted by Moore (10 nm feature size in 2019) and Taniguchi (sub-micrometer machining tolerance and ~1 nm surface roughness Ra in 2019), leading to the advent of advanced micromachining processes (Hansen et al., 2011; Matsumoto et al., 2023; Rajurkar et al., 2006a; Zhang et al., 2019a). Furthermore, the demands on the multifunctionality of these sophisticated products have resulted in the emergence of novel materials with new compositional recipes and extreme properties, thereby bringing challenges to existing micromachining processes. Miniature products such as microelectromechanical systems (MEMS), micro-sensors, micro-molds, miniature-lenses, micro-impellers, micro-turbines, microfluidic chips, optoelectronic components, wearable electronics, human-implants, etc. continue to demand precise micromachining of complex shapes (Dimov et al., 2006; Saxena et al., 2018). To guarantee the high-end performance of these miniature products, stringent requirements have to be met dimensional tolerances, shape accuracy, and surface/sub-surface integrity.

Conventional mechanical micromachining processes are limited by the hardness of the workpiece materials, downscaling of tools, and issues such as tool failure and wear which always exist with difficult-to-cut materials. To address the difficulties related to mechanical micromachining methods, several non-conventional micromachining technologies have been developed such as micro-electric discharge machining (micro-EDM) (Li et al., 2021a), micro-electrochemical machining (micro-ECM)

(Lu et al., 2022; Speidel et al., 2022), short/ultra-short pulsed laser micromachining (Parandoush and Hossain, 2014), ion beam machining, and electron beam machining (He et al., 2021). Micro-EDM and laser micromachining impose a thermal load on the workpiece, adversely affecting the surface integrity. The utilization of femtosecond pulse lasers has shown much less thermally induced defects but it is rather a slow and cost-intensive process. The requirements of vacuum environments for electron beam processing or ion beam processing limit their usage. This has led to accelerated research and development into micro-ECM technology which does not suffer from the above problems.

The micro-ECM process involves material removal by the controlled anodic dissolution of the workpiece where the workpiece is not subjected to thermal load and hence the surface/sub-surface integrity is nearly preserved (Bhattacharyya et al., 2001; Rajurkar et al., 2013; Zhao and Kunieda, 2019). Considering the ways to restrain the material dissolution area, micro-ECM technologies can be divided into several configurations including tool-based ECM (Kumar et al., 2014), mask-based ECM (Wu et al., 2020a), and jet-ECM (Speidel et al., 2022). The mask-based ECM process etches materials patterned by masks thereby machining shallow pits or holes with a limited small aspect ratio. Nevertheless, it is difficult to fabricate high aspect ratio and three-dimensional (3D) features. The jet ECM process has the capability to fabricate 3D structures by controlling the angle of the nozzle and its motion path. In the tool-based ECM processes, the use of columnar and cylindrical tools in conjunction with high-precision coordinated relative motion allows flexible processing of both 3D microstructures and micro-holes. Columnar and cylindrical micro-tools have a wider range of applications than using wire tools (Sharma et al., 2020), and they are also simpler compared to complex-shaped tools (Klocke et al., 2013), making them more widely studied and applied at present.

A micro-ECM instrument typically involves basic components similar to an electrolytic cell (micro-tool as cathode, workpiece as an anode, electrolyte, and power supply). The micro-tool is the most critical factor influencing processing capability, dimensions, and accuracy. Researchers often overlook the characteristics and functions of micro-tools when exploring new mechanisms and processes. In addition to their basic function as cathodes, the new functions and structures of micro-tools need to be designed with the aim of solving essential issues in micro-ECM. The selected materials and fabrication processes need to consider reproducibility, simplicity, and batch size factors. Up to now, the available review literature focuses on micro-ECM process fundamentals, removal mechanisms, and applications. The basic concepts of micro-ECM and the difference between micro-

ECM and macro-ECM were addressed by Bhattacharyya et al. (2004). They have highlighted the influence of various predominant factors such as machining accuracy, power supply, design of the micro-tool, the role of the inter-electrode gap, etc. Several aspects of technology have advanced since then. Rajurkar et al. (2006b) have discussed the technical developments and state-of-the-art micro and nano machining by EDM and ECM processes. They have mostly reported the applications where micro-ECM technologies were successfully adopted before 2006. Spieser and Ivanov (2013) have summarized the challenges of micro-ECM development, including the machining processes, power supply units, tool preparation, measurement, and handling. Saxena et al. (2018) have presented an extensive literature source with a wide coverage of research developments in micro-ECM technology and its hybrid variants by reviewing the related concepts, aspects of tooling, and advanced process capabilities. Most recently, Speidel et al. (2022) reported a review on jet ECM manufacturing highlighting the process physics and removal mechanisms, however, only jet ECM processes were involved in the latter study. Some micro-tools were touched on in the aforementioned review papers but not extensively. Research on micro-ECM tooling requires more attention for further development of micro-ECM technology up to the industrial level.

In this paper, we fill an important gap in the literature by reviewing the tooling aspects of micro-ECM technology in a single article. Although this paper builds on prior state-of-the-art, it yet gives extensive attention to the developments of tooling technology and takes into consideration a broad range of knowledge related to micro-ECM tooling. Specifically, this work provides a systematic overview of research advances in the design and fabrication of micro-tools for micro-ECM, including almost all aspects such as the function of micro-tools, their basic structures, materials, fabrication processes, etc. The review also covers special micro-tools for hybrid processes based on micro-ECM and nano-scale tools. It is important to note the definition of microscale in this paper. In general, scales in the range of 1-100 μm are referred to as microscales, but given the required stiffness of a tool, micro-tools with dimensions of 50-1000 μm are considered mainly in this paper as these dimensional ranges are commonly used. In addition, a number of innovative approaches to the design and fabrication of macroscale tools (mm range) with the prospect of size reduction or downscaling are also included. Additionally, some tooling designs developed for electric discharge micromachining (micro-EDM) technology can also be used for micro-ECM technology and hence are also covered here for cross-inspirations. The various aspects intersect with each other and are discussed in detail in each sub-

section. The paper also infers current and future research trends in micro-ECM tooling at the end.

2. Definition, chronology and review framework

2.1 Definition

In a micro-ECM process, a micro-tool is a columnar part of the desired shape that is connected to the cathode of a power source (Fig. 1a). This tool traces a defined scanning path on the workpiece surface which is connected to the anode of the power source. The electrolyte is separately supplied and a feature of the desired shape is machined when the electric current flows through the circuit, as illustrated in Fig. 1(b). Cations leave the workpiece and electrons leave the micro-tool to reach their respective opposite ends (Fig. 1c). The electrolytic reactions can be restated as follows:

Reduction reaction at the tool:

$$2H_2O + 2e^- \rightarrow H_2 \uparrow + 2OH^- \quad (1)$$

Oxidation reaction at the workpiece:

$$Me - ne^- \rightarrow Me^{n+} \quad (2)$$

Since only hydrogen evolution reaction takes place on the surface of the micro-tool, the micro-tool is not subjected to process-related wear. In addition to the requirements of size, shape, and electrical conductivity, micro-tools also can have design requirements to serve special functions such as accelerating electrolyte flow, suppressing stray currents, etc.

In the literature, the tools are called by various names, such as electrodes or cathodes. In this review, it is referred to as the ‘micro-tool’ or ‘tool’. Further, we will use the following definitions: In the EDM-based micro tool fabrication process, the micro-tool acts as the workpiece, and the other pole is called the ‘electrode’. In ECM-based micro-tool fabrication, the tool acts as the workpiece, and the other pole is called the ‘cathode’.

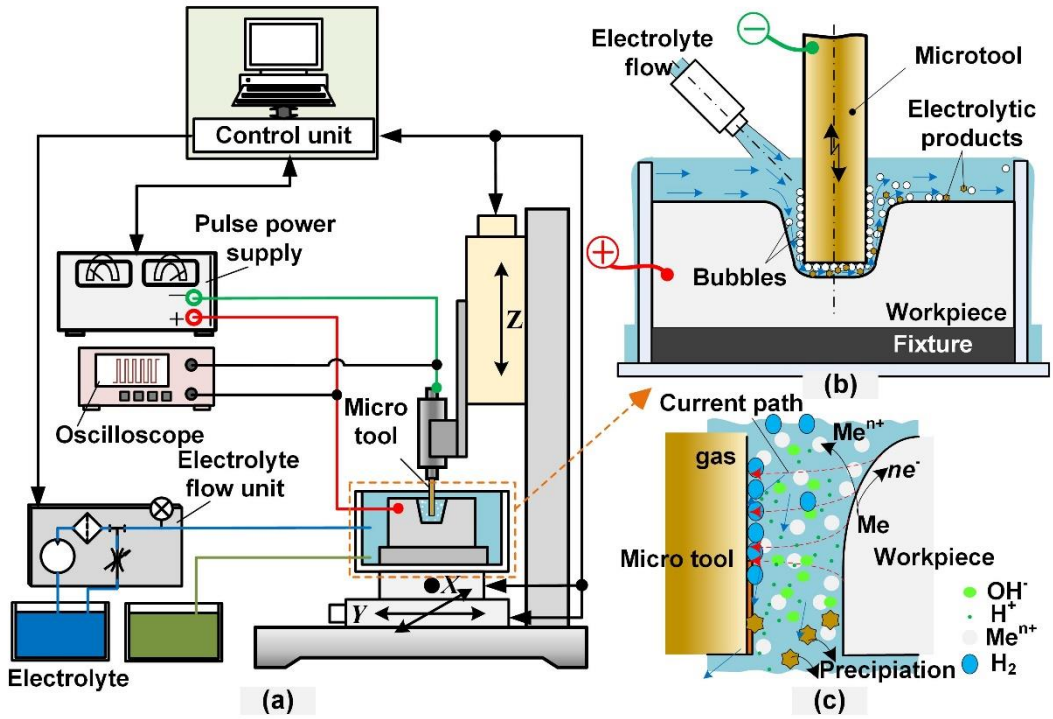

Fig. 1. Schematic showing: (a) experimental setup of the micro-ECM process, (b) the electrochemical cell, and (c) the reactions and species.

2.2 A short chronological review

Fig. 2 shows a chronological representation of some key advances in micro-tools for the micro-ECM process. The scope of the ECM technique was at the macroscopic scale of several millimeters until the 1980s due to the challenges of micro-tool fabrication and material dissolution constraints. In 1985, the wire electrical discharge grinding (WEDG) technique was applied to micro-EDM (Masuzawa et al., 1985) and also provided inspiration for tool fabrication for micro-ECM. In the same year, the sidewall insulating films prepared by the chemical vapor deposition (CVD) effectively suppressed stray corrosion and further improved the feasibility of micro-ECM (Osenbruggen and Regt, 1985). In the 1990s, the use of short-pulse (several ms) power supplies significantly reduced the size of machining gaps and further improved the machining accuracy (Rajurkar et al., 1998). With the more sophisticated numerical control (NC) technology, columnar microtools were increasingly utilized in the ECM process of holes and 3D structures (Kozak, 1998). Since 2000, there has been a surge of interest in the fabrication and application of micro- and sub-micro-tools, inspired in particular by the ultra-short-pulse ECM technology (Ahn et al., 2004; Kirchner et al., 2001; Schuster et al., 2000). The stray current was suppressed by controlling the period of the applied ultrashort voltage pulse. During 2000-2010, significant research was published on different process improvements in the fabrication of

micro tools (Kock et al., 2003), special-tip tools (Kim et al., 2005), and array tools (Park and Chu, 2007). Although many micro-rods or pins are not directly used in micro-ECM, they also drive the possibilities for more applications. Due to the influence of EDM technology, the majority of micro-tools are made of tungsten or tungsten carbide and have a relatively simple structure. From 2010 to the present, scholars have increasingly considered practical issues in the inter-electrode gap (IEG) and processing area in micro-ECM and have started to adopt new tool structures and materials (Kamaraj et al., 2012). The brass tube tool is one of the most successful examples (Zhang et al., 2021; Zhang et al., 2020a; Zhang et al., 2016b). Electrolyte renewal is achieved by using the inner hole of the tool to flush the electrolyte at high speed (Clare et al., 2018; Mitchell-Smith et al., 2019). Various techniques for the preparation of insulating films on the tool sidewall have also been developed. In addition, significant research has been published related to progress in the novel structure of micro-tools (Liu et al., 2018a), new materials (Meng et al., 2020), nano-tip tools (Wang et al., 2016c), and composite function tools (Saxena et al., 2020c).

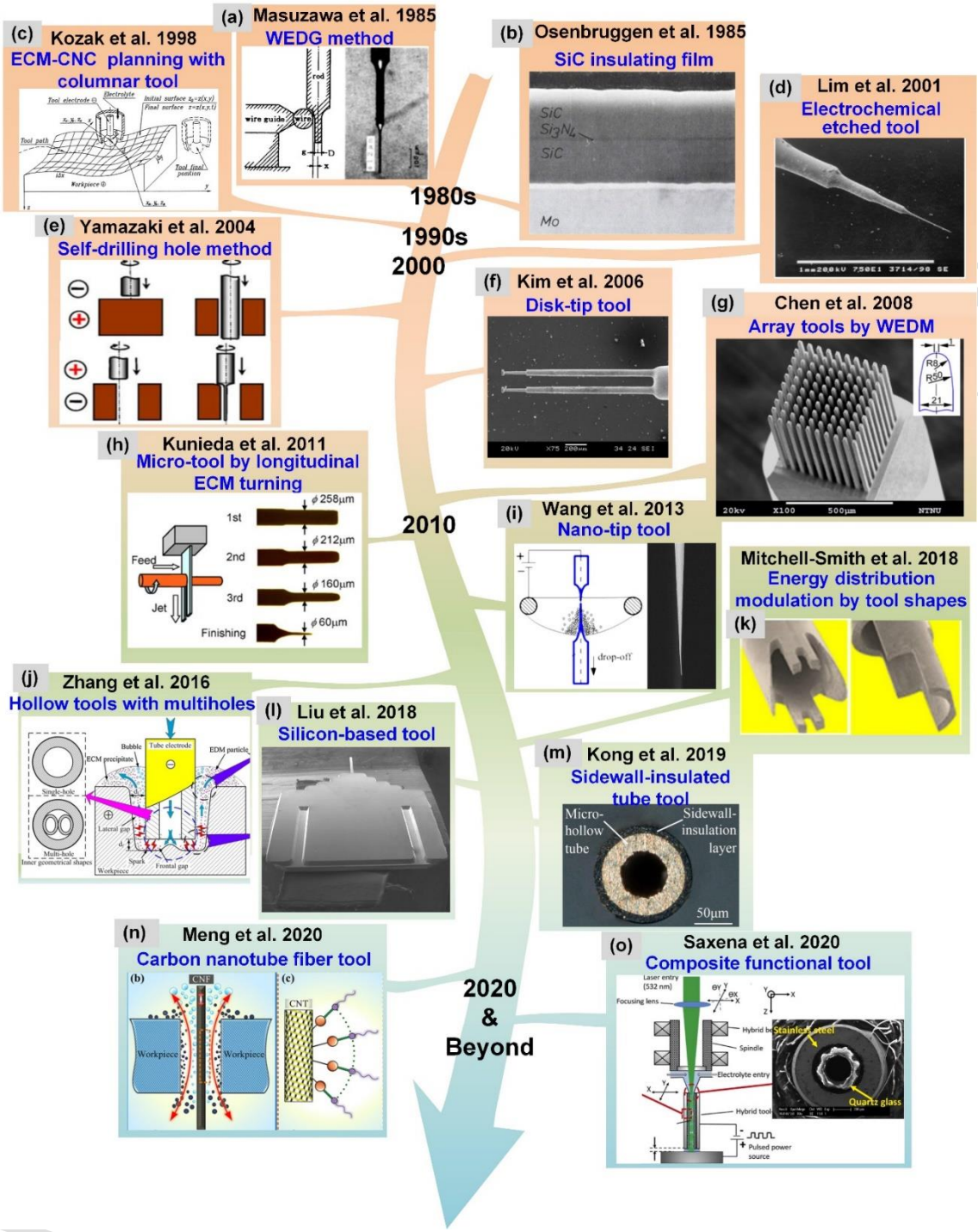

Fig. 2. Chronological representation of key advances in the design and fabrication of micro-tools for micro-ECM: (a) Proposing the wire electrical discharge grinding (WEDG) technique for micro-tool fabrication (Masuzawa et al., 1985); (b) CVD deposited SiC-Si_3N_4-SiC insulating films on the molybdenum tool (Osenbruggen and Regt, 1985); (c) ECM-CNC planning using a columnar tool (Kozak, 1998); (d) Micro-tool fabricated by electrochemical etching (Lim and Kim, 2001); (e) Micro-tool fabricated by EDM using the self-drilled hole method (Yamazaki et al., 2004); (f) Disc-

end micro-tool fabricated by the reverse EDM (Kim et al., 2006); (g) Array micro-tools machined by wire-EDM (Chen, 2008); (h) Micro-tool machined by ECM turning (Kunieda et al., 2011); (i) Nano-tip tool with a high aspect ratio fabricated by the liquid membrane method (Wang et al., 2016c); (j) Tube tool with various inner features (Zhang et al., 2016a); (k) Energy distribution modulation by the mechanical design of micro-tool shapes (Mitchell-Smith et al., 2017); (l) Silicon-based tool fabricated by MEMS technology (Liu et al., 2018a); (m) Tube tool with sidewall insulating film (Kong et al., 2021); (n) Carbon nanotube fiber used as a micro-tool in wire-ECM (Meng et al., 2020); (o) Composite function tool used for laser-ECM hybrid process (Saxena et al., 2020c).

2.3 Framework and logic of this review

The structural design and material selection put demands on the fabrication processes of micro-tools. At the same time, tool design also needs to be integrated with the development of manufacturing technology by considering manufacturability, economy, and efficiency. Fig. 3 depicts the framework of this review paper. Considering the complex interelectrode gap phenomena and problems in micro-ECM, section 3 describes the basic functions of micro-tools, which are necessary to enhance the machining stability. Section 4 summarizes the common materials currently used for micro-tool bodies and insulating films in the literature. Some potentially viable materials that yet need to be extensively validated are also included. Section 5 and 6 provides an overview of several fabrication processes for the micro-tools and insulating films. The feasibility of the fabrication of tools of different structures and materials is analyzed by comparing technical characteristics, efficiency, and applicability, echoing sections 3 and 4.

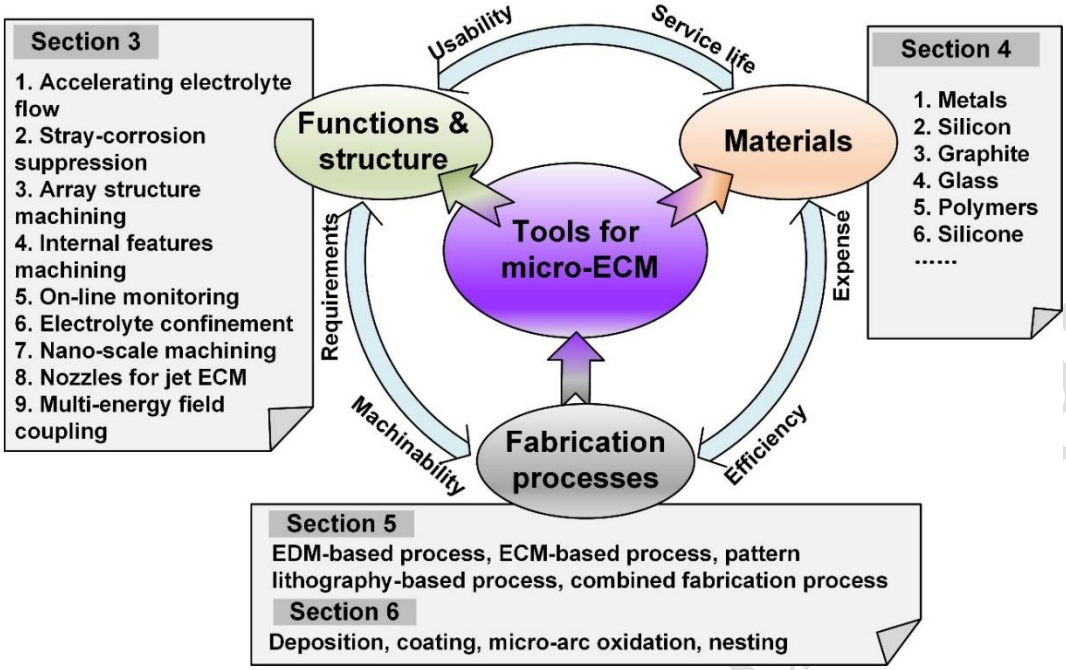

Fig. 3. Framework and logic of this paper.

3. Functional design of the micro-tools in micro-ECM

Dimension, structure, and material are basic elements of micro-tools, which in combination determine the applicability, tool functions, usability, and service life. In tradition ECM sinking processes, the dimension and shape of the tool need to be calculated backward according to processing targets, and the key is to establish an anode shape prediction model. Additionally, the interelectrode gap (IEG) should remain uniform throughout machining to guarantee the shape accuracy during EC sinking. The earliest research developed empirical and mathematical models, such as the multiple regression techniques (Ippolito and Fasalio, 1976), the cos θ method (Kawafune K et al., 1967), and the conformal mapping technique (Collett DE et al., 1970), to design the tool dimensions according to overcuts and side gaps. Nevertheless, they are restricted to limited parameter ranges and stable workpiece shapes. Recently, researchers started to use numerical methods such as the finite difference method (FDM) and finite element method (FEM) to determine the potential distribution and material removal rate. With the application of multiphysics models based on COMSOL software, the size and shape prediction of workpieces and tools is becoming more accurate.

In most cases, there is no unique solution for the micro-tool dimensions, and it is necessary to consider the adopted processing parameters. The frontal and side interelectrode gap (IEG) are very important as well as difficult to maintain parameters during micro-ECM. The frontal IEG determines

the copying accuracy and the side IEG determines the dimensional accuracy. S. Hinduja and M. Kunieda (2013) have introduced the approaches of anode prediction and dimension design in their review paper. This study focuses on the design for functionality, structure, and materials of micro-tools. The discussions on tool design with specific functional requirements are provided in the following subsections.

3.1 Tool designs for facilitating electrolyte flow and removing electrolysis by-products

In micro-ECM, the gap between the micro-tool and the workpiece is in the range of ~100 μm (Bhattacharyya et al., 2004). When machining high-aspect-ratio structures, the electrolyte flushing becomes less effective and prevents the renewal of fresh electrolytes, making it difficult to remove electrolytic products. Short circuits or tool collisions often occur, causing interruptions to the process and limiting the maximum achievable aspect ratio. Even if the micro-ECM process can continue, the change in physical and chemical properties of the contaminated electrolyte deteriorates the machining accuracy. Several studies have been carried out to facilitate electrolyte flow by designing special shapes of micro-tools. Compared to cylindrical tools, changing the cross-sectional shape or using an internal structure can increase the debris removal space and accelerate the longitudinal flow rate of the electrolyte. To date, edge-cutting tools (Egashira et al., 2018; Yang et al., 2009), slotted tools (Nastasi and Koshy, 2014; Puthumana and Joshi, 2011), tools with oblique holes (Kumar and Singh, 2019), polygonal tools (Mullya et al., 2020), tools with oblique grooves (Kumar and Singh, 2018), and spiral tools (Liu et al., 2019a; Tsui et al., 2008; Zou et al., 2020) have been used in micro-ECM and micro-EDM technologies, as illustrated in Fig. 4.

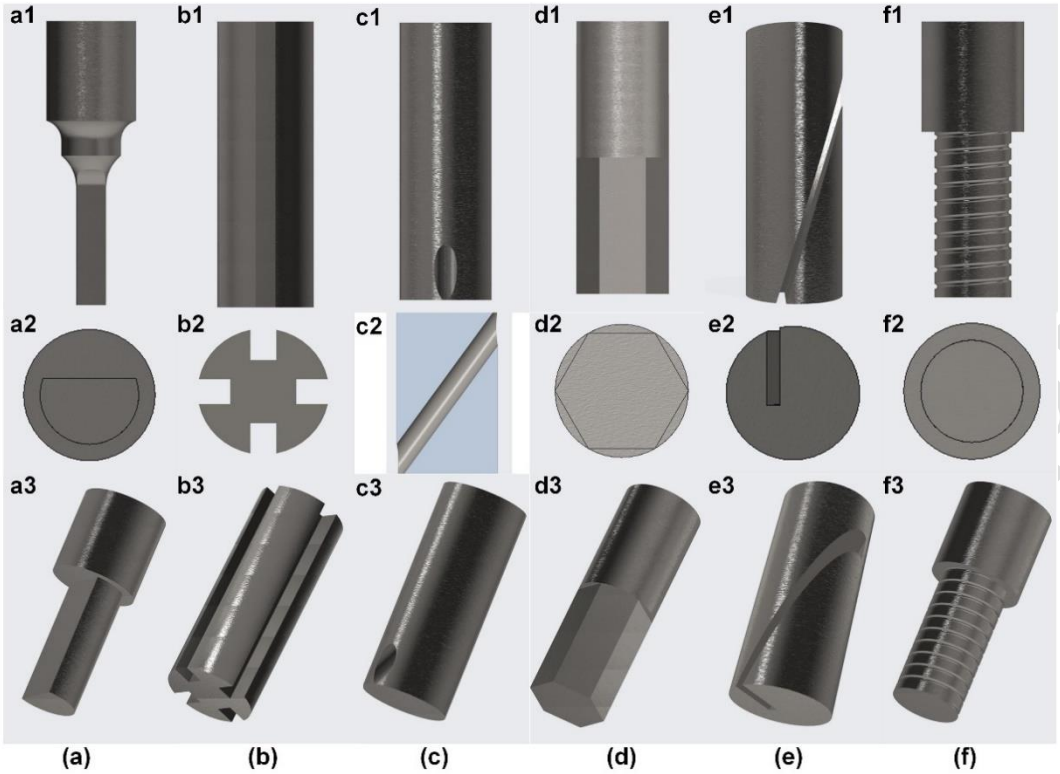

Fig. 4. Micro-tools with special shapes for facilitating electrolyte flow: (a) Edge-cutting micro-tool; (b) Slotted micro-tool; (c) Micro-tool with oblique holes; (d) Polygonal micro-tool; (e) Micro-tool with oblique grooves; (f) Spiral micro-tool.

High-speed rotation of the cylindrical tool drives the electrolyte flow in the tangential direction, leading to a small longitudinal flow rate, as shown in Fig. 5(a). In contrast, high-speed rotation of the edge-cutting micro-tool or the polygonal micro-tool accelerates the fluid flow along the axial direction, transporting the solid products from the processing area to the outside (Fig. 5b). The edge-cutting microtool provides more flow space for the electrolyte. Assisted by ultrasonic vibrations, the maximum machining depth was increased by approximately 30%, and the machining efficiency was improved by approximately 83% (Yang et al., 2009). In addition, a variety of cross-sectional shapes such as double-side edge-cutting tools (Zheng et al., 2007), polygon cross-sectional tools (Goiogana and Elkaseer, 2019), and trapezoidal cross-sectional tools (Liu et al., 2020c) were also derived. From computational fluid dynamics (CFD) results, it has been observed that the variation in the amount of residual electrolytic products between the trapezoidal cross-sectional tool decreases with the increase of rotating speed, as illustrated in Fig. 5(e). The electrolytic products can be reduced to 13%, resulting in a remarkable product removal performance (Liu et al., 2020c).

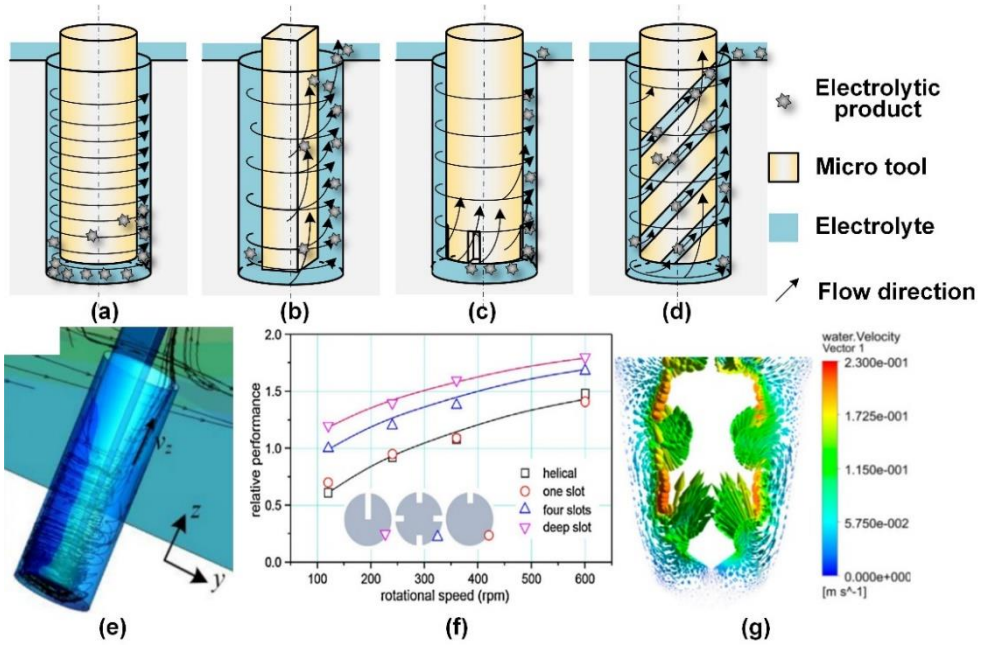

Fig. 5. Schematic diagram of electrolyte flow using (a) A cylindrical tool; (b) An edge-cutting tool; (c) A slotted tool; (d) A spiral tool. (e) Streamlines in the machining gap using a trapezoidal cross-sectional tool (Liu et al., 2020c); (f) Comparison of section geometries on tool performance using various slotted tools (Nastasi and Koshy, 2014). (g) Velocity vector distribution diagram of the electrolyte using a spiral tool (Liu et al., 2019a).

An end-slotted tool consists of slots with various widths, numbers, and heights, which usually have a larger cross-sectional area than an edge-cutting tool, as displayed in Fig. 5(c). CFD simulation results indicated that a tool with deep radial grooves had the most prominent flushing effect on the working liquid (Nastasi and Koshy, 2014) (Fig. 5f). The creation of a micro-hole in the tool body as a flow channel can alter the flow field so that the products are removed through the hole (Kumar and Singh, 2018). Analogously, the use of oblique grooves on the micro-tool sidewalls is also effective in eliminating products in the processing area. Kumar and Singh (2018) have shown a 300% increase in the machined aspect ratio compared to a cylindrical tool due to its self-flushing effect. Referring to the debris removal of mechanical drilling, a spiral drill was used as the micro-tool, and the so-called 'micro-spiral pumping effect' caused by the high-speed rotation of the tool drives out the electrolytic products (Wang et al., 2006). As shown in Fig. 5(d), the spiral flow of liquid within the IEG is similar to a vertical vortex, consisting of a circumferential vortex and an axial annular flow (Liu et al., 2019a) (Fig. 5g). The negative pressure absorbs fresh electrolytes and pours them into the processing area along the sidewalls (Liu et al., 2019b). With the spiral micro tools, micro holes with maximum aspect

ratios of up to 8 were processed. However, this method depends on the drill's size specification, and it is difficult to reduce its diameter to less than 100 μm.

The application of a non-cylindrical tool relies on the application of a high speed of rotation. While removing the solid products, achieves an equivalent electric-field-distribution effect to that of using a cylindrical tool. To coincide the geometrical and rotational centers, this must be achieved either by a precise fixture design or by fabricating the micro-tool in situ, thereby eliminating errors caused by the clamping.

The use of tubular tools is another effective approach for facilitating electrolyte flow (Li et al., 2021b; Pattavanitch and Hinduja, 2012; Wang et al., 2010). The electrolyte is flushed directly into the processing area through the inner hole, and flows out from the IEG, consequently removing the electrolytic products (Fig. 6a). By adopting a tubular tool with an inner diameter of 60 μm and length of 6.5 mm, the electrolyte flow velocity is up to approximately 10 m/s with the inlet pressure of 1.05 MPa (Kong et al., 2017), as displayed in Fig. 6(b). Zhang et al. (2020b) have established a multi-physics model of gas-liquid flow and electric current to study the flow field and current density distribution at different electrolyte pressures. The high-speed flow of electrolytes in the processing area enhanced the mass transfer and improved the shape accuracy of the microstructure. As a result, narrow grooves with a depth-to-width ratio greater than 6 were processed. Apart from that, a combination of spiral and tubular structures for a micro-tool has also been presented. Matching external flushing with counterclockwise rotation of the micro-tool improves the electrolyte flow within the gap and reduces the precipitate concentration (Ji et al., 2021; Zhang et al., 2019b; Zhang et al., 2019c). It has been proven that a trapezoidal spiral structure was beneficial in reducing the accumulation of the by-products and effectively removing the precipitates in Fig. 6(c).

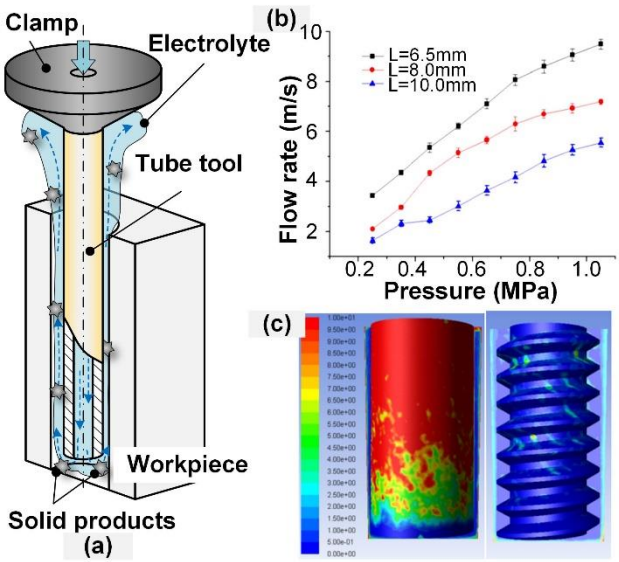

Fig. 6. (a) Schematic diagram of electrolyte flow using a tubular tool; (b) Relationships between the flow-rate and the electrolyte pressure (Kong et al., 2017); (c) Axial velocity in the machining gap (Zhang et al., 2019b).

The disadvantage of using a tubular tool is that it leads to the formation of residual islands (Fig. 7a) on the workpiece when the inner diameter is large (Zhang et al., 2016b). Moreover, the machining efficiency is theoretically lower than with a solid tool due to the reduced area of the end face. Optimizing the inner diameter and internal shape of the tubular tool can eliminate the residual island and improve the machining efficiency (Zhang et al., 2016a). The use of internal multi-hole tubular tools was found to be effective in removing residual islands, as illustrated in Fig. 7(b). It was also determined that the double-perforated tubular tool was the optimal structure. In addition, a conceptual porous structure based on a tubular tool was also proposed by Koyano et al. (2017). The electrolyte can carry out electrolytic processing through the porous structure while ensuring the flatness of the surface and eliminating residual islands, as shown in Fig. 7(c). Although the dimensions of these tools are in the millimeter range, they inspire the design of novel tool structures and fabrication processes.

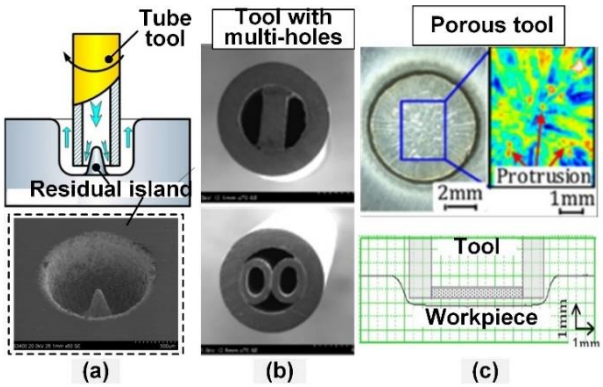

Fig. 7. (a) Residual islands on the workpiece; (b) Tools with multi-holes and the machined hole (Zhang et al., 2016b); (c) 3D printed porous tool and the machined profiles (Koyano et al., 2017).

Based on the aforementioned contents, the micro-tools for accelerating electrolyte flow in micro-ECM and their performance, application, and remarks are summarized in Table 1.

Table 1. The specification of various micro-tools for accelerating electrolyte flow in micro-ECM.

No.	Tool types	Dimensions (diameters/lengths)		Applied rotating speed (RPM)	Applications	Remarks
		Diameters & features	Lengths			
1	Edge-cutting tool	0.12 mm	0.6 mm	582	Machining micro holes (depth of 300 μm)	(Egashira and Mizutani, 2002; Yang et al., 2009)
2	Polygonal tool	~0.2 mm	1mm	500-1200	Machining blind holes (depth of 600 μm)	(Liu et al., 2020c)
3	End-slotted tool	Diameter of 2-15.8 mm, various dimensions and number of slots	1mm	~1000	Increasing removal rate by 150 % in EDM processes	(Mullya et al., 2020; Nastasi and Koshy, 2014)
4	Designed tool with inclined through holes	0.8-3.5 mm	~10 mm	500-1500	Machining micro holes (depth of 2-121.37 mm, diameter of ~ 4.5 mm)	(Kumar and Singh, 2018, 2019)
5	Designed tool with inclined slots	0.07-8 mm	~4 mm	500-1500	Increasing achieved aspect ratio by 300 %	(Kumar and Singh, 2019)
6	Spiral tool	0.1-0.8 mm	~4 mm	~30000	Machining micro holes (aspect ratio of ~3)	(Liu et al., 2020a; Liu et al., 2019a; Tsui et al., 2008; Zou et al., 2020)
7	Hollow tool	Outer diameter of 0.1-2 mm, inner diameter of 0.06-0.8mm	~10 mm	~100, and inlet pressure of 0.1-2 MPa	Machining micro-holes (aspect ratio of ~6)	(Li et al., 2021b; Wang et al., 2010; Zhang et al., 2020b; Zhang et al., 2016a)

3.2 Tool designs for suppression of stray corrosion and improvement of processing localization

Stray currents between the tool sidewalls and the workpiece create a secondary dissolution on the machined surface, causing overcut and sidewall taper during the machining of deep structures. This is one of the critical issues that make micro-ECM difficult to achieve precision micromachining in an

industrial context. Currently, there are three ways to reduce or eliminate stray currents through the micro-tool design. (1) Increasing the distance between the tool sidewall and the workpiece, such as special end shapes of the micro-tools (compare Figs. 8a and 8b); (2) Using sidewall insulating films to isolate the stray current path, as in Fig. 8(c); (3) adopting auxiliary electrodes to actively control the spatial current distribution, as in Fig. 8(d).

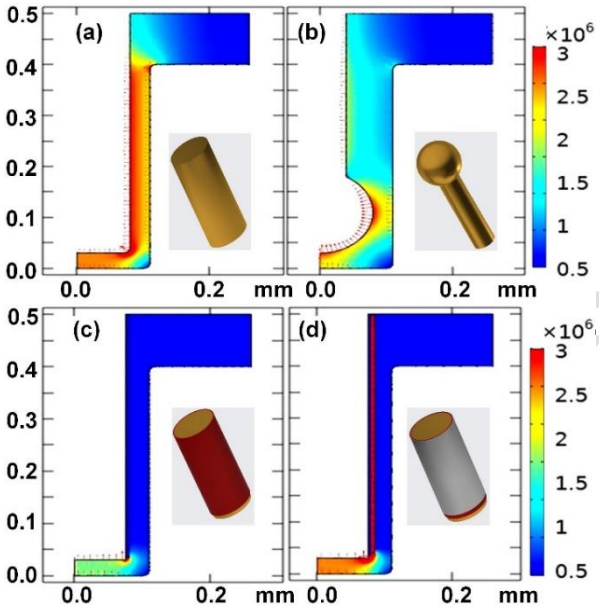

Fig. 8. Simulation results of the current density distribution using (a) A common cylinder tool; (b) A sphere-tip tool; (c) A sidewall-insulated tool; (d) A micro-tool with auxiliary electrodes. More simulation details are in supplementary materials S1.

To increase the gap between the tool sidewalls and the workpiece, the micro-tool is usually designed to have a thick head and a thin neck. In contrast to the tapered shape using a cylindrical tool, the reverse-tapered tool can compensate for the taper caused by stray currents (Sheu, 2014). However, the reverse-tapered tool needs to be matched to processing parameters and machining depth. Further reducing the diameter of the neck, the shape of the tool evolves into a flat-end tool with a disk-shaped end (Kim et al., 2006; Rathod et al., 2013; Wang et al., 2016b) as illustrated in Fig. 9(a), which results in a very tiny taper of the machined microstructure (Fig. 9b). High-aspect-ratio micro-holes were machined using a flat-end tool assisted by ultrasonic vibration. The aspect ratio was up to 10, and the taper angle was only 1°, demonstrating its excellent effects in stray-corrosion suppression. Similar processing performances are achieved using spherical-tip tools (Liu et al., 2015; Yang et al., 2011; Yi and Zhang, 2015). Sub-micron-sized sphere-ended tools were prepared by Wang et al. (2015) (Fig. 9b). The achieved aspect ratio was greatly increased (Fig. 9d). However, the sphere-end tool is more

difficult and time-consuming to prepare than the flat-ended tool. Overall, tools with thick heads and thin necks are better at inhibiting stray corrosion and accelerating electrolyte flow. Nevertheless, the special-tip tools with thin necks are more easily deformed by electrolyte scouring and mechanical collisions. Therefore, they are limited by specific processing conditions in micro-ECM.

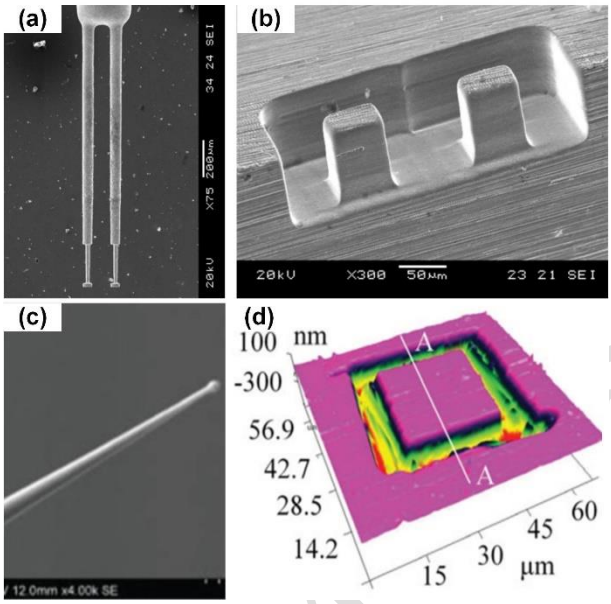

Fig. 9. (a) A disk-tip tool and (b) Machined microstructure (Kim et al., 2006). (c) Sphere-tip tool and (d) the machined microstructure (Wang et al., 2015).

Insulating the sidewalls of the micro-tool is a direct and ideal way to eliminate stray corrosion by blocking the current path. Currently, the tool structure based on a ‘metal substrate + insulating film’ is commonly utilized. The deposition of a SiC film on tungsten tools was an early attempt to insulate the tool sidewalls (Li et al., 2003). This has been followed by techniques such as coating organic adhesive, nesting insulating tubes, as well as fabricating metal oxide films, including an evaluation of their effectiveness in suppressing stray currents. The taper of the processed structures such as cantilevered beams, micro holes, and micro slots were all less than 15°. The relative position of the end faces of the insulating film and the tool substrate shows a critical impact (Liu et al., 2017b; Liu et al., 2016). When the end face of the insulating film is retracted to the tool, the bare tip length of the tool affects the current distribution and the lateral overcut of the machined profiles. When the insulating film extends beyond the tool end face, the stray currents are restrained more effectively and the processing accuracy is further improved. Nevertheless, the risks of damage, breakage, and destruction of the insulating layer are also increased (Liu et al., 2017c).

On a micro-scale, the insulating films on the metal substrates must be thin, uniform, and exhibit

high bonding force to the substrate, which poses some major challenges such as poor adhesion of the insulating film or the low strength of the insulating film itself. The insulation film is easily peeled off and damaged in the electrochemical environment, destroying its function as a current blocker. Hu et al. (2013) investigated the effect of insulating film hydrophobicity on the adsorption of hydrogen bubbles generated during electrolytic reactions. On a hydrophobic film of silica with a thickness of several micrometers, microbubbles reside and adhere at the front end of the tool in combination with the insulating film, thereby protecting the insulating film and improving its durability, as shown in Fig. 10(a). Liu et al. (2020b) attributed the susceptibility of silica film to the differences in expansion coefficients of the film and the tool substrate. A silicon-based tool with silica film was proposed and validated. The use of heavily-doped silicon instead of metallic materials resulted in the physical properties of the substrate and the silica film being closed and improved the durability of the insulating film (Fig. 10b). To prevent peeling off the insulation films, an electroplated layer on the exposed part of the tool was also adopted to protect the films (Hung et al., 2021) as shown in Fig. 10(c). Apart from that, Fang et al. (2013) have demonstrated that a micro-tool tip structure reduced the interfacial stress at the interface of the tool and the insulating film. When the tip angle was increased to 18°, the durability of the coating was increased by approximately 60% (Fig. 10d). In addition, the use of nested rigid tubes (Yao et al., 2016), protective electroplating (Hung et al., 2014), and laser deposition layers (Chang et al., 2015) have also been proposed to improve the durability of the insulating films.

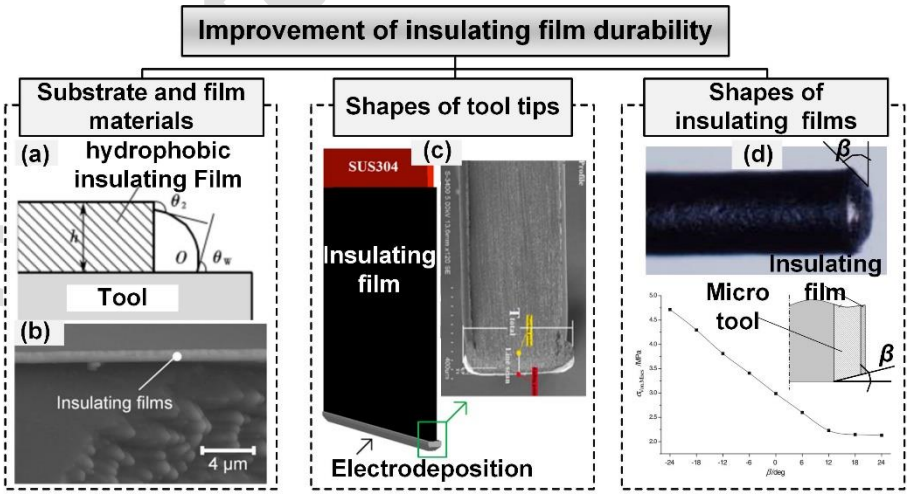

Fig. 10. Improvement of the durability of insulating films: (a) Optimizing the material of tool substrate and insulation film (Hu et al., 2013); (d) Silicon-based tool (Liu et al., 2020b); (c) Micro-tool with special tips (Hung et al., 2021); (d) Optimizing the shape of the insulating film (Fang et al., 2013).

To further constrain stray currents, Zhu and Xu (2002) proposed a tool with an auxiliary electrode.

A metallic bush outside the insulating film was connected with the workpiece, and so the electric field at the side gap area was substantially weakened to achieve better stray-current suppression. However, the tool structure is complex and difficult to prepare, making it difficult to reduce its size and apply it to the common metal micro-tools.

Overall, the micro-tools for suppressing stray corrosion in micro-ECM and their performance, application, and associated remarks are summarized in Table 2.

Table 2. The specification of various micro-tools for stray-corrosion suppression in micro-ECM.

No.	Tool types	Dimensions (diameters/lengths)		Applications	Remarks
		Diameters & features	Lengths		
1	Reverse-tapered tool	Diameter of ~150μm, tip taper of 53μm	~2 mm	No applications	(Sheu, 2014)
2	Flat-tip tool	Disc diameter of 45-200μm, neck diameter of 20-127μm,	0.3-1.2 mm	Machining microgroove and holes (taper angle of <1°)	(Kim et al., 2006; Wang et al., 2016b)
3	Sphere-tip tool	Sphere diameter of 0.9-70μm, neck diameter of 0.2-45μm	~1mm	Machining microgroove and holes (taper angle of <1°)	(Liu et al., 2015; Sheu, 2014; Yang et al., 2011)
4	Sidewall-insulated tool	0.8-3.5 mm	~10 mm	Machining microgroove and holes (taper angle of < 18°)	(Gaihong et al., 2009; Hung et al., 2014; Li and Hu, 2013; Rathod et al., 2014; Wang et al., 2014)
5	Tool with auxiliary electrode	Diameter of ~8μm	1.4-4 mm	100% decrease in standard deviations of machined micro-holes	(Zhu and Xu, 2002)

A dedicated design of the tool structure can serve the dual functions of facilitating electrolyte flow and suppressing stray corrosion. Sidewall-insulated spiral micro-tools can be achieved by depositing an insulating film on the spiral drill (Tsui et al., 2011). Using a ceramic and epoxy bilayer as an insulating film reduces stray corrosion. It was found that tool surface corrosion and the addition of a surfactant to the sol-gel improved the adhesion of the film to the spiral edge (Hung et al., 2013), as shown in Fig. 11(a). Sidewall-insulated tubular tools are relatively simple and easy to prepare. Kong et al. (2021) have prepared tubular tools with a sidewall insulating film using an electrophoretic coating in an aqueous epoxy acrylic solution, as shown in Fig. 11(b). The taper of the micro-holes processed with this tool was reduced by more than 60% and an aspect ratio of more than 5 was achieved. The difficulty with this solution is that it should be ensured that the insulating material does not clog the tube tool. Liu et al. (2021a) used a glass tube as the insulating substrate and the silver-plated layer as the working cathode (Fig. 11c). This novel sidewall-insulated tube tool can further inspire tool preparation schemes based on novel substrate materials and film preparation methods.

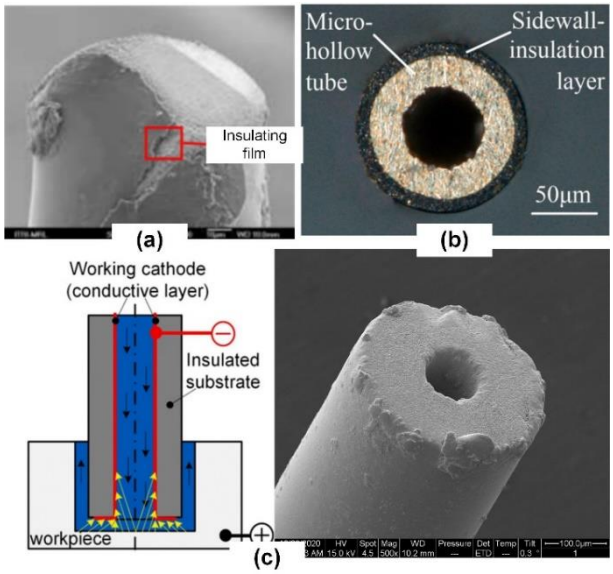

Fig. 11. Micro-tools with dual functions of accelerating electrolyte flow and suppressing stray corrosion: (a) Sol-gel coated spiral drill (Hung et al., 2013); (b) Sidewall-insulated tube tool (Kong et al., 2021); (c) Silver-plated glass tube tool (Liu et al., 2021a).

3.3 Tool designs for machining of array microstructures

Batch fabrication of multiple holes and slots or fabrication of an array of features are highly demanded in a wide range of applications. The use of a single micro-tool with machining trajectory and programming is not only inefficient but also produces poor dimensional accuracy and consistency. Therefore, there is an urgent demand for the utilization of array-type micro-tools. An array of disk-type tools was fabricated using a combination of wire-EDM (WEDM) techniques, mask treatment, and chemical etching procedures. The tool accuracy was low due to the unavoidable influence of stray currents (Wang et al., 2016a), as shown in Figs. 12(a) and 12(b). In contrast, array tools formed by LIGA-based processes are more uniform (Hu et al., 2008), as in Fig. 12(c). Various cross-sections of the micro-tool including square, triangle, hexagon, and gear were achieved. Ma (2010) coated the array-type tools with a liquid epoxy resin and cured it to obtain sidewall insulations and process an almost taper-free array structure as shown in Fig. 12(d) and 12(e). Array-type tools have an irreplaceable position in scenarios that emphasize high repeatability and efficient processing, but their design and preparation methods are still somewhat lacking for now.

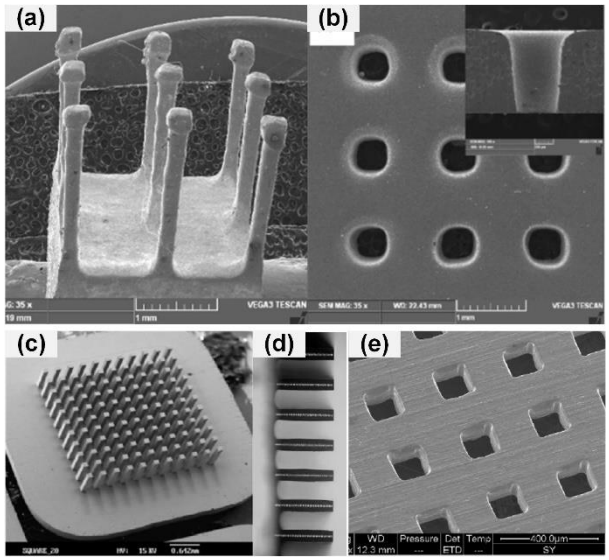

Fig. 12. Array-type tools: (a) Array of disk-tip tools; (b) SEM micrographs of micro-holes drilled using the disk tool array (Wang et al., 2016a); (c) Array-type tools fabricated by LIGA; (d) Sidewall-insulated array-type tools; (e) ECM-machined by sidewall-insulated array-type tools (Ma, 2010).

In addition to array tools for processing holes and grooves, there are also tools for fabricating shallow pits and textures with complex shapes on workpiece surfaces. Microstructures are fabricated in bulk on tool surfaces by techniques such as lithography, micro-milling, and femtosecond laser cutting, and used in micro-ECM processes. More details are discussed in Section 5.5.3.

3.4 Tool designs for machining of complex internal features

With the miniaturization and functional diversification of mechanical products, there is an increasing need for machining holes with internal features. For example, diesel injector nozzles require reverse-tapered holes to improve combustion efficiency and reduce energy loss. The use of bamboo-shaped cooling holes in aero-engine blades can improve cooling efficiency. To this end, a tool with a winding-controlled conductive area ratio was proposed to machine the inner surface of complex holes (Mi and Natsu, 2017). From the simulation results of current density, the evolution of the inner feature shape of the hole was investigated to control the rate of material etching at different machining locations, enabling the machining of complex internal shapes such as reverse-tapered holes (Fig. 13a), internal drums, spirals, and bamboo holes. Wang and Zhu (2009) fabricated micro-tools with conductive patterns on the sidewalls using a photolithographic mask method and machined spiral-shaped flow channels in the holes (Fig. 13b). A bamboo-knotted structure was obtained using a tool with partial insulating films. The above process requires a pre-machined hole, which is then precisely

aligned with the hole using a specially designed tool. In contrast, the machining of micro holes with complex internal structures could be achieved by controlling the processing parameters, machining complex internal features in a single step (Liu et al., 2017a), but it requires a high degree of precision in parameter regulation and is less efficient.

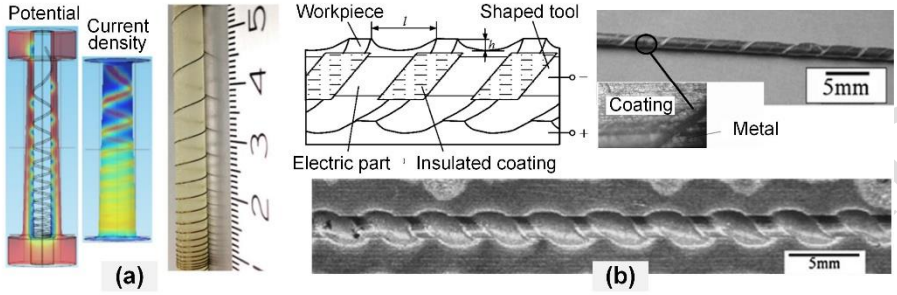

Fig. 13. Tools for the fabrication of complex internal features: (a) Winding wire tool (Mi and Natsu, 2015); (b) Local-insulated tool (Wang et al., 2009).

3.5 Tool designs for on-line monitoring of ECM processing

In the micro-ECM process, the processing signals including the machining current, voltage, temperature, and electrolyte conductivity are continuously evolving. For deterministic material removal, it is essential to capture these evolving parameters at all locations in the IEG where the process is acting. Li et al. (2020) proposed a concept of silicon tool-based chip-on-tool technology. As illustrated in Fig. 14(a), the conductivity and temperature monitoring units were designed on a silicon tool body for real-time process monitoring. The precision and accuracy of the micro-ECM process also depend highly on the generation and removal of gas bubbles that evolve in the IEG. Zhang et al. (2014) employed transparent electrodes of SiC and Ga_2O_3 for monitoring the gas bubble evolution (Fig. 14 b). These transparent tools gave insights into the evolution and coalescence of gas bubbles and the effect of Joule heating on gas bubble formation.

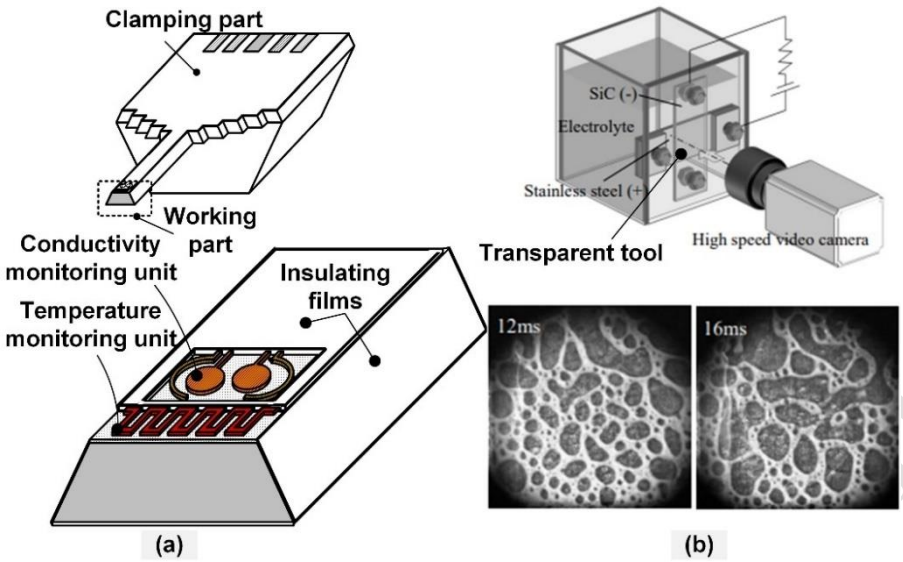

Fig. 14. (a) Concept diagram of silicon tool-based chip-on-tool technology (Li et al., 2020); (b) Observation of gas bubbles in stationary electrolyte using a transparent electrode as a cathode (Zhang et al., 2014).

3.6 Tool designs for local electrolyte confinement

In the ECM process, the spreading of electrolytes on the workpiece or immersion of the workpiece in the electrolyte chamber can lead to corrosion. This has necessitated research in developing tools that facilitate electrolyte confinement. There have been two major developments in this field where one involves the use of solid porous balls analogous to a ballpoint pen and in another concept a tool with vacuum suction of electrolyte is employed. In the work of Wang and Natsu (2022), a spherical porous tool was used in the micro-ECM process as shown in Fig. 15(a). When immersed in an electrolyte bath, the electrolyte is absorbed in the porous tool due to capillary action and when it contacts the workpiece, the electrolyte spreads over a small area due to surface tension. This allows the machining of channels by rolling the tool over the workpiece surface. Guo et al. (2017) have proposed a scanning microelectrochemical flow cell (SMEFC) setup to confine the electrolyte in a small region. As shown in Fig. 15(b), this system consists of an electrolyte circulation system, a hollow tool, and a vacuum insert connected to a Venturi tube via an electrolyte recycling tank. With this method, it was possible to fabricate surficial cavities and channels in a controllable manner.

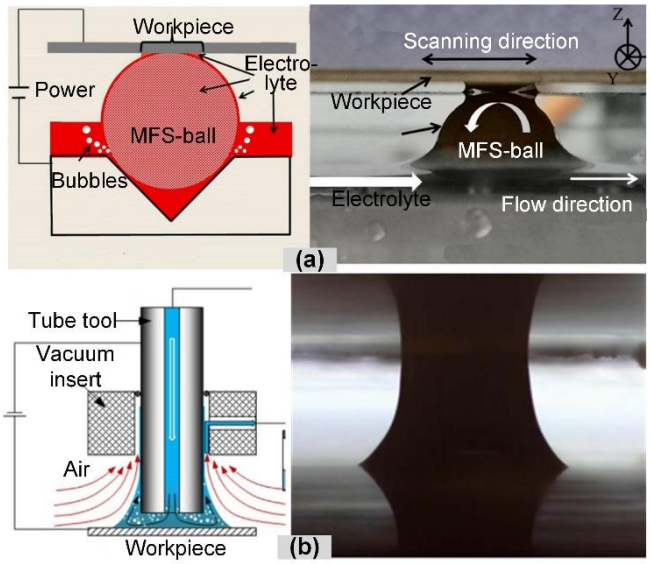

Fig. 15. ECM tools for electrolyte confinement: (a) A tool with a solid porous ball to absorb electrolyte through capillarity analogous to the mechanism of a ballpoint pen (Wang and Natsu, 2022) (b) A tool with vacuum suction of electrolyte (Guo et al., 2017).

3.7 Tool designs for machining of sub-micro and nanostructures

The characteristic dimensions of features fabricated by the ECM process are determined by the potential distribution, which is determined by the size, shape, and curvature of the tool and the IEG. Schuster et al. have proposed the use of ultrashort voltage pulses based on the ‘‘electric filter’’ principle (Kock et al., 2003; Schuster et al., 2000) for fabricating features at the sub-micrometer scale. Because the electrode process exhibits a charging time (τ) of the electrical double layer, the electrochemical reactions can be confined in a highly localized manner by setting the τ shorter than the pulse width. As a result, the electrochemical reactions are confined to a machining accuracy of ~1 μm. Hence, by reducing the tool size, the electrochemical reaction can be limited to the sub-micro and even nanoscale (Huh et al., 2017; Malshe et al., 2010), As an example, with an ultra-short pulse coupled with an atomic force microscope (AFM) cantilever tip (Fig. 16 a and 16b), the dimension of the machined groove can be confined to be less than 100 nm (Han et al., 2022; Lee et al., 2010). The alternative way is to decrease the size of the electrolytic cell, which then acts as both the electrolytic cell and the tool. This method is called scanning electrochemical cell microscopy (SECCM) in Fig. 16(c). The distinct characteristic of SECCM lies in an electrolytic cell (usually fabricated by a micropipette with single or multiple channels), in which a micro/nano-scale orifice is employed as the scanning probe and brought into contact with the conductive substrate to construct the electrochemical system (Zhan et al.,

2017). By employing a SECCM tool (Fig. 16d), metal nanowires, nanopillars, and micropatterns can be achieved by electrochemical deposition (McKelvey et al., 2013; Momotenko et al., 2016). A similar two-channel capillary-based droplet cell was used to remove material from the workpiece. As shown in Fig. 16(e), one of the channels is used as an electrolyte inlet, while the second one is the outlet (Lohrengel et al., 2004). The partition wall is removed close to the tip of the capillary by etching and, thus, the electrolyte flows in the channel. The carrier contains a micro reference electrode, the counter electrode, electric connectors to the power, and fittings for the electrolyte tubes (Lohrengel et al., 2007). This method is currently possible at the micro-scale (Fig. 16f), but achieving nano-fluidic flow is very difficult. The use of highly polished gold foils has also been reported to fabricate nanostructures smaller than the wavelength of light on gold workpieces using ultrashort pulses (Ma and Schuster, 2011).

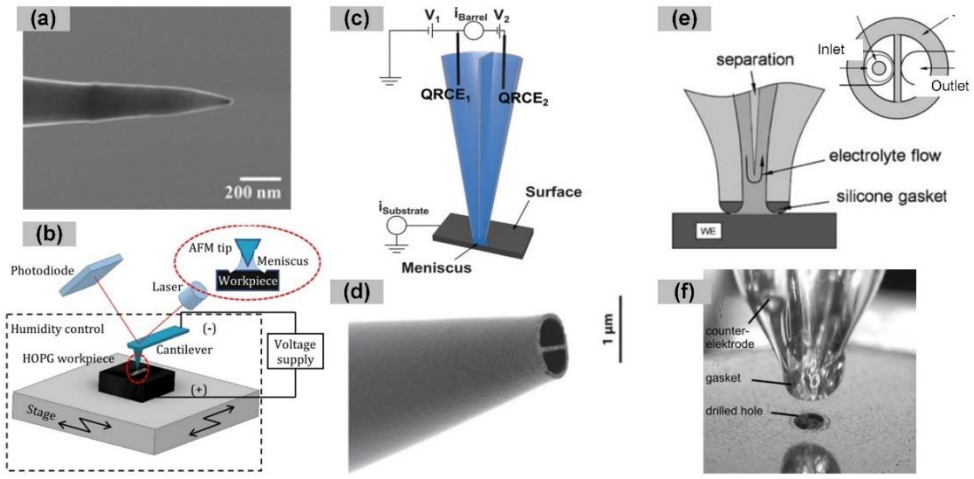

Fig. 16. (a) SEM images of Au tips (Huh et al., 2017); (b) Schematic diagram of the AFM-based electrochemical etching apparatus (Han et al., 2022); (c) Schematic of the SECCM configuration; (d) SEM image of a typical SECCM probe (McKelvey et al., 2013); (e) Schematic views of the theta capillary tool (Lohrengel et al., 2004); (f) Capillary tip above the sample surface (Lohrengel et al., 2007).

3.8 Nozzles for jet-ECM micro-processing

Jet-ECM technology has been developed in parallel for micro-scale processing, and it has been reviewed extensively in ref. (Speidel et al., 2022). The electrochemical jets can be created in varying diameters depending on the nozzle diameter and current density can be manipulated through nozzle shape (Mitchell-Smith et al., 2017). However, there are fluidic limits that prevent downscaling of this technology. The electrochemical jets have been applied for micro-fabrication (pits, cavities, channels)

(Hackert-Oschätzchen et al., 2012), selective micro-deposition (Li et al., 2022), as a cost-effective EBSD analysis tool (Speidel et al., 2021) and as an on-machine metrology tool. Besides this, the jets have been applied for controlled surface structuring (Lutey et al., 2021), three-dimensional machining (Natsu et al., 2008), plasma electrolyte polishing (Quitzke et al., 2022), selective anodizing (Kuhn et al., 2017) and selective cathodic hydrogenation (Zhao et al., 2020) as well.

3.9 Tool designs for achieving multi-energy field coupled processing

3.9.1 Electric discharge and electrochemical energy coupling

Considering the energy source in EDM, the electric spark energy is derived from the plasma discharge between the tool and workpiece through the breakdown of the dielectric medium (Zhan and Zhao, 2020). The electrochemical energy is derived from the electrochemical reaction that takes place at the interface of the tool and workpiece (Fig. 17a). These differences in the mechanism of the location of the energy action lead to differences in the construction and design of the tools.

In the spark-assisted chemical engraving (SACE)[1] (also known as electrochemical discharge machining (ECDM)) process, the micro-tool directly interacts with the workpiece. To improve the aspect ratio, spiral tools (Tang et al., 2017) or double-sided trimming tools (Zheng et al., 2007) were adopted to accelerate electrolyte renewal. To confine the material removal area on the workpiece sidewalls or protect the tool from discharge erosion, sidewall-insulated tools were utilized for better machining performance (Tang et al., 2017). They also had the effect of determining the shape of the gas film. Han et al. (2008) found that the micro-tool with a ceramic layer creates a spherical distribution of the gas film, resulting in better geometric uniformity of the film and a significant improvement in the geometric accuracy of the machined channel. Besides, micro-tools with surface nano-bumps or weaving were prepared to form thin and uniform gas films on the tool surface (Han et al., 2017), thus enhancing the ECDM performance (Fig. 17 b). Yang et al. (2010) investigated the wettability and processing characteristics of different tool materials and their effects on gas film formation. The surface roughness of the tool material determines the wettability, which in turn affects the agglomeration state of the gas film and the machining stability (Kolhekar and Sundaram, 2018; Wüthrich et al., 2005). The shape of the micro-tool is a critical factor influencing the morphology of

[1] In certain literatures the terms SACE and ECDM are used interchangeably. In this paper, the authors have referred to SACE as the process where sparks are generated at the electrolysis gas film around the tool.

the gas film in the ECDM process. The average drilling speed of a sharp-tip tool was approximately 10 times faster than a cylindrical tool due to the higher discharge density at the tip (Zou et al., 2021). Yang et al. (2011) found that the curved surface of the spherical tool reduced the contact area on the workpiece, facilitating the flow of electrolytes and enabling the rapid formation of a gas film. Considerable efforts have been made to control the gas film and the discharge point using various tool shapes or surface morphology (Arab et al., 2019a; Cheng et al., 2010; Pu et al., 2020; Yang et al., 2010), but the current difficulty is how to reduce the severe wear and tear phenomenon of micro-tools in SACE processes. The authors believe that the use of reliable sidewall-insulated tools may be a solution.

In the EDM-ECM hybrid machining (EC machining and EDM discharge occurring at different positions or timing sequences), Zhang et al. (2015b, 2016b) proposed an electrochemical discharge drilling (ECDD) method based on a tubular micro-tool (Fig. 17 b), which simultaneously improved machining efficiency and accuracy due to different material removal mechanisms around the bottom and side walls of the tool by EDM and ECM, respectively. The process is based on the use of a tubular tool to ensure smooth flushing of the products from the bottom. The disadvantage of this process, however, is that stray corrosion inevitably leads to a taper in the machined holes.

3.9.2 Laser and electrochemical energy coupling

Laser-electrochemical hybrid machining (L-ECM) has a wide range of applications in the processing of difficult-to-cut materials such as metal matrix composite and high-temperature alloys. The laser energy is derived from the laser source and the electrochemical energy is from the power supply. The laser beam is introduced into the electrochemical dissolution region inside the workpiece via a tubular tool to make laser-electrochemical energy fully coupled (Fig. 17 d). Water-guided laser machining technology, which uses a jet of water from a tubular tool to introduce the laser into the process area, was an early attempt (Qiao et al., 2021). The emergence of L-ECM based on total beam reflection has shown the combined effects of laser and electrochemical energy, improving processing efficiency and reducing defects. Wang et al. (2019, 2021) have bonded capillaries made of fluoropolymer to the inside of a tube tool for reflecting the laser beam, and coated the outer surface of the tubular tool with ceramic as an insulating film (Fig. 17 e). The micro-tool designed by Saxena et al. acts as a cathode and a reflective multimode waveguide for the laser. The goal here was to minimize the dependence of laser propagation on the refractive indices of the electrolytes, thereby allowing experimental flexibility in using different electrolytes for processing materials. In their work, a quartz

glass hollow capillary was used to increase the receiving angle of the laser into the tool and to prevent damage to the metal end (Fig. 17 f) (Saxena et al., 2020b, c). Inside the tool, the laser propagates through multiple diffuse and specular reflections from the internal surface of the workpiece. However, these structures still do not eliminate laser energy loss in the electrolyte, as the laser is transmitted in the liquid. Also, thermal effects have a negative impact on the service life of the micro-tool. Addressing the absorption of laser light by electrolytes and exploring the effect of tool structures and materials on laser-electrochemical energy coupling needs further attention.

3.9.3 Mechanical-electrochemical (discharge) energy coupling

The Mechanical-electrochemical (discharge) energy-based machining (M-ECM, M-ECDM) processes are under development with the objective of machining difficult-to-cut materials for improved productivity and better surface quality (Fig. 17 g). There are three types of combined mechanical-electrochemical (discharge) machining technology: hybrid electrochemical grinding, hybrid electrochemical milling, and hybrid electrochemical discharge grinding. Zhu et al. (2011) have presented a specially designed tool used for hybrid electrochemical grinding, which is the metal rod with coated abrasives as the cathode removes material electrochemically and mechanically, as shown in Fig. 17 (h). the workpiece material removal occurs in two phases. Phase 1 is entirely electrochemical action. Phase 2 is a combination of electrochemical action and mechanical grinding. The abrasive grains act to remove the soft, non-reactive passivation layer, thus improving the machining efficiency and surface quality.

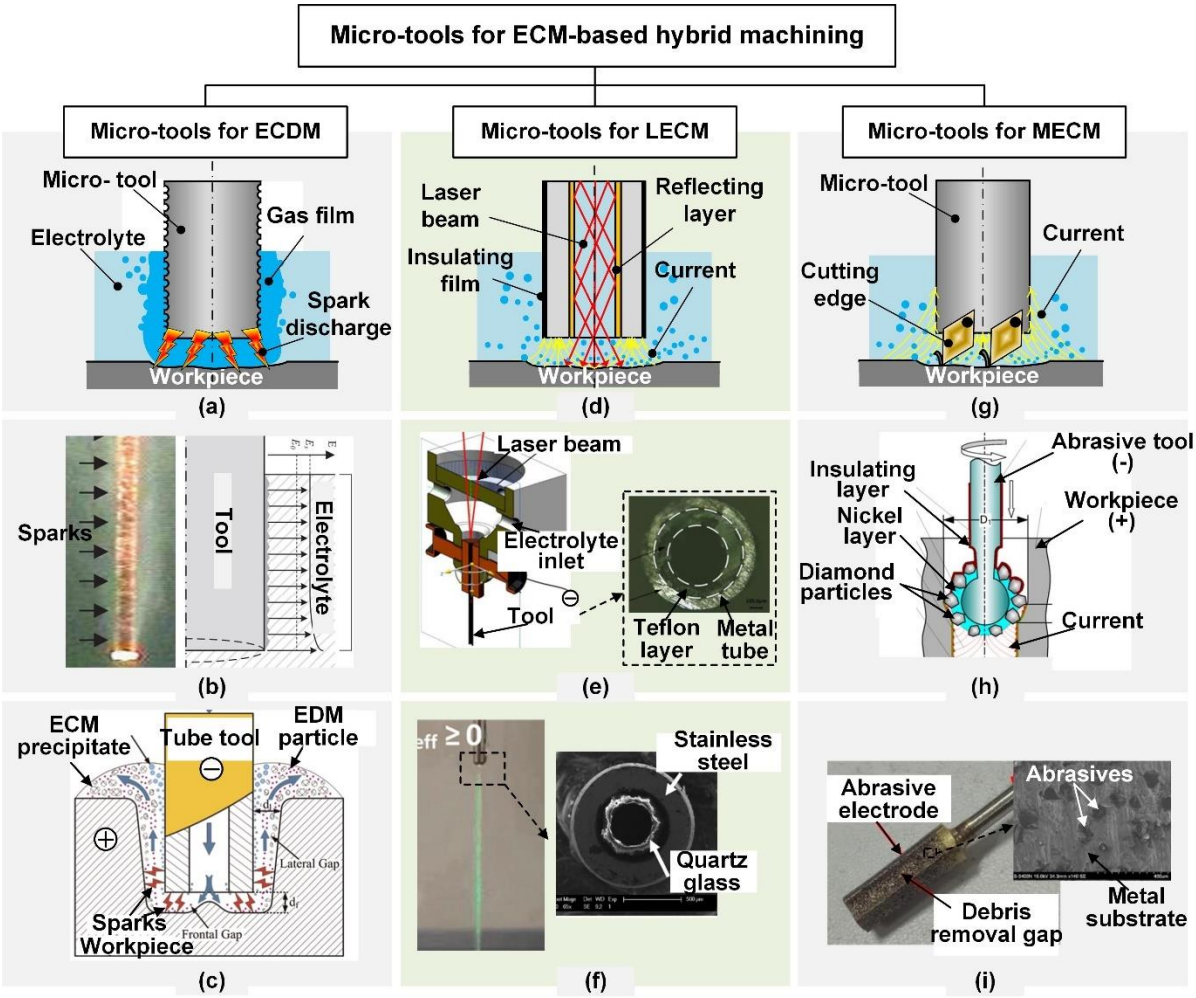

Fig. 17. Micro-tools for ECM-based hybrid machining: (a) Schematic diagram of the ECDM process; (b) Micro-tool with surface bumps (Han et al., 2017); (c) Diagram of the tube-tool electrochemical discharge drilling process (Zhang et al., 2016b); (d) Schematic diagram of the L-ECM process; (e) Micro-tool with laser reflector (Wang and Zhang, 2021); (f) Micro-tool with quartz capillary and inner reflective layer (Saxena et al., 2020c); (g) Schematic diagram of the M-CDM process; (h) Tool for hybrid electrochemical grinding (Zhu et al., 2011); (i) Micro-tool for hybrid electrochemical discharge grinding (Liu et al., 2020d).

The tools used for hybrid electrochemical milling are a combination of a milling cutter and a cathode, which mainly comprises the tool body, a ceramic insert, and shims. The workpiece materials are removed mechanically by rotating the cutting edge of the ceramic insert and electrochemically by reactions (Van Camp et al., 2018; Wang and Qu, 2021). Because the size of ceramic inserts is difficult to reduce to micrometer size, the reported tool is not suitable for micromachining for now. The tool used for a hybrid electrochemical discharge grinding method is a combination of diamond abrasives

and metal substrate. Densely packed abrasive grains are not as easily damaged by electrochemical discharge behavior as cutting edges of milling cutters. Thus, grinding and ECDM energy have a high degree of coupling (Chak and Rao, 2007; Liu et al., 2018b; Liu et al., 2013). A typical tool for electrochemical discharge grinding is shown in Fig. 17(i).

4. Structure and materials of micro-tools for micro-ECM

4.1 Monolithic columnar micro-tools and materials

There are several demands on the physical and chemical properties of tool materials: (1) Excellent electrical conductivity to conduct current. (2) High strength to maintain a stable shape under the impact of electrolyte flow. (3) High stiffness, not easily damaged and deformed during accidental mechanical impacts. (4) Excellent corrosion resistance to maintain the size and shape of the process for high precision. (5) Excellent ductility and machinability, can be easily shaped into micro-sizes, complex structures.

Metals or alloys are the most common materials for micro-tools for micro-ECM, such as brass, tungsten, tungsten carbide, stainless steel, platinum, titanium, nickel, and molybdenum. Non-metal conductive materials are also feasible as micro-tools, as shown in Fig. 18.

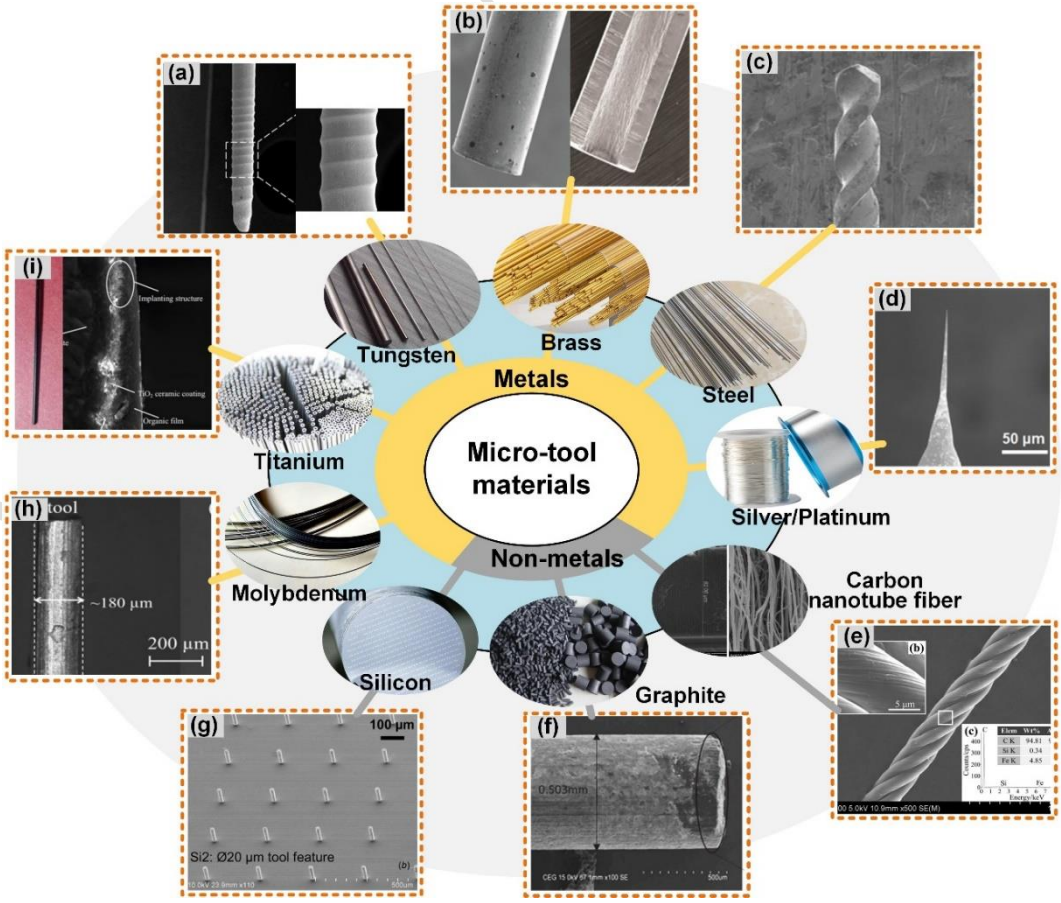

Fig. 18. Materials for micro-tool substrate and some application examples: (a) Tungsten spiral tool (Fang et al., 2020); (b) Brass tube tool (Zhang et al., 2016a); (c) Steel spiral drill (Zou et al., 2020); (d) Platinum nano-tip tool (Yi and Zhang, 2015); (e) Carbon nanotube fiber tool (Meng et al., 2020); (f) Graphite tool (Pradeep et al., 2019); (g) Silicon tool (Li et al., 2013); (h) Molybdenum tool (Arab et al., 2021); (i) Titanium tool (Wang et al., 2014).

Table 3 lists the physical parameters of the various materials used for micro-tools. Tungsten (Li et al., 2003; Qi et al., 2018) or tungsten carbide (Egashira et al., 2018) micro-tools were first widely used in micro-EDM due to their high melting point and were eventually introduced into micro-ECM experiments. Due to their excellent stiffness and strength, they can be used to produce micro-tools with special shapes and complex structures, such as edge-cutting, spherical, spiral tools, and micro-tools with oblique holes. In contrast, the strength of brass tools is lower, and they are prone to deformation or fracture in some cases. Due to its superior ductility, brass is generally used as the tube micro-tool. It can be formed using the die drawing preparation process with various combinations of inner diameter, outer diameter, and internal structures. Brass tube tools are available in sizes down to 0.05 mm and can have a variety of internal configurations. Despite this, the most widely used size of the tube micro-tool is in the range of 0.1-0.5 mm (Kong et al., 2017; Zhang et al., 2016a). The advantage of titanium and aluminum materials is that the stable oxides generated on their surface can be used directly as reliable sidewall insulation. With their excellent corrosion resistance, they are also often used as tool materials (Hung et al., 2019; Wang et al., 2014). However, the size of titanium and aluminum tools is difficult to reduce to less than 100 μm. Silver and platinum have excellent electrical conductivity, but are expensive and have low stiffness. The use of silver and platinum in the fabrication of sub-micron scale tools has been reported so far (Wu et al., 2013; Yi and Zhang, 2015), but their use is very limited. Nickel has deficient physical properties such as strength and hardness than stainless steels and tungsten carbide, but it can be used to prepare micro-tools by electroforming based on the LIGA process and is therefore also often used as array micro-tools.

Table 3. Alternative materials for micro-tool substrate and their properties.

No.	Material	Conductivity (S/m)	Melting point (°C)	Strength (MPa)	Corrosion resistance	Machinability	Remarks
1	Brass	1.6×10^7	930	~469	Medium	Easy	(Liu et al., 2021b; Zhang et al., 2016a)
2	Tungsten	1.79×10^7	3422	479	Medium	Difficult	(Liu et al., 2015; Masuzawa et al., 1985)
3	Platinum	9.5×10^6	1768	~165	High	Easy	(Sugita et al., 2013b; Yi and Zhang, 2015)

4	Silver	6.3×10^7	961	140	High	Easy	(Wu et al., 2013)
5	Molybdenum	2×10^7	2623	324	High	Very difficult	(Arab et al., 2021)
6	Titanium	2.38×10^6	1668	240	High	Difficult	(Hung et al., 2019; Wang et al., 2014)
7	Aluminum	3.8×10^7	660	90	Medium	Easy	(Hung et al., 2019)
8	Stainless steel	1.45×10^6	~1510	~621	High	Difficult	(Rashedul et al., 2021)
9	Graphite	$\sim10^5$	~3600	~14	High	Very difficult	(Pradeep et al., 2019; Sugita et al., 2013a)
10	Carbon nanotubes	$\sim10^4$	~3127	~200	High	Difficult	(Meng et al., 2014)
11	Heavily doped silicon	$\sim10^4$	~1410	165	Medium	Easy	(Li et al., 2013; Liu et al., 2020b)

Electrical conductivity is the primary consideration in the selection of tool materials. The results of a software simulation of the tool conductivity against the current density are shown in Fig. 19. When the tool conductivity is 5×10^7 S/m (brass), the spatially distributed current density is up to 180 A/cm^2 (Fig. 19a). The current density at the surface of the workpiece rarely changes when varying in the range of 5×10^7-5×10^4 S/m (Fig. 19c). This indicates that materials such as stainless steel (~10^6 S/m) (Bian et al., 2021), graphite (~10^5 S/m) (Pradeep et al., 2019; Sugita et al., 2013a), carbon nanotubes (~10^4 S/m) (Meng et al., 2020), and heavily doped silicon (~10^4 S/m) (Li et al., 2013; Liu et al., 2018a) can also be used as tool materials theoretically. When the conductivity is 5×10^3 S/m, the current density is up to 150 A/cm^2, which can be used as a tool material by increasing the voltage, but the heat generated by the tool increases at the same current density. When the conductivity is reduced to 5×10^2 S/m, the current density decreases sharply to 59 A/cm^2, and the current density distribution is shown in Fig. 19(b). It indicates that low-conductive tools cannot be used for micro-ECM processes.

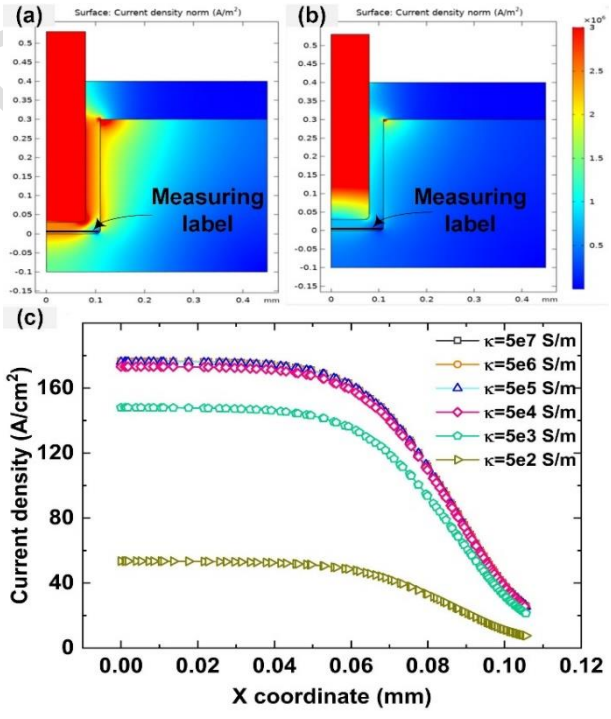

Fig. 19. Simulation results of the current density using micro-tools with various conductivity: (a) Current density with the tool conductivity is 5×10^7 S/m; (b) Current density with the tool conductivity is 5×10^2 S/m; (c) Current density with various tool conductivities. More simulation details are in supplementary materials S2.

In addition to metals, non-metallic conductors or heavily-doped semiconductors are also feasible as tools in micro-ECM. Pradeep et al. (2019) performed ECM using graphite tools with a diameter of 500 μm. Although the electrical conductivity of graphite is high enough, it is difficult to reduce it to a smaller size without deformation. Meng et al. (2014) have proposed a method of welding carbon nanotubes on a tungsten rod to produce carbon nanotube tools with a diameter of 30 μm. The conductivity of the carbon nanotube tools was enhanced by surface nickel plating. They also surface-treated the carbon nanotubes hydrophilically to improve chip evacuation and achieve improved machining accuracy. Carbon nanotube fibers are an emerging material that has proven its viability in micro-ECM, but further attempts and verification of widespread use are still in the early stages. Liu et al. (2020b) experimented with heavily doped monocrystalline silicon tools with a doping concentration of 10^{20} cm^{-3}. Silicon-based tools with a section size of about 91 × 52 μm and a high aspect ratio (> 20) are obtained by wet etching. The processing efficiency is proven to be almost identical to that of using a brass tool. Based on the MEMS process, it is possible to further reduce the silicon tools to the sub-micron or even nano-scale, and it is suitable for batch manufacturing. However, silicon tools are also highly brittle and prone to breakage in use.

4.2 Conductive substrate with insulating films and their materials

The common sidewall-insulated tool structure consists of a conductive substrate and an insulating film. The conductive materials are described in section 4.1. Currently, materials for insulating films can be divided into four categories: (1) high polymer materials such as polyimide, silicone, epoxy resin, etc. Most polymer films are made by solidifying the liquid state into a solid. Their advantage is that they can be formed to a thin film thickness and can be prepared in-line and repaired in situ. The disadvantage is that the films formed are inherently soft and have low strength. They are easily damaged during the electrolytic process and the thickness uniformity and consistency of the films formed are inferior. (2) Silicon-based film materials such as SiO_2, Si_3N_4, SiC, etc. They are desirable film materials with outstanding compactness, uniform thickness, strength, hardness, and corrosion resistance. They are also suitable for batch preparation. However, the adhesion on the metal substrate

is weak after deposition at high temperatures and cooling using CVD processes. (3) Metal oxides such as titanium oxide, aluminum oxide, etc. Existing studies have proven that metal oxides have reliable insulating properties and can be grown directly on titanium and aluminum. However, this is limited to a few metallic materials. The relatively poor machinability and ductility of metals such as titanium and aluminum make it challenging to reduce the size of tools. (4) Sintered materials, such as ceramics and glass. These materials usually have high resistance, high wear resistance, and excellent corrosion resistance. However, their brittleness and difficulty in size reduction limit their application prospects on the micro-scale. In addition, diamond-like carbon (DLC) coating materials also have the potential to be used as insulating materials, but their applications have not been reported in micro-ECM technologies.

The available research offers the possibility of a variety of material combinations, but a comprehensive analysis that considers the properties of the insulating layer material itself and its bonding properties with the conducting substrate still needs further exploration.

Table 4. Alternative materials for insulating films and their properties

No.	Material	Conductivity (Ω·m)	Melting point (°C)	Strength (MPa)	Corrosion resistance	Machinability	Examples
1	Polyimide	10^{15}-10^{17}	223	80	High	Medium	(Li and Hu, 2013; Liu et al., 2021b)
2	Silicone	10^{9}-10^{15}	400-450	~30	High	Easy	(Gaihong et al., 2009; Hu et al., 2013)
3	Epoxy resin	10^{9}-10^{21}	150	~34	High	Easy	(Rathod et al., 2014)
4	Silicon-based materials	10^{13}-10^{16}	1410	~180	High	Difficult	(Ferraris et al., 2013; Li et al., 2003)
7	Ceramics	10^{9}-10^{22}	1985 (Al_2O_3)	~300	High	Very difficult	(Han et al., 2008; Park et al., 2006)
8	Glass	10^{15}-10^{19}	1700	7-9	High	Very difficult	(Liu et al., 2021a; Liu et al., 2022b)
9	Diamond	10^{14}-10^{16}	~3550	8000	High	Difficult	(Tang et al., 2017)

4.3 Insulated substrate with conductive film and its materials

In recent years, a novel structure of micro-tools with a conductive film as the cathode has been introduced. Malleable engineering plastic is used as a substrate. On the substrates, thin metal film materials such as gold, silver, platinum, copper, and nickel act as the cathode, which can be prepared by metal sputtering, evaporation, or electroless plating. Lyubimov et al. (2017) used a plastic substrate with an optimized conductive coating (Figure 20a), and the feasibility of metalized plastic tools was demonstrated. The minimum thickness of the conductive layer of copper, nickel, and platinum tools was determined and the maximum permissible current about the thermal temperature of the thin metal

layer was defined. The use of a hollow structure as a substrate and the preparation of metal films on the inner and end surfaces allows the formation of a sidewall-insulated tube tool. The substrate materials are available in glass, plastic, and ceramics, while the metal films need to be suitable for chemical plating preparation methods. Liu et al. (2021a) prepared a silver layer on the quartz glass tube as the tool substrate by electrodeless plating of silver (Fig. 20a). The silver-plated glass tube tool was successfully prepared by using ammonium persulphate to etch the inner wall surface of the glass tube to roughen it. A polyimide film was used as a mask layer to define the chemically plated area, and experimental results proved its reliability for long-term applications. Although it is still limited to laboratory applications, it offers new ideas for the design of tools for micro-ECM.

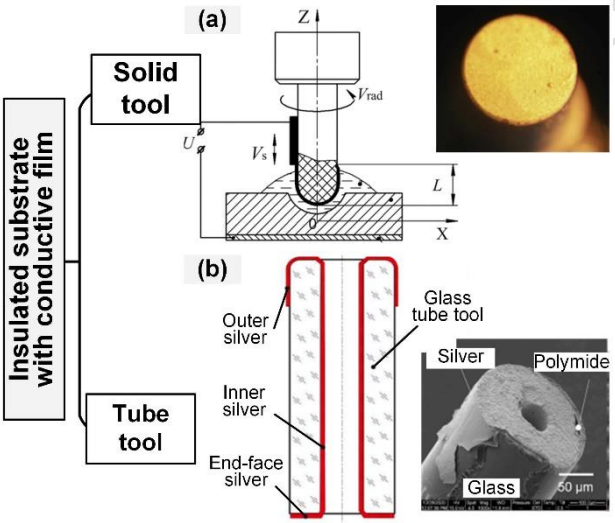

Fig. 20. Insulated substrate with the conductive film: (a) Plastic substrate with metal film (Lyubimov et al., 2017); (b) Glass tube with platted silver film (Liu et al., 2021a).

5. Fabrication processes of micro-tools

5.1 EDM-based processes

Micro-EDM is one of the most efficient technologies to produce micro-components, which can in situ produce the metal micro-tools of desired dimensions, thereby maintaining the concentricity of the fabricated tool with the machine spindle. Up to now, five different EDM-based techniques have been developed and are available commercially for micro-tool fabrication, including the wire electrical discharge grinding (WEDG) method, rotating-sacrificial-disk electrode discharge grinding method (D-EDG), block electrical discharge grinding method (BEDG), reverse electrical discharge machining (R-EDM) method, and wire electrical discharge machining (WEDM) method. In the WEDG process, low-

energy machining with a point discharge mode can be achieved. The constantly moving wire electrode allows for compensation of electrode wear (Wang and Bai, 2014) (Fig. 21a). The use of a high-speed rotating disc electrode can replace the wire electrode and avoid wire breakage (D-EDG in Fig. 21b). The use of large-area block electrodes allows for an increase in simultaneous discharge points (BEDG in Fig. 21c). But the phenomenon of tip discharge leads to uneven losses in the block electrode, creating severe taper in the subsequent machining of the micro-tool (Ravi and Chuan, 2002). Reverse electrical discharge machining is the process of counter-copying a micro-tool by means of discharges through pre-formed negative microstructures on a thin plate (Fig. 21d). Micro-tools can be obtained by the successive steps of performing small holes (called self-drilling holes) and then counter-copying by reversing the polarity of the power supply. WEDM is commonly used for the fabrication of micro-tool arrays (Fig. 21e).

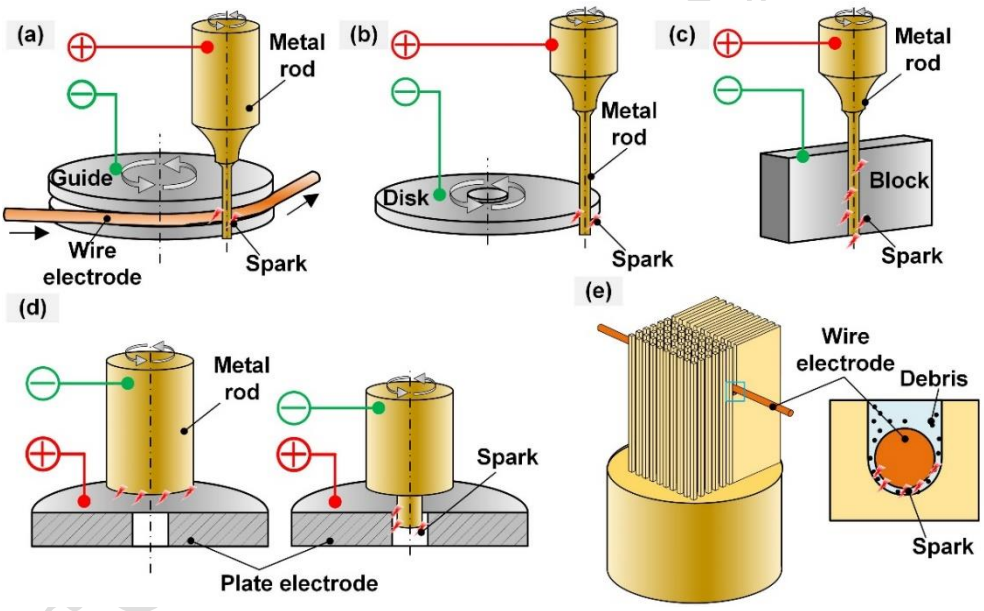

Fig. 21. Schematic diagram of EDM-based processes: (a) Wire electrical discharge grinding (WEDG); (b) rotating-sacrificial-disk electrode discharge grinding (D-EDG); (c) block electrical discharge grinding (BEDG); (d) reverse electrical discharge machining (R-EDM); (e) wire electrical discharge machining (WEDM).

5.5.1 Wire electrical discharge grinding (WEDG)

The WEDG method was first introduced by Masuzawa et al. (1985), which provides an effective approach for fabricating micro pins, micro spindles, and micro-tools. Micro-tools with diameters in the range of 2.5-25 μm were fabricated and the shaping accuracy is high with an error of less than 1 μm (Li et al., 2019; Masuzawa and Tönshoff, 1997). Based on this, all kinds of micro-tools of various

cross-sectional shapes such as edge-cutting tools and polygonal tools were obtained through WEDG (Fig. 22a and 22b) (Tzu-WeiHuang and Dong-YeaSheu, 2020). To improve the efficiency, a new approach combining twin wires with two discharge circuits was proposed (Fig. 22c), so-called the 'twin-wire EDG' (Sheu, 2008). As shown in Fig. 22(d), tapered micro-tools were fabricated by feeding a rotating micro-rod along the centerline between the inclined wires (Bellotti et al., 2021). To eliminate the adverse effects of positioning errors of the machine tool, the tangential-feed WEDG (TF-WEDG) method is proposed by Zhang et al. (2015a). In Fig. 22(e), the slope of the curves is decreasing with the reduction of the distance S_T, the removal resolution is higher if the tool is closer to the symmetry axis of the wire guide. Several micro-tools with diameters less than 70 μm were machined repeatedly (Fig. 22f), and the consistent accuracy of micro-tools along axial direction was confined to 1 μm.

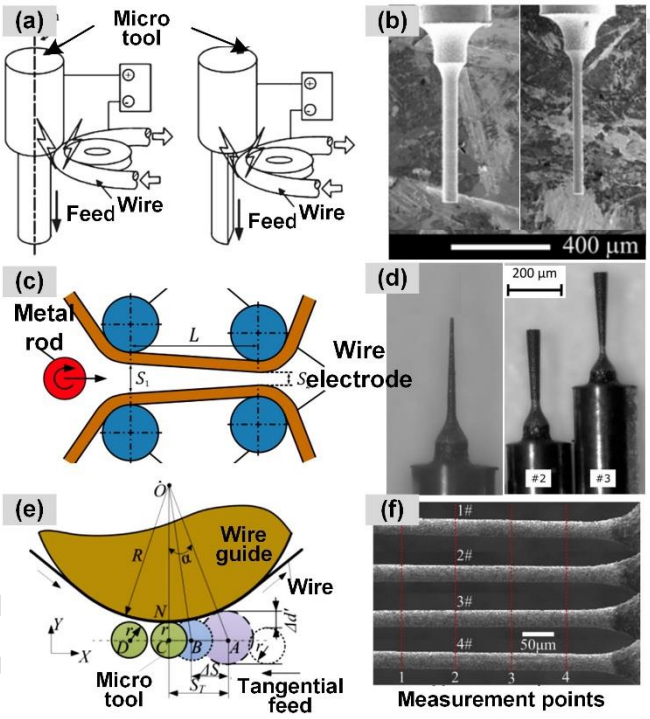

Fig. 22. Wire electrical discharge grinding (WEDG) technologies and the obtained micro-tools: (a) Fabrication of edge-cutting tool by WEDG, and (b) Machined tools with cross-sections of circle and semicircle (Yang et al., 2009); (c) Schematic diagram of the twin-wire EDG, and (d) Tapered tools (Bellotti et al., 2021); (e) Schematic diagram of the TF-WEDG, and (f) Cylindrical micro-tools (Zhang et al., 2015a).

5.1.2 Rotating-sacrificial-disk electrode discharge grinding method (D-EDG)

The use of a disk instead of a wire can avoid the issue of wire breakage. Moreover, the tool wear is distributed uniformly over the whole disk. Lim et al. (2003a) have compared three different types of

sacrificial electrodes including wire, disk, and blocks to assess their performance for tool fabrication. The dimensional change of the rotating electrode is almost negligible in tool fabrication. The rotating electrode with 0.5 mm thickness can produce a smooth surface like a stationary electrode as it is wide enough to finish a smooth surface.

5.1.3 Block electrical discharge grinding method (BEDG)

The moving-BEDG method is essential to reduce processing error caused by electrode wear, which is more beneficial for machining straight and thin micro-tools in a short time (Zhao et al., 2006). From the scanning EDM results in Fig. 23(a) and 23(b), a 500 μm diameter changes to 20 μm in 20 minutes (Mohri and Tani, 2006). The machining speed increases depending on the machining time. This suggests that it is essential to stop machining at a suitable time to get the desired diameter of the micro-tool. To further enhance the efficiency and accuracy, Yin et al. (2016) have developed the BEDG by two block electrodes without measuring the device online (so-called EDG-TBE method), as shown in Fig. 23(c). The desired diameters of micro-tools were mainly determined by the width of the narrow slit and the discharge gaps. Fig. 23(d) compares the tool diameters concerning machining time using the BEDG and EDG-TBE methods. The machining efficiency of the EDG-TBE method is higher than that of the BEDG method, and the machining error is less than 2 μm. Micro-tools with diameters of 86 μm and 46 μm were obtained as illustrated in Fig. 23(e). Inspired by the moving BEDG and WEDG methods, Song et al. (2013) presented a strip-EDM turning method using a wide conductive strip as the electrode. The strip-EDM method did not result in a broken-electrode problem or cusps on the machined surface. The MRR of the strip-EDM turning was 74.3% higher than the MRR for wire-EDM turning.

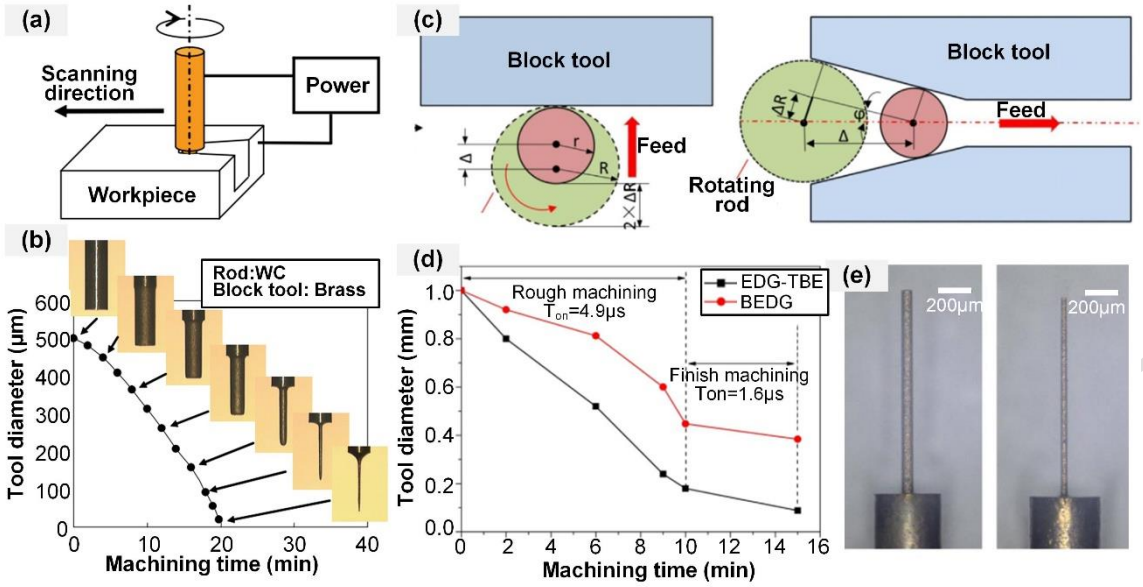

Fig. 23. **Block electrical discharge grinding method** (BEDG) technologies and the obtained micro-tools: (a) Schematic diagram of the moving BEDG, and (b) Relationship between tool diameter and time (Mohri and Tani, 2006); (c) Schematic diagram of the EDG-TBE, (d) Relationship between tool diameter and time, and (e) Cylindrical micro-tools (Qingfeng et al., 2016).

5.1.4 Reverse electrical discharge machining (R-EDM)

Yamazaki et al. (2004) proposed self-drilled holes to form a micro-tool that does not need its initial positioning, and the operation is easy and short as shown in Fig. 24(a). In this procedure, a small hole is machined by rotating and feeding a rod that has negative polarity on a plate electrode. Then, the rod polarity is inverted and the rod is fed into the plate electrode. A micro-tool with varying diameters can be fabricated by measuring the machining gaps between the rod and the machined hole in advance. Micro-tools obtained by R-EDM still had taper errors after copying many times (Fig. 24b). Contrary to WEDG, this process can produce reference holes using the rod without finding the reference point. Moreover, this procedure is simple and has the capability to produce complex shapes and array tools (Kim et al., 2006) (in Section 5.4.2).

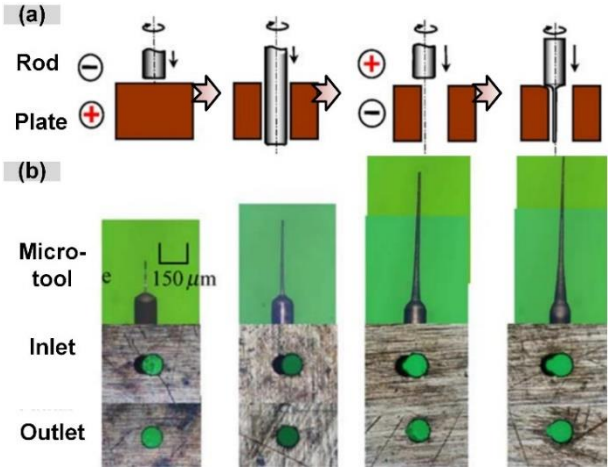

Fig. 24. (a) Schematic diagram of the EDM method with a self-drilling hole; (b) Micro-tools and the hole profiles after fabrication (Yamazaki et al., 2004).

5.1.5 Wire electrical discharge machining (WEDM)

The WEDM method is primarily utilized in fabricating array microtools with polygon structures (Fofonoff and Donoghue, 2004; Rakwal et al., 2009). Chen et al. (2008) have presented the WEDM mechanisms and developed a precise NC machine tool for the micro-WEDM process (Fig. 25a). To reduce the wire electrode jitters, the vibration suppression system is utilized to suppress the vibrations of the wire. 10×10 squared array micro-tools with a width of 21 μm, height of 700 μm, and spacing of 24 μm were fabricated as shown in Fig. 25(b) and 25(c). Arab et al. (2019b) used a reciprocating WEDM machine to fabricate the multi-tip array tool and selected sufficient tension for avoiding wire wobbling and reducing overcut. As a result, the 3×3 multi-tip array micro-tools with a high aspect ratio were obtained as shown in Fig. 25(d) and 25(e).

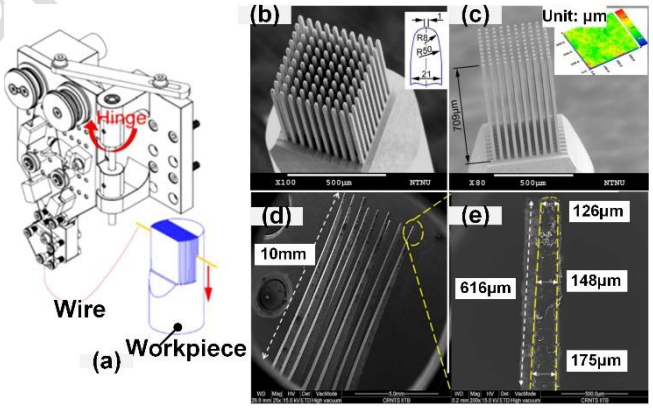

Fig. 25. (a) A precise CNC machine tool for the micro-wire EDM (WEDM); (b) Tool arrays from an isometric view; (c) Tool arrays from a front view (Chen, 2008); (d) 3 × 3 multi-tool tip array; (e) Details of the tool surface (Arab et al., 2019b).

5.2 ECM-based processes

Compared to the EDM-based processes, the ECM-fabricated tools have a smooth surface with no residual stresses or heat-affected defects. In an electrolytic cell, a metal rod with high-speed rotation acts as an anode. Depending on the difference in cathode shape and the relative motions, ECM-based processes can be divided into three categories. By using a cathode of comparable or even larger size to the metal rod immersed in the electrolyte (Fig. 26a), metallic materials are removed from different locations on the metal rod at the same time, which is the electrochemical etching method. As in Fig. 26(b), using the cathode of a thin sheet or a small self-aligned hole, the high-aspect-ratio tool requires relative movement between the metal rod and the cathode for material removal at different locations, so-called the electrochemical turning-like method. In Fig. 26(c), the process is similar to WEDG when a fast-moving wire is used as the cathode. The tool fabrication relies on precise relative movements, which is the wire electrochemical grinding (WECG).

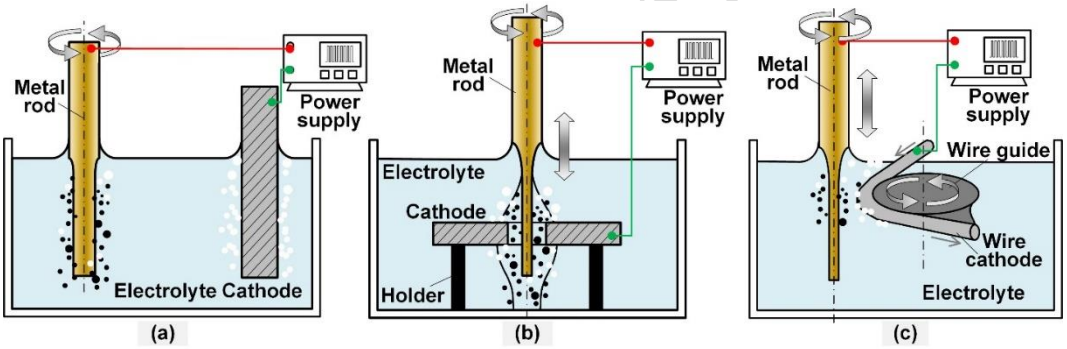

Fig. 26. Schematic diagram of ECM-based processes: (a) Electrochemical etching; (b) Electrochemical turning-like method; (c) wire electrochemical grinding (WECG).

5.2.1 Electrochemical etching

The electrochemical etching is the simplest approach as only a few relative movements are required. The cathode can be of various shapes such as columns, flat plates, cylinders, etc. (Lim et al., 2003b; Zhang et al., 2017). Lim and Kim (2001) found that a diffusion layer forms around the rod due to the generated electrolytic products. Because the diffusion layer has an ionic concentration gradient, the diffusion layer obstructs the movement of ions from a bulk solution to a material surface. Hence, the local dissolution rate decreases in inverse proportion to the thickness of the diffusion layer. By considering the 'black film' formed on the metal rod, a FEM-based numerical model was established to predict the tool profiles (Patro et al., 2019). The material removal rate decreases with time due to the formation of diffusion layers. By adopting the DC voltage of 4V, the diameter of the tool was

reduced from 0.6 mm to 0.42 mm during 360s, and the varying rate of the diameter decreased with the processing time.

Pulsed power supplies have been used more frequently in high-precision tool fabrication (Kamaraj and Sundaram, 2013; Lee et al., 2005). Processing parameters such as applied voltage, pulse frequency, pulse duty cycle, electrolyte concentration, electrolyte temperature, and the rotating speed of the metal rod affect the thickness of the diffusion layer and the tool shape. The influence of different parameters on the uniformity of tool diameter was investigated by Fan and Hourng (2009). As illustrated in Fig. 27(a), The higher the applied voltage, the greater the inverse taper angle of the tool obtained by corrosion. As processing time increases, the diameter shrinkage occurs, affecting the machinable tool length. When the applied voltage is 2 V, the local diffusion layers are thinner, and the bottom material is preferentially removed due to the large curvature of the bottom of the metal rod. Thus, no inverse tapered structure is formed. As shown in Fig. 27 (b) and 27 (c), the larger the pulse period and the smaller the pulse duty cycle, the better the diameter size uniformity and the smaller the inverse taper of the processed tool. This is because the long period and small duty cycle allow sufficient time for the product around the tool to be transported into the bulk electrolyte, avoiding concentrated polarization and an excessively thick diffusion layer.

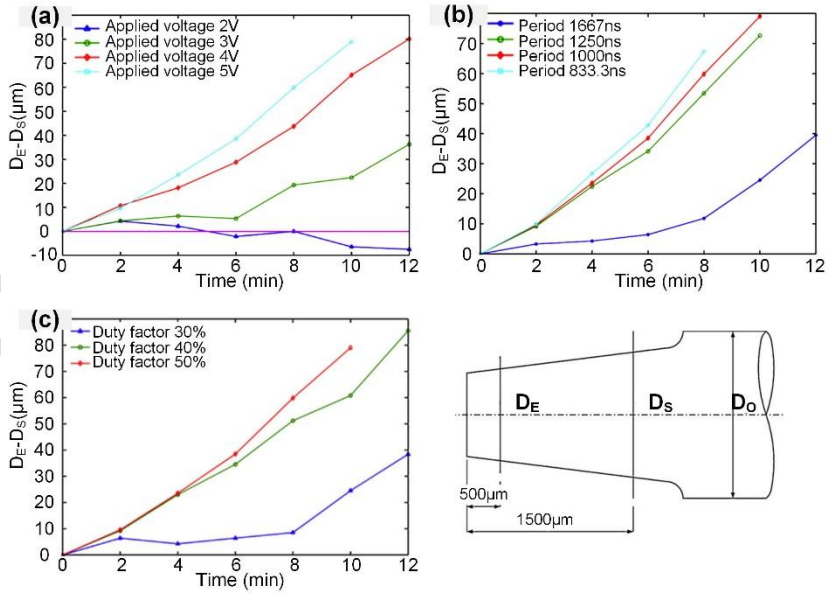

Fig. 27. Shape of the micro-tools: (a) With the various voltages of 2-5 V; (b) Various pulsed periods; (c) Duty factors of 30-50 % (Fan and Hourng, 2009).

With constant process parameters, the typical evolution of the metal rod shape with increasing machining time is shown in Fig. 28 (a). The tapered tool formed by the lower part of the diameter

shrinkage coming off is shown in Fig. 28 (b) and 28(c) (Ju et al., 2011; Lim and Kim, 2001). In contrast, a linearly decreasing voltage or duty factor can be used to fabricate cylindrical micro-tools with uniform diameters. A high removal rate and a smaller ΔD can be simultaneously obtained by applying gradual reducing voltage at a particular rate and remaining in a low voltage to make the uniform thickness of the diffusion layer along the micro-tool. The metal rod material is removed more uniformly and forms into high aspect ratio as displayed in Fig. 28(d). Linear decaying of the applied voltage or duty factor yields micro-tools in nearly cylindrical forms, as shown in Fig. 28(e) (Fan et al., 2010). Besides, the tool can also be fabricated to a cylindrical shape under the condition of low applied voltage, high electrolyte concentration, and large cathodic area. A tungsten tool with a diameter of 500 μm was fabricated in 20 min into a cylindrical tool as shown in Fig. 28(f) (Fan and Hourng, 2009).

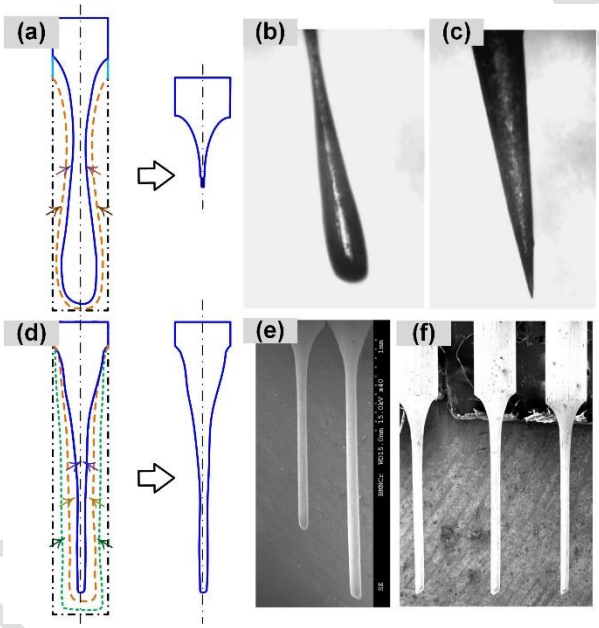

Fig. 28. (a) Typical geometries of the micro-tool using constant parameters; (b) Typical appearances of tungsten tips under a low current; (c) Tungsten tips under a high current (Lim and Kim, 2001); (d) Typical geometries of the micro-tool using varying parameters; (e) Various length micro-tools fabricated by varying parameters (Fan et al., 2010); (f) Micro-tools fabricated by optimal parameters (Fan and Hourng, 2009).

5.2.2 Electrochemical turning-like method

Material dissolution only occurs close to the cathode. Hence, precise control of the relative movement between the metal rod and the cathode allows better control of the shape of the micro-tool with different cross-sections (Liu et al., 2010; Liu et al., 2011). Ghoshal and Bhattacharyya (2013) have studied the effects of the applied voltage, vibration frequency, vibration amplitude, and electrolyte

concentrations on the tool dimensions. As the applied voltage increases, the time for the tool to reach its minimum diameter or the cut-off time for radial shrinkage decreases. The amplitude of vibration has the most significant effect on the growth of cavitation bubbles and energetic collapse. For each voltage, there exists an appropriate amplitude of vibration for minimum standard deviation and the main idea is to make the current density uniform throughout the length. With the optimum combination of processing parameters (voltage of 5 V and amplitude of 3 μm), the diameter of the micro-tool varies as shown in Fig. 29.

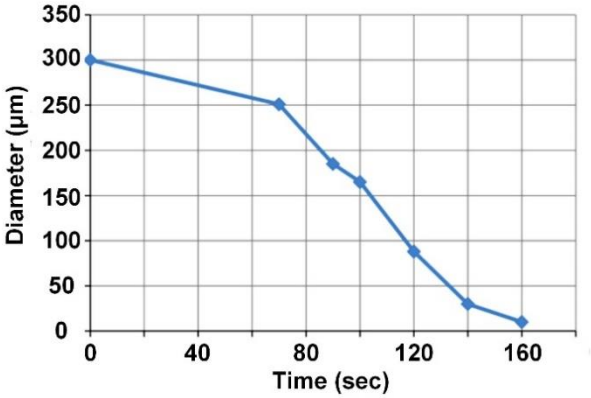

Fig. 29. Diameter of the cylindrical fabricated tool according to machining time (Ghoshal and Bhattacharyya, 2013).

The relative position of the cathode end face has a significant influence on the geometric evolution behavior of the metal rods (Chiou et al., 2012; Han and Kunieda, 2017). When the initial highest position of the rod end is higher than the cathode, the geometry of one end of the workpiece is easily formed into a V-shape with a large shortening in length (Fig. 30a). When the initial highest position of the rod end is lower than the cathode, a reversed taper is formed and it is more likely to cut off the rod (Fig. 30b). When this relative position is adjusted to a preset position at each stroke, the ratio of the length to the diameter is increased, but the average decreasing rate in diameter remains invariable (Fig. 30c). Mathew and Sundaram (2012) have established a mathematical model using the IEG to predict the diameter of the fabricated tool based on the velocity of the cathode. The micro-tools with a diameter of 14.2-53.1 μm and a very high aspect ratio (280-450) are obtained as displayed in Fig. 30 (d). In addition to the shape of the cathode, there have also been studies into the removal of areas by thin layers of electrolyte (Ao et al., 2019). The typical evolution of the metal rod shape with increasing machining time is shown in Fig. 30 (e). A high aspect ratio (195.47) micro-tool with an average diameter of 24.3 μm and good surface quality is fabricated successfully with the help of the liquid

membrane (Fig. 30f and 30g).

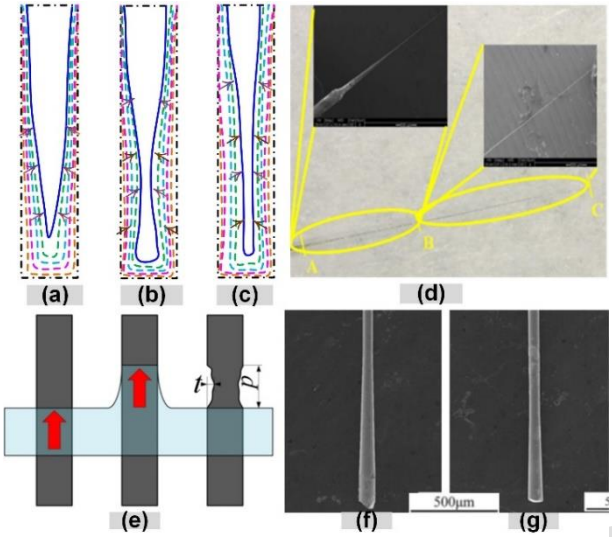

Fig. 30. Typical geometries of the micro-tools machined by the workpieces under the different highest positions (Y_0): (a) Y_0=100 μm, and (b) Y_0=-150 μm (Chiou et al., 2012). (c) Typical geometries of the micro-tool machined at optimal parameters; (d) A high aspect ratio (450) micro-tool machined by the pulsed ECM (Mathew and Sundaram, 2012). (e) Mechanism of the ECM-based liquid membrane method; (f) Tool-tips fabricated using the thickness of electrolyte of 250 μm; (g) Tool-tips fabricated using the thickness of electrolyte of 500 μm (Ao et al., 2019).

The high-aspect-ratio cylindrical tool with nano-tips can be machined by using a liquid membrane in ECM, as shown in Fig. 31(a). At first, a meniscus forms at the rod/electrolyte interface when the rod is located at the center of the circumferential cathode. The shape of the meniscus determines the profile of the etched material on the anodic rod within the liquid membrane (Wang et al., 2013; Wu et al., 2020b). As the anodic rod moves upward and downward periodically, an inverse conical shape forms on the lower end of the rod. The diameter of the rod becomes so tiny that the lower part drops off. As a result, the lower part is used as the fabricated nano-tip tool (Wang et al., 2016c). From the experimental result, small voltage and low electrolyte concentrations lead to improvements in the aspect ratio, uniformity of the diameter, and decreasing the average diameter. A sub-micrometer tool with an average diameter of 140.8 nm and an aspect ratio of 50 was successfully obtained (Zeng et al., 2013), as shown in Fig. 31(b) and 31(c).

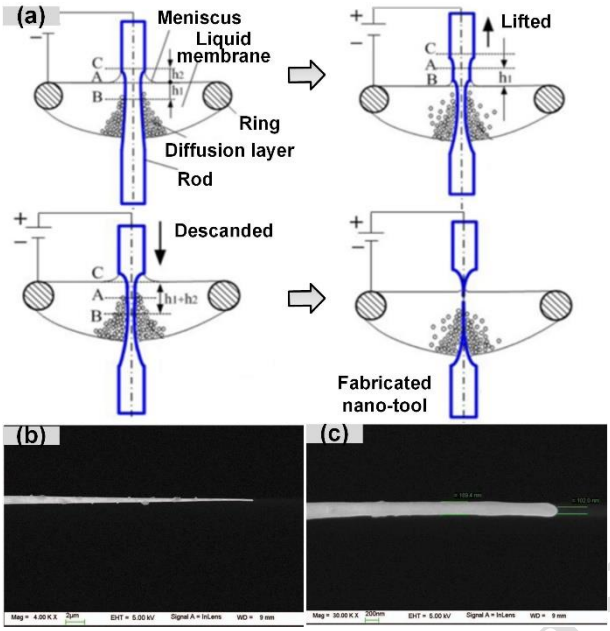

Fig. 31. (a) A schematic of the machining process using liquid membrane ECM when the straight reciprocating motion is applied to the tool; (b) Machined high-aspect-ratio sub-micrometer tool; (c) Enlargement of the tool tip (Wang et al., 2013; Zeng et al., 2013).

5.2.3 Wire electrochemical grinding (WECG)

WECG uses a moving wire cathode, and the micro-tools are processed by a radial and axial feed motion with a metal rod. Han and Kunieda (2018, 2020) proposed a WECG method for the preparation of tungsten micro-tools using a neutral electrolyte and a bipolar current. Processing parameters such as the motion rate of the wire cathode, the material, the diameter of the wire, the speed of the metal rod, and the shape of the guide affect the maximum length and accuracy of the machined micro-tool. As the feed rate increases, both axial and radial gaps decrease. Compared with the rod fed in the axial direction method, the current efficiency was lower due to the stronger influence of the stray current flowing through the side and end surface of the machined micro-rod. The pattern of change in the shape of a metal rod is shown in Fig. 32(a). The shape of the micro-tool changes as a result of the different feed directions (Fig. 32b and 32c). With the WECG method, the minimum rod diameter of 11 μm was obtained with a high aspect ratio of 36 (Fig. 32d and 32e), since the influence of tool wear caused by the bipolar pulse current was eliminated with the winding wire cathode, realizing micromachining ability equivalent to micro-EDM method.

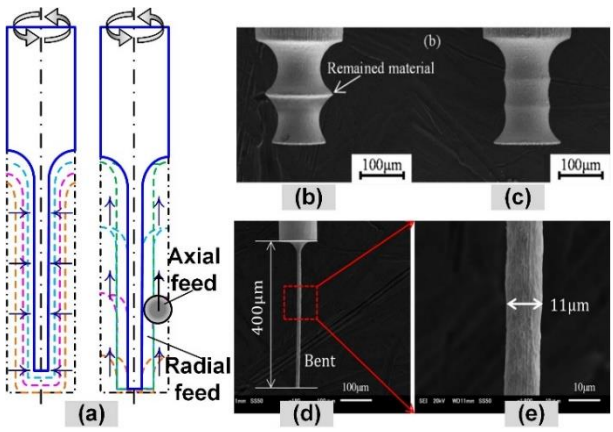

Fig. 32. (a) Typical geometries of the micro-tools machined by WECG; micro-rods machined with different feed intervals (b) 100 μm, (c) 50 μm (Han and Kunieda, 2018); (d) Micro-tool with a minimum diameter of 11 μm; (e) Enlargement of the tool tip (Han and Kunieda, 2020).

5.3 Template lithography-based methods

The use of the photolithography technique enables the preparation of patterns on micro and even nano scales. High-precision micro-tools can be achieved by means of subsequent electroforming and deep etching processes. Ma (2010) has presented a LIGA process for the preparation of array micro-tools with various cross-sectional shapes. X-ray exposure of the polymethyl methacrylate (PMMA) photoresist results in a photoresist structure with a mask pattern (tool cross-sectional shape). By performing the electroforming process, nickel columnar tools with tool bases were obtained to improve the strength and integrity of the array micro-tools, as illustrated in Fig. 33(a). Micro-tools with a dimension of 100 μm, an aspect ratio of 8, and an array of 11×11 were prepared for use as micro-tools for micro-ECM in Fig. 33(b) and 33(c).

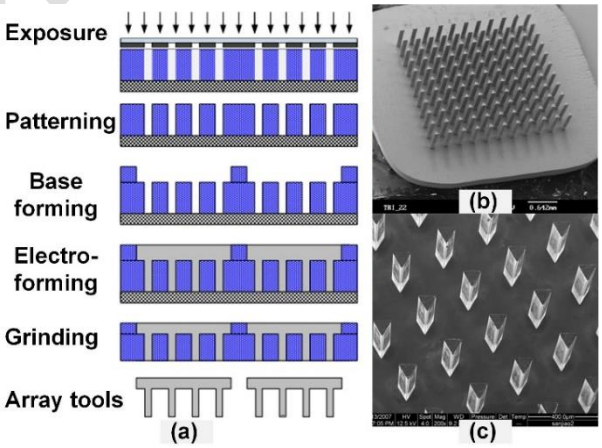

Fig. 33. (a) A LIGA process for the preparation of array micro-tools; (b) Array tools; (c) Details of the array tools with the cross-section of triangular (Ma, 2010)

Liu et al. (2020b) have presented a fabrication process of silicon-based micro-tools based on MEMS technology, where the micro-tool shape is patterned on a silicon wafer by photolithography. The silicon-based tool body was fabricated by wet etching, and metal films were deposited by a sputtering process to increase the electrical conductivity to reduce the contact resistance (Fig. 34a). As a result, silicon-based tools (Fig. 34b and 34c) with dimensions of 86 ×54 μm and 800 nm thick SiO_2 and Si_3N_4 films are successfully fabricated and used in micro-ECM processes.

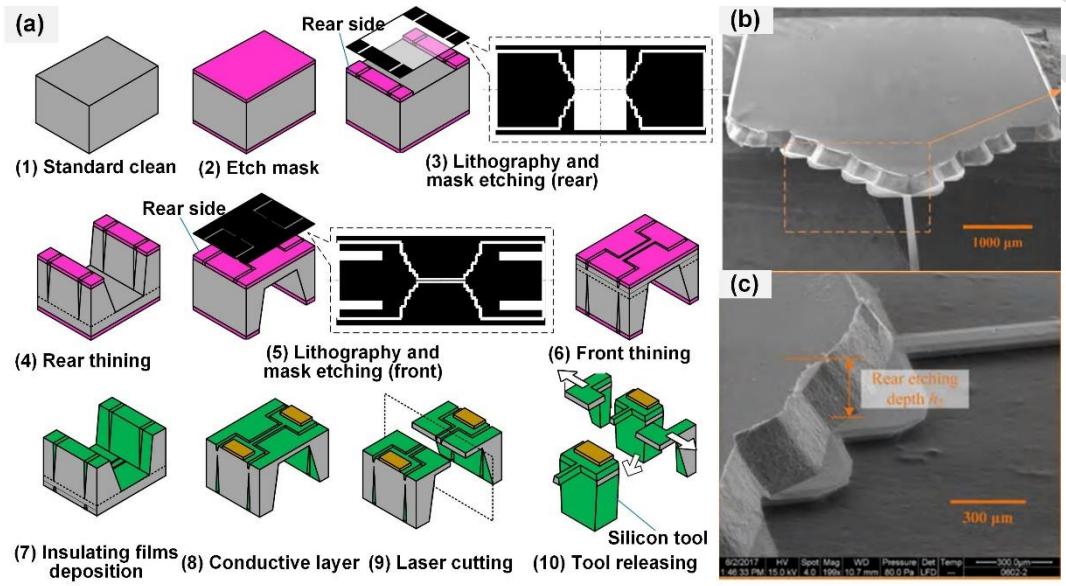

Fig. 34. (a) Fabrication process of silicon-based micro-tools; (b) Silicon-based micro-tool; (c) Details of the micro-tool (Liu et al., 2020b).

5.4 Combined fabrication process

5.4.1 Combined process of micro-turning and EDM-based procedures

Micro-turning offers high machining efficiency, but the cutting forces cause the deformation of the micro-tool especially when the tool diameter is less than 100 μm. EDM-based techniques can machine micro-tools without subjecting them to cutting forces, but their efficiency is very low. Therefore, the combined process of micro-turning and micro-EDM can fabricate micro-tools and eliminates all downsides of the sacrificial electrode fabrication methods. On specially designed machines, the micro-tools can be fabricated automatically and efficiently (Rahman et al., 2010). The EDM procedure (WEDG, BEDG, or R-EDM) is performed via the use of a fabricated micro-tool with the required length by micro-turning. CuW tool with a diameter of 45 μm and brass tool with a diameter of 19.3μm (Jahan et al., 2009) were obtained. This process decreases significantly the machining time in comparison to moving BEDG, which takes more than a few hours. Furthermore, this process needs

very little operator interference and is suitable for automation because of the lower error possibility.

5.4.2 Combined process of LIGA and EDM procedures

The LIGA process can form structures characterized by high precision and micro-scale. Negative-type microstructures with array alignment and complex shapes can be formed and act as electrode of the R-EDM procedure with a high degree of conformability. Fig. 35(a) depicts the combined machining procedures of LIGA and R-EDM. Production of many of the negative-type microstructures (Fig. 35b) is performed on an electroplated metal plate. The WC-Co rod is fed into an electrode through EDM to fabricate a micro-tool with a positive type of patterned structure (Takahata et al., 2000). To achieve a consistent cross-section throughout the length, the micro-tool has to be changed prior to the occurrence of its deformation along its thickness between each electrode and the micro-tool. Fig. 35(c) shows a WC-Co micro-tool of the positive type that has a length of 1 mm fabricated by employing three of the serial negative-type microstructures. Besides, the negative-type array structure formed by the LIGA process can also be used for R-EDM of array micro-tools (Hu et al., 2008).

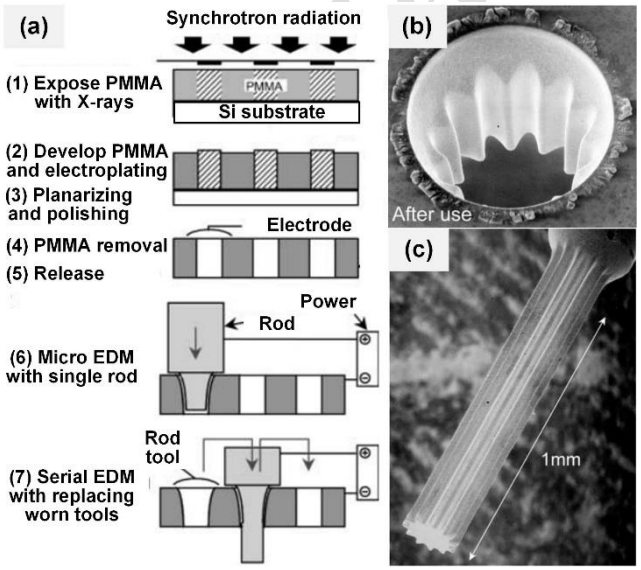

Fig. 35. (a) Flow of microfabrication process combining LIGA and EDM; (b) Negative electrode after R-EDM; (c) 1 mm long WC-Co micro-tool with a gear pattern (Takahata et al., 2000).

5.4.3 Combined process of EDM-based and ECM-based procedures

The electrochemical dissolution process removes the heat-affected defects created by EDM and improves surface quality. Furthermore, the square tool structure machined by WEDM can be electrochemically etched into a smoother edge, forming a near-cylindrical structure or sharp tips (Wang and Zhu, 2008). Fig. 36(a) shows the procedures to fabricate the array of micro-tools with sharp tips.

WEDM processes are used to fabricate micro-tool with 4-μm diameter and 30-μm length. Then, the submicron tips were etched using the ECM process. Fig. 36 (b) illustrates the micro-tool with a 1-μm diameter and 20-μm length. Using a similar process, it is also possible to machine 3×3 arrays of micro-tools as shown in Fig. 36 (c) and 36 (d) (Wang et al., 2016a).

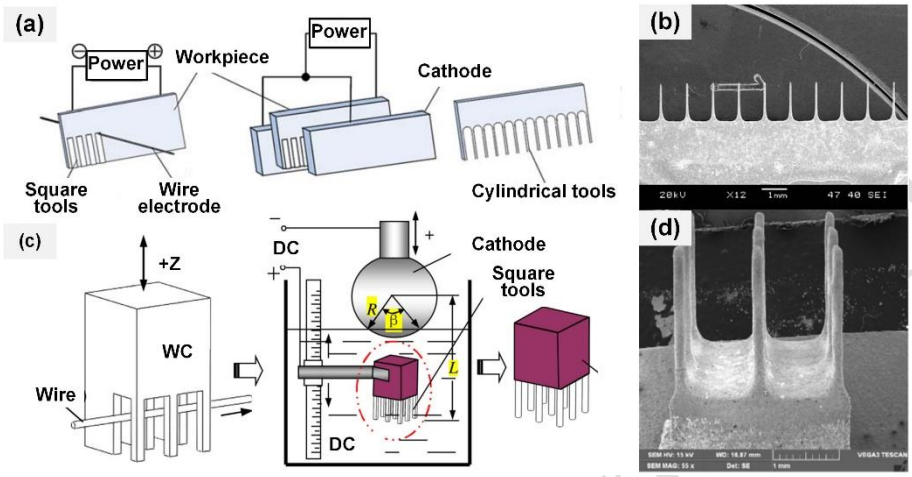

Fig. 36. Fabrication procedure and array micro-tools. Single row micro-tools: (a) Fabrication process; (b) Array tools (Wang and Zhu, 2008). 3×3 array micro-tools: (c) Fabrication process; (d) Array tools (Wang et al., 2016a).

Sheu et al. (2014) have utilized one pulse electro-discharge (OPED) to fabricate spherical-tip micro tools. The OPED process was carried out on the same machine after micro-tools were fabricated by ECM-based procedure. The diameter of spherical tips is possible to predict by controlling the OPED energy, and spherical tips can be coincident by selectable pulse duration and peak current of OPED procedure. Liu et al. (2015) have discussed the effects of the tool polarity, the peak current, the discharge duration, and the gap voltage on the sphere diameters. The diameter of the microsphere of about 60 μm has been obtained.

5.5 Other methods

5.5.1 Electroforming and electrodeless plating

The electroforming process was utilized for forming micro-tools in a layer-by-layer manner (Yin et al., 2014). Fig. 37(a) shows a copper tool deposited in the electrolyte (250 g/l $CuSO_4 \cdot 5H_2O$ + 75 g/l H_2SO_4). In the deposition process, an insulated tool (Pt 90%-Ir 10% alloy) with about 100 μm radius of the tip was obtained. The deposit speed of the micro-tool reaches 5 μm/s (Li et al., 2003). In addition to fabricating the tool substrate, the electroforming process was also used to fabricate the nanoscale features on the micro-tool surface. The surface hydrophobic structure formed by template deposition

helps form a stable gas film on the tool surface, which can isolate stray currents (Zhan and Zhao, 2021). During the fabrication process, polystyrene microspheres with a diameter of 1 μm were arranged to form the monolayer, and copper was deposited to fill the gaps of microspheres by electroforming in Fig. 37(b) (Liu et al., 2022a).

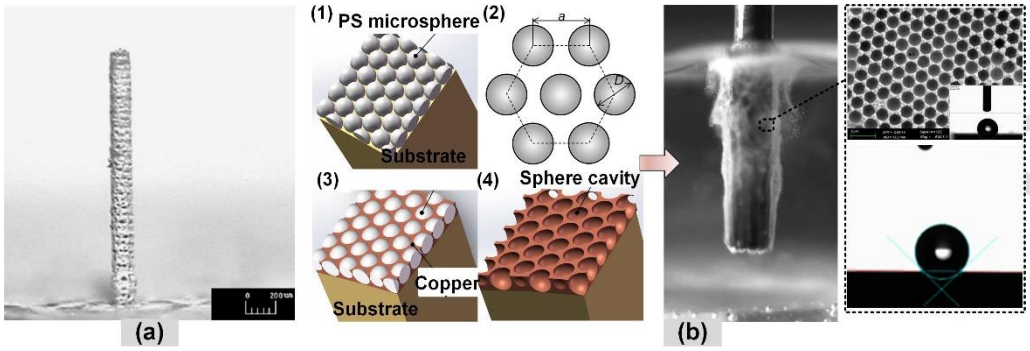

Fig. 37. (a) Electrochemical deposited micro-tool (Li et al., 2003); (b) Tool with the cavities on its surface acting as the hydrophobic features (Liu et al., 2022a).

The electrodeless plating process is suitable for the preparation of thin-film cathode layers and does not require conductive seeds. The connection strength between the coating and the substrate depends on the material and surface morphology of the substrate (Lyubimov et al., 2017). The thickness of the plating is generally controlled by reaction time (Liu et al., 2021a). Zhu et al. (2011) have plated the nickel layer on the abrasive tool used for the M-ECM process. The abrasive particles (diamond particles) in the tool protrude beyond the conductive bond surface (nickel layer). This establishes a small gap between the tool nickel layer and the hole side wall.

5.5.2 Assembly and welding

Metal tubes are usually manufactured in bulk from ductile metal by a drawing process. Special fixtures and spindle designs are required for their conductivity, fluid conduction, and rapid clamping. For micro-tubes with diameters of less than 200 μm, assembly and nesting are utilized for mounting and connecting the liquid path. A tubular tool was prepared by Kong et al. (2015). through a metal tube welding approach, as shown in Fig. 38(a). It was made by layer-by-layer nesting welding of a micro-tube, a support tube, and a large tube. Fig. 38 (b) shows that the tube tool with an outer diameter of 130 μm, an inner diameter of 65 μm, and a length of about 3 mm. For the L-ECM process, Saxena et al. (2020) assembled quartz micro-tubes and stainless steel tubes to synchronize the functions of transferring laser beam and electrolyte. To allow successful insertion without breakage, a 50 μm allowance has been used. This gap was filled with transparent UV-curing glue. Inside the tool, the laser

propagates by means of multiple diffuse and specular reflections from the internal metallic surface (Saxena et al., 2020a, 2020c), as illustrated in Fig. 38(c).

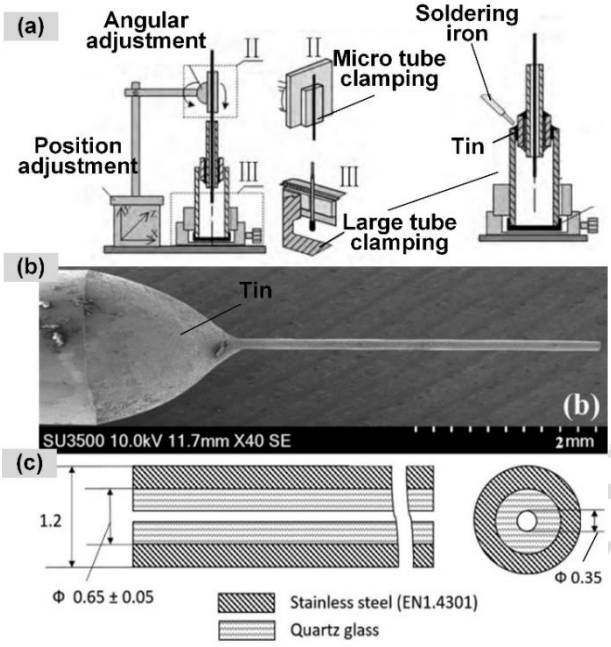

Fig. 38. (a) Fabrication procedure for the micro-tools using a welding method (Kong et al., 2015); (b) A micro-tubular tool (Saxena et al., 2020c); (c) Sketch of the hybrid tool for L-ECM processes (Saxena et al., 2020b).

5.5.3 Laser micromachining and micro-milling

Short-pulsed lasers can be used to create microscale surface textures and features on the tool cathode which can be replicated onto the workpiece through ECM. Fang et al. (2020), fabricated two and three-dimensional patterns on the tool cathode through nanosecond pulsed laser machining. Grooves of 50 μm height and 73 μm width, half-spheres of 34 μm height and 132 μm diameter, and hexagonal shapes of 7 μm height, 82 μm side length and 8˚ slope angle were used as test features on the tool and were validated by using an industrial pulsed-ECM machine. However, there were some deviations in the replication precision of PECM due to the molten materials on the periphery of cathode features, which requires higher frequency pulsed lasers like pico- and femtosecond lasers to minimize these defects. ECM tools with simple shapes can also be manufactured through micro-milling and lithography in the case of shaver slots (Silva et al., 2000), square holes, and optical structures.

6. Fabrication processes of sidewall-insulated films

6.1 Thin-film deposition method

SiO_2, Si_3N_4, and SiC are ideal materials for insulating films. In MEMS technology, the process of

preparing these silicon-based films using CVD techniques is relatively well-developed. The batch preparation of silicon-based insulating films with sub-micrometer thickness can be achieved by arranging micro-tools vertically or horizontally in suspension within the vapor deposition chamber as displayed in Fig. 39(a). The first application of silicon-based films was in a macro-scale ECM process. A SiC-Si_3N_4-SiC structural film with a total thickness of 13.4 μm on a molybdenum tool was deposited (Osenbruggen and Regt, 1985). Li et al. (2003) applied the CVD technique to deposit the SiC film on the tungsten tools with a diameter of approximately 200 μm. In addition, insulating films consisting of the parylene C and diamond were also prepared using the deposition process. In the study by Ferraris et al. (2013), the coating thickness of the parylene C layer on tungsten carbide tools could be controlled within 2-5 μm on dedicated equipment, resulting in a tool diameter within 128-136 μm (Fig. 39b and 39 b). Tang et al. (2017) deposited the diamond coating layer on the tool surface using the hot filament chemical vapor deposition (HFCVD) method. The diameter of the micro-tool body is 250 μm, and the diamond coating layer has a thickness of 4 μm.

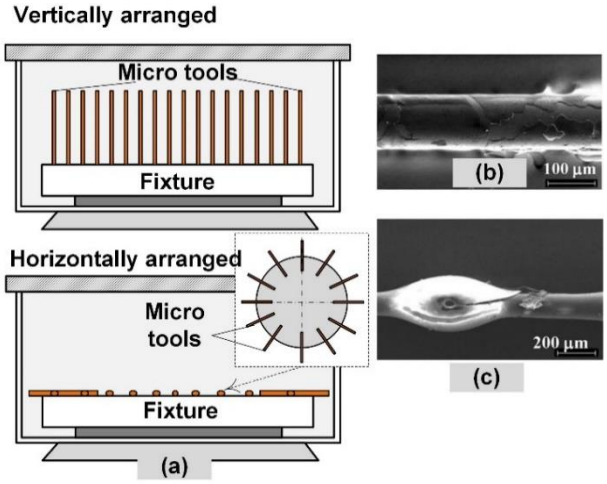

Fig. 39. (a) Schematic of the insulating film deposition process by CVD; (b) Delaminated ceramic coating; (c) Polymer drop on a parylene C coated tool (Ferraris et al., 2013).

6.2 Adhesive material coating method

Silicone, epoxy, and polyester resin-based materials have excellent insulating properties. Their liquid form can cling to the tool substrate and its shape changes with the tool feature. After curing, the coating materials have excellent corrosion resistance and strength. Coating methods such as drop coating, spin coating, and lift coating have been validated, consisting of the procedure of adhesive-material coating, curing, and end-face treatment in sequent.

Fig. 40(a) shows a diagram of the drop-coating process. The spindle rotates the tool substrate at

high speed, and the adhesive materials with the appropriate viscosity and flowability are applied to the tool substrate from the sides downwards (Jo et al., 2009). The tools covered by the coating film are then left to cure in a ventilated area. Depending on the type of adhesive materials, curing can also be carried out by heat or UV light. The thickness of the coating film can be adjusted by optimal parameters such as rotating speed, moving rate, and extrusion pressure, but the uniformity is poor. The use of high-speed rotation to improve the homogeneity of the resin layer by centrifugal force has also been investigated. However, the centrifugal force is small and the effect is limited due to the tiny diameter of the micro-tools. Park et al. (2006) applied a 3 μm thick layer of enamel to the surface of a micro-tool with a diameter of 60 μm by applying diluted enamel dropwise, as shown in Fig. 40(b). The enamel proved to be resistant to most chemicals and was suitable for the preparation of insulating films for micro-tools for micro-ECM.

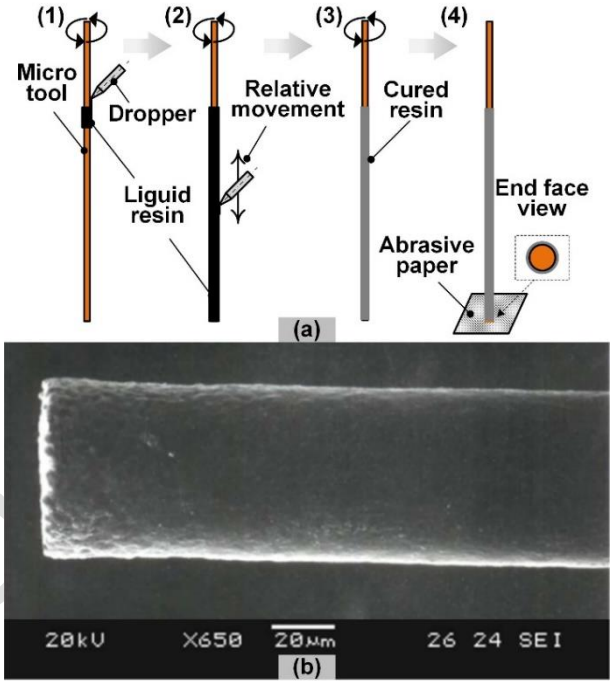

Fig. 40. (a) Schematic diagram of the drop-coating process; (b) Sidewall-insulated tool with enamel coating (Park et al., 2006).

In contrast to the drop-coating method, the micro-tools are placed horizontally in the spin-coating method (Fig. 41a). The thickness of the insulating film can be precisely adjusted by using optimized process parameters, such as the viscosity, the rotating speed, and the coating time. As the tools are further away from the rotating center, the adhesive materials are thrown off the tool substrate by the appropriate centrifugal force, thereby thinning the insulating film and improving its homogeneity. Liu

et al. (2009) determined the optimum values for the spin-coating process parameters through orthogonal experiments. With a rotating speed of 1000 rpm, and a coating time of 17 min, the sidewall insulating film with a thickness of 3-8 μm was prepared, as illustrated in Fig. 41 (b). The spin coating method can also be applied to the preparation of insulating films for array micro-tools. The disadvantages of this method are a large amount of wasted resin and the fact that it is not suitable for tube tools.

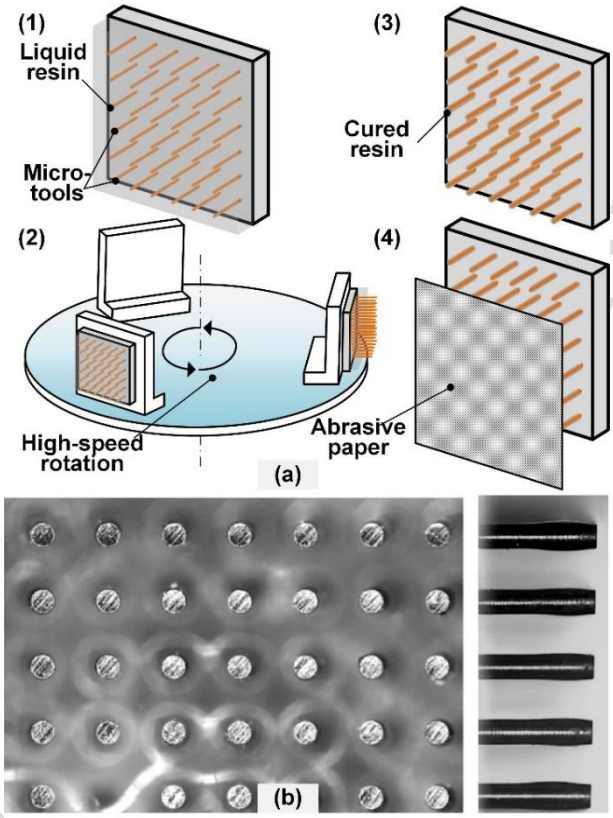

Fig. 41. (a) Schematic diagram of the spin-coating process; (b) Sidewall-insulated array tools with polished end face polishing (Gaihong et al., 2009).

A schematic diagram of the lift-coating process is shown in Fig. 42(a). The sidewall of the micro-tool was in-situ insulated by dipping the tool in an insulating solution. Micro-tool to be insulated was moved downward at high speed, retracted back immediately, and dried in air at room temperature. The thickness of the insulating film can be defined by the prefabricated hole. Rathod et al. (2014) have presented the lift-coating method for micro-tools using a liquid solution made of polymer and resin dissolved in isopropyl alcohol and the use of acetone for opening the front end of the micro-tool. This method can also be used to remove the previously applied coat completely so that the micro-tool can be reinsulated again for reuse. In-situ fabricated tungsten micro-tool of 104 mm diameter was insulated

with 4.5-mm thick film, as illustrated in Fig. 42(b).

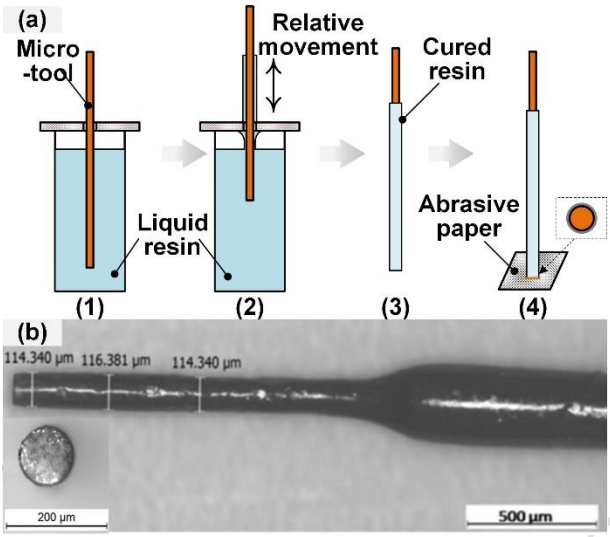

Fig. 42. (a) Schematic diagram of the lift-coating process; (b) In-situ fabricated micro-tool with an insulating film (Rathod et al., 2014).

6.3 Micro-arc oxidation and electrophoresis coating method

Micro-arc oxidation (MAO) is commonly used to modify the surface of aluminum, magnesium, titanium, and their alloys with an oxidation ceramic coating. In the MAO process, the specimens as a positive pore are immersed in a certain solution, the electrolytic bath as the negative pore is filled with electrolyte, and a large number of micro-arc discharges caused by dielectric breakdown of oxide coatings, occurring on the entire tool surface when the supplied voltage is higher than a critical value (Fig. 43a). By combining the MAO and cathodic electrophoresis coating techniques, the double insulating layers, which consisted of TiO_2 ceramic coating and organic film were fabricated by Wang et al. (2014) (Fig. 43b). Hung et al. (2019) have presented a combined preparation process of hot-dip aluminizing and MAO techniques. To form an effective insulating film on a stainless-steel substrate, an aluminum-rich layer was first formed on the stainless steel surface the aluminum-rich layer, then it was converted into an aluminum oxide insulating layer through MAO.

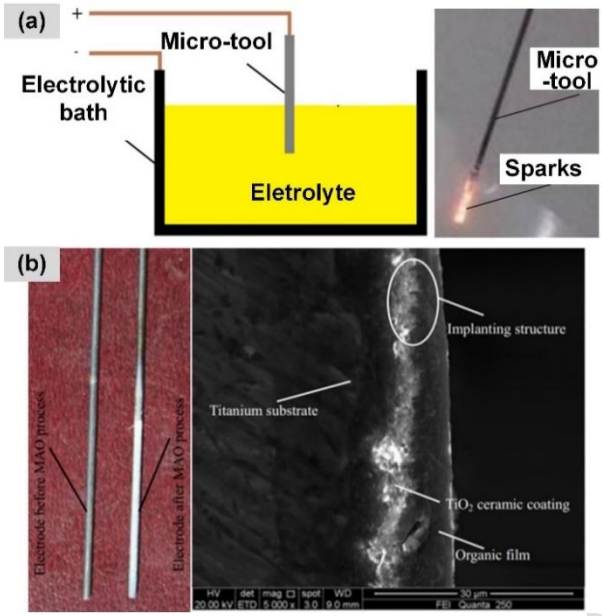

Fig. 43. (a) A micro-tool during the metal arc oxidation (MAO) treatment; (b) Micro-topography of the cross-section of the micro-tool (Wang et al., 2014).

6.4 Insulating-tube nesting method

This method uses an insulating tube with the same or slightly larger inner diameter which is assembled and mounted on the outside of the micro-tool. It is a simple way of preparing the insulating film, as shown in Fig. 44(a). The difficulty lies in selecting the right tube material and size, which is limited by the manufacturing process of the insulating tube. It usually has a thick wall and is difficult to apply for processing 3D microstructures. Currently, there are polyimide and glass tubes being used for the nesting method (Li and Hu, 2013; Liu et al., 2021b) (Fig. 44 b). The advantages of this method are the simplicity of the process, the uniform wall thickness of the insulation layer, and its suitability for tube micro-tools, but it is difficult to achieve automation and batch preparation.

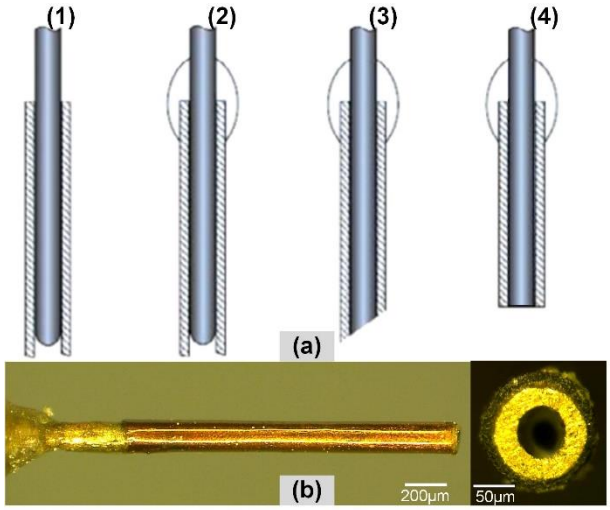

Fig. 44. (a) Schematic diagram of the tube nesting process (Li and Hu, 2013); (b) A sidewall-insulated tube micro-tool (Liu et al., 2021b).

7. Scopes on future directions

Although some progress has been made in the structural design, material selection, and preparation of micro-tools for micro-ECM, there exists a huge potential for tooling development in the field of micro-ECM.

7.1 Using additive manufacturing (AM) to fabricate customized tools

With the advancements in AM techniques for the metals, it is possible to develop customized micro-tools for the ECM process which was not possible or very difficult in the past. This includes tools with complex shapes, customized flushing channels, and porous tools (Hwang et al., 2020). In a recent work by Koyano et al. (2022), an ECM tool with a porous structure was fabricated by the laser powder bed fusion process (Fig. 45 a). With microscale pores, the machined surface becomes free of residual unmachined features. Through these pores, the high-pressure electrolyte is supplied inside the IEG. An array of micro tube tools (Fig. 45 b) was also achieved using the AM process. The material is stainless steel 316L and the tools have an outer diameter size of approximately 800 μm and an inner diameter of approximately 300 μm. The AM method has unique advantages for forming complex-shaped microfabrication electrodes, but its rough surface may affect the quality of the process and therefore needs to be further explored in the future in terms of printing resolution with metal powders.

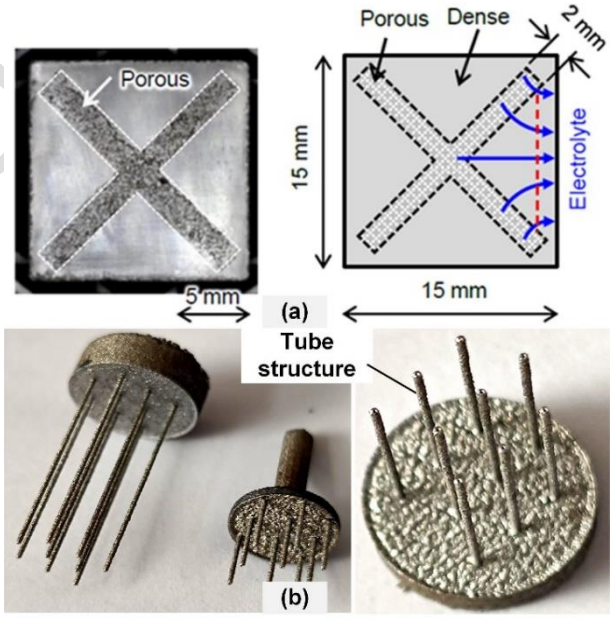

Fig. 45. (a) A porous ECM tool of square cross-section fabricated by laser powder bed fusion (Koyano et al., 2022); (b) Tubular micro-tools fabricated by AM.

7.2 Soft-actuators as ECM tools

To realize the micro-ECM process of complex geometries, difficult-to-reach locations and internal features, the soft actuators can be exploited as ECM tools (Uchiyama and Kunieda, 2013). The soft-actuators possess a unique combination of compliance, and flexibility in positioning and can be controlled by air/fluid flow. This is beneficial for applications involving surficial machining with limited precision. Fig. 46(a) shows the initial development of soft actuators for the ECM process and Fig. 46(b) shows an actuator for polishing the inside surface of cylindrical workpieces (De Smet et al., 2023).

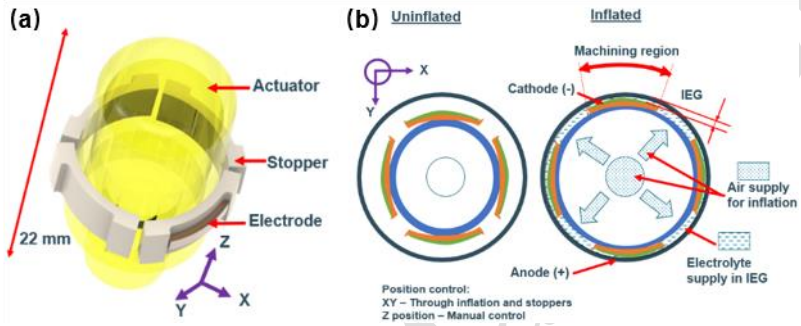

Fig. 46. (a) Prototype of an inflatable actuator for ECM on an internal cylindrical surface (b) Schematic of the electrochemical machining process with soft-actuator (De Smet et al., 2023).

7.3 In situ efficient fabrication of micro-tools and insulating films

The transfer and secondary clamping of micro-tools damage their positioning accuracy. Tool corrosion, wear, or insulation failure also deteriorates the ECM process. In-situ fabrication and repair of the substrate and insulating film of micro-tools are therefore essential. With micro-tools, there come other practical challenges such as micro-tool clamping/holding in spindle while supplying electrolyte internally at higher electrolyte pressures. It is challenging to control tool-runout with micro-tools and maintain concentricity with the rotation axis. It is easy to integrate EDM-based tool fabrication in a micro-ECM setup. Based on the WEDG or R-EDM processes, the in-line dressing of the tool to achieve the required dimensions and desired surface quality can be achieved by switching the type of working fluid, the polarity, and the power supply. The difficulty lies in the rapid creation of dimensional and references positioning models for micro-tools, as well as the development and optimization of process parameters and machining trajectories in process solutions. Additionally, there is a need for further research on in-line preparation techniques for sidewall insulating films. It is unacceptable to guarantee the functionality of the micro-tools by removing them for the offline repair of the insulating film or

replacing them during the process. The study of in-situ and rapid preparation techniques for tool substrate and sidewall insulating film will be a future trend.

7.4 Virtual tool design

With the trend of sustainable manufacturing, it is important to cut down the costs, lead times, and material wastage associated with tool design and fabrication. For general ECM processes (Jain and Rajurkar, 1991) and freeform surfaces (Sun et al., 2006) finite element simulation models have provided reliable results for designing the tool shape, surface patterns, and dimensions by taking into account generic ECM phenomena like flow field, temperature distribution, side gap, potential/current density distribution, edge effects, electrolyte conductivity, etc. These models have also been successfully applied for developing micro-ECM tools for complex internal micro-features (Mi and Natsu, 2017) which can reduce the needed experimental validations but not eliminate them, since it is challenging to accurately incorporate the complex multi-physical gap phenomenon of micro-ECM for precise tooling shape and dimensions prediction. These challenges are even more pronounced when developing hybrid ECM tools as certain physical phenomena still lack complete understanding. Recent developments in machine learning seem interesting for employing the methodology to design the tool shape, dimensions, and coatings by specifying the required ECM feature. However, extensive experimental runs are needed to make a reliable machine learning model for a specific application which seems excessive at first, but in the future, it might help eliminate the experimental costs and material wastage with improved tool dimensional accuracy after reliable models are developed.

7.5 Exploring new materials, methods, and novel functions

The experimentation and validation of micro and nano-tools such as carbon tube fibers and heavily-doped silicon, break away from the conventional thinking of using metals as micro-tools. The creation and development of these new materials can help researchers design and fabricate special tools with smaller sizes and more complex shapes. Similarly, new micro-tools made from 3D-printed plastics and chemically plated films as cathodes are challenging the conventional thinking of using metallic materials as substrates. With the help of AM processes, MEMS technology, and focused ion deposition, the preparation of new tools of special shapes and materials will play an even greater role in the exploration of processes and mechanisms for the micro-ECM process. In recent years, micro-tools with composite functions have attracted a lot of attention and research (Lu et al., 2022). The use of a tubular tool structure that combines electrical conductivity, light transmission, internal liquid

supply, and side-wall insulating functions is a typical application that will also be further explored in depth in the future and will open new avenues of applications that were difficult or impossible before. Based on the micro-tool made of silicon materials, the preparation of silicon-based tools with sensing, detection, and wireless transmission functions, and their application in micro-ECM and its hybrid processes also have a wide scope of imagination.

7.6 Nano-scale/downscaled tools

For the fabrication of a sub-micrometer tool with a high aspect ratio or smaller dimensions, the available machining methods are usually adopted from the integrated circuits industry such as lithography, LIGA, and focused ion beam machining. The static liquid membrane ECM process has been adopted to prepare conical-shaped tools with a tip radius of several dozen or even several nanometers. The reduction of machinable dimensions down to a few micrometers can be realized by using specialized downscaled tools such as single, multiple, and braided carbon nanotubes as tools (Meng et al., 2020), conductive AFM tips (Malshe et al., 2010), STM tips (Ju et al., 2009), and Fluid FM® tips (Hirt et al., 2015) with an integrated microfluidic channel to dispense electrolytes for micro/nanopatterning and deposition. Inspired by nanotechnology and nanoengineering, all these are under extensive research to be used as ECM tools.

7.7 Further developments of composite or hybrid tools

The ongoing developments towards hybrid and sequential manufacturing (micro) processes have also necessitated developments of composite or hybrid tooling approaches. This implies that a single tool has to serve several purposes instead of the traditional function of supplying one process energy. Some of the examples where further developments of composite or hybrid tools include (1) tools capable of supplying multiple process energies (such as laser, electrochemical reactions, ultrasonic vibrations, etc.) in the same machining zone, (2) tools capable of doing on-machine metrology (Bisterov et al., 2022), and (3) tools that can do both electrochemical subtractive and additive manufacturing on the same machining axis.

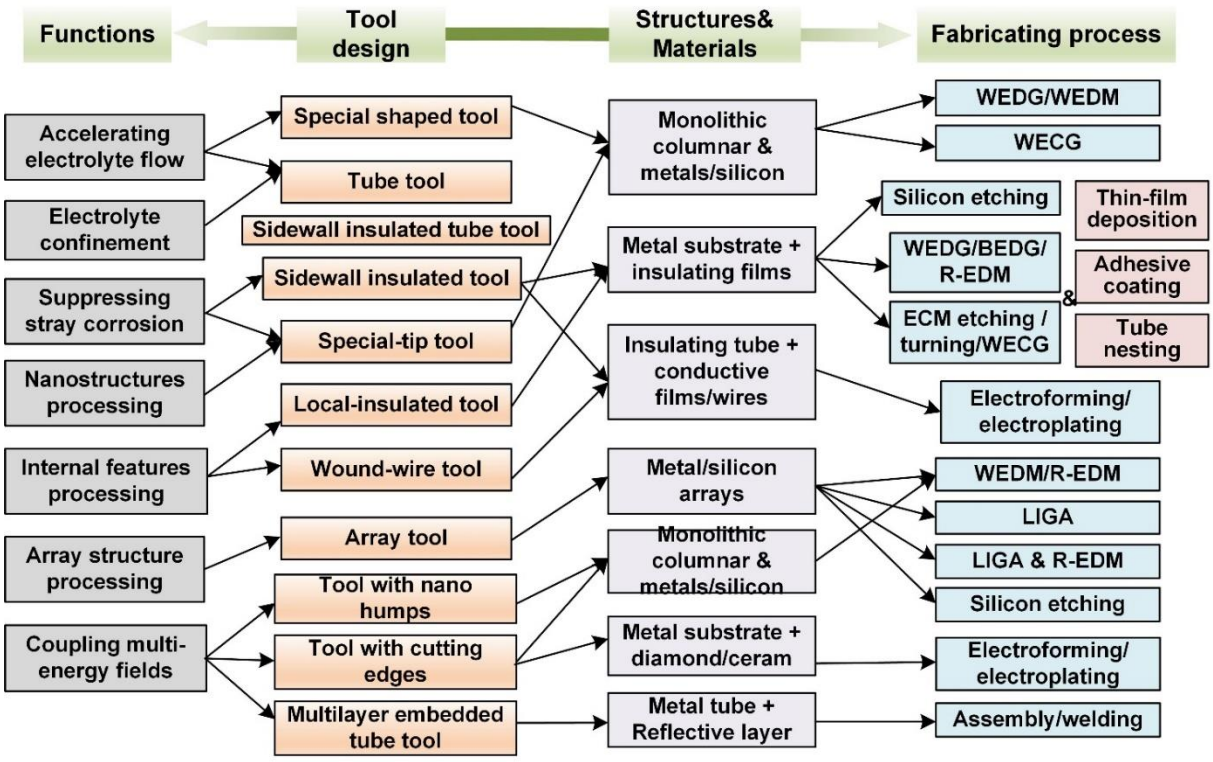

Fig. 47. A summary of the relationships between tool functions, structures, materials, and fabrication processes.

8. Conclusions and summary

This review article has focused on the tooling aspects of micro-ECM technology which was not exhaustively covered in the existing state-of-the-art. The achievable dimensions as well as shape precision depend on the micro-tool in micro-ECM processes apart from other parameters such as flow-field, side IEG, etc. In order to develop novel tool designs and their fabrication routes, several cross-innovations are required alongside inspiration from adjacent technologies such as micro-EDM. A tool in micro-ECM not only serves as a cathodic electrode but it serves several important functions such as facilitating electrolyte flow, suppression of stray machining, facilitating process localization, machining of an array or complex internal features, online monitoring, local electrolyte confinement, and achieving multi-energy field coupling. The micro-ECM tool design which is supported by simulation and experimental validations requires additional functionality-specific modifications. Metals or alloys are the most common materials for micro-tools for micro-ECM, such as brass, tungsten, tungsten carbide, stainless steel, platinum, titanium, nickel, and molybdenum along with side insulation coatings. Non-metal conductive materials such as graphite, silicon, and CNT are also feasible as micro-tools. The major fabrication routes for micro-tools for the micro-ECM process are (i)

EDM-based processes such as WEDG, D-EDG, BEDG, R-EDM, and WEDM process, (ii) Electrochemical etching (iii) Electrochemical turning, (iv) Wire electrochemical grinding, (v) Lithography based processes, (vi) Combined process such as EDM and ECM, and (vii) micro-milling and laser-based fabrication (viii) Other processes such as electroforming, electrodeposition, and assembly/welding. Therefore, this article covers a wide spectrum of knowledge on the micro-tools (as summarized in Fig. 47 for the micro-ECM process and will be a useful reference for researchers.

For now, the fabrication processes of micro-tools are not yet upscaled for large-scale production. Tooling costs are still high. With rapid developments in AM, laser micromachining, soft-robotic actuators, and nanomanufacturing technologies, it is possible to fabricate advanced tools for micro-ECM processes such as using AM process to make micro-tools, laser surface structuring of hydrophobic features on tool periphery to suppress stray machining or using soft actuators for surficial machining and using AFM tips, CNTs, and custom probes as downscaled tools. Besides, in the future, tool design for micro-ECM and hybrid ECM processes also requires improved simulation and machine-learning models to reduce costs, material waste, and lead times.

Data availability statement

The data used to support the findings of this study are available from the corresponding author upon request.

Acknowledgments

This work was supported by the National Natural Science Foundation of China [grant number 52205439], Research Foundation Flanders (FWO) postdoctoral mandate [grant number 12ZZ622N], Beijing Institute of Technology Ben Yuan funding, Basic scientific research projects of state administration of science of China [grant number JCKY2021204A006], and FWO senior research project fundamental research [grant number G099420N].

Declaration of Interest statement

The authors declare that they have no known competing financial interests or personal relationships that could have appeared to influence the work reported in this paper.

CRediT author statement

Guodong Liu: Conceptualization, Methodology, Software, Writing - Original Draft, Writing - Review & Editing, Visualization. **Md Radwanul Karim**: Writing - Original Draft,

Methodology. **Muhammad Hazak Arshad**: Validation, Investigation. **Krishna Kumar Saxena:** Writing - Review & Editing, Formal analysis. **Wei Liang:** Validation, Investigation**. Hao Tong**: Methodology, Data Curation. **Yong Li:** Supervision, Funding acquisition. **Yuxin Yang**: Writing - Review & Editing. **Chaojiang Li:** Conceptualization, Resources, Writing - Review & Editing. **Dominiek Reynaerts:** Supervision, Project administration.

References

Ahn, S.H., Ryu, S.H., Choi, D.K., Chu, C.N., 2004. Electro-chemical micro drilling using ultra short pulses. Precis. Eng. 28, 129–134.

Ao, S., Li, K., Liu, W., Xu, J., Dai, Y., Qin, X., Luo, Z., 2019. Electrochemical micro-machining of high aspect ratio micro-tools with a reverse conical shape tip using electrolyte liquid membrane. Int. J. Adv. Manuf. Technol. 105, 1447–1455.

Arab, J., Kannojia, H.K., Dixit, P., 2019a. Effect of tool electrode roughness on the geometric characteristics of through-holes formed by ECDM. Precis. Eng. 60, 437–447.

Arab, J., Mishra, D.K., Kannojia, H.K., Adhale, P., Dixit, P., 2019b. Fabrication of multiple through-holes in non-conductive materials by Electrochemical Discharge Machining for RF MEMS Packaging. J. Mater. Process. Technol. 271, 542–553.

Arab, J., Pawar, K., Dixit, P., 2021. Effect of tool-electrode material in through-hole formation using ECDM process. Mater. Manuf. Process 36, 1019–1027.

Bellotti, M., Wang, Y. Q., Li, Z., Qian, J., Reynaerts, D., 2021. Fabrication of tapered micro rods using twin static wire electrical discharge grinding process, CIRP Conference on Electro Physical and Chemical Machining, Zurich, pp. 499–504.

Bhattacharyya, B., Doloi, B., Sridhar, P., 2001. Electrochemical micro-machining: new possibilities for micro-manufacturing. J. Mater. Process. Technol. 113, 301–305.

Bhattacharyya, B., Munda, J., Malapati, M., 2004. Advancement in electrochemical micro-machining. Int. J. Mach. Tools Manuf. 44, 1577–1589.

Bian, J., Ma, B., Ai, H., Qi, L., 2021. Experimental Study on the Influence of Tool Electrode Material on Electrochemical Micromachining of 304 Stainless Steel. Materials 14.

Ceylan1, H., Dogan, N.O., Yasa, I.C., Musaoglu, M.N., Kulali, Z.U., Sitti, M., 2021. 3D printed personalized magnetic micromachines from patient blood–derived biomaterials. Sci. Adv. 7, eabh0273.

Chak, S.K., Venkateswara Rao, P., 2007. Trepanning of Al2O3 by electro-chemical discharge machining (ECDM) process using abrasive electrode with pulsed DC supply. Int. J. Mach. Tools Manuf. 47, 2061–2070.

Chang, Y. J., Ho, C. C., Hsu, J. C., Hwang, T. Y., Kuo, C. L., 2015. Atmospheric dual laser deposited dielectric coating on electrodes for electrochemical micromachining. J. Mater. Process. Technol. 226, 205–213.

Chen, S. T., 2008. Fabrication of high-density micro holes by upward batch micro EDM. J. Micromech. Microeng. 18, 085002.

Cheng, C. P., Wu, K. L., Mai, C. C., Yang, C. K., Hsu, Y. S., Yan, B. H., 2010. Study of gas film quality in electrochemical discharge machining. Int. J. Mach. Tools Manuf. 50, 689–697.

Chiou, Y. C., Lee, R. T., Chen, T. J., Chiou, J. M., 2012. Fabrication of high aspect ratio micro-rod using a novel electrochemical micro-machining method. Precis. Eng. 36, 193–202.

Clare, A.T., Speidel, A., Bisterov, I., Jackson Crisp, A., Mitchell-Smith, J., 2018. Precision enhanced electrochemical jet processing. CIRP Annals 67, 205–208.

Collett D E, Hewson-Browne R C, Windle D W, 1970. A Complex Variable Approach to Electrochemical Machining

Problems. J. Eng. Math. 4. 29–37.
Dabbagh, S.R., Sarabi, M.R., Birtek, M.T., Seyfi, S., Sitti, M., Tasoglu, S., 2022. 3D-printed microrobots from design to translation. Nat. commun. 13, 5875.
De Smet, Elias, Arshad, Muhammad Hazak, De Meester, Andreas, Saxena, Krishna Kumar, Gorissen, Benjamin, Reynaerts, Dominiek, Elastic inflatable soft actuators for electrochemical machining on internal surfaces of metallic workpieces, Proceedings of euspen's 23rd International Conference and Exhibition, Copenhagen, Denmark, June 2023.
Dimov, S.S., Matthews, C.W., Glanfield, A., Dorrington, P., 2006. A roadmapping study in Multi-Material Micro Manufacture. Elsevier.
Egashira, K., Hayashi, A., Hirai, Y., Yamaguchi, K., Ota, M., 2018. Drilling of microholes using electrochemical machining. Precis. Eng. 54, 338–343.
Egashira, K., Mizutani, K., 2002. Micro-drilling of monocrystalline silicon using a cutting tool. Precis. Eng. 26, 263–268.
Fan, Z. W., Hourng, L. W., 2009. The analysis and investigation on the microelectrode fabrication by electrochemical machining. Int. J. Mach. Tools Manuf. 49, 659–666.
Fan, Z. W., Hourng, L. W., Wang, C. Y., 2010. Fabrication of tungsten microelectrodes using pulsed electrochemical machining. Precis. Eng. 34, 489–496.
Fang, S. Q., Ernst, A., Llanes, L., Bahre, D., 2020. Laser Surface Texturing of PECM Tools and the Validation. Procedia CIRP 95, 891–896.
Fang, X., Qu, N., Li, H., Zhu, D., 2013. Enhancement of insulation coating durability in electrochemical drilling. Int. J. Adv. Manuf. Technol. 68, 2005–2013.
Fang, X., Yang, T., Chen, M., Zhu, D., 2020. Fabrication of a Large-aspect-ratio Single-thread Helical Electrode using Multiple Wire Electrochemical Micromachining. Int. J. Electrochem. Sci., 7796–7808.
Ferraris, E., Castiglioni, V., Ceyssens, F., Annoni, M., Lauwers, B., Reynaerts, D., 2013. EDM drilling of ultra-high aspect ratio micro holes with insulated tools. CIRP Annals 62, 191–194.
Fofonoff, T.A., Donoghue, J.P., 2004. Microelectrode array fabrication by electrical discharge machining and chemical etching. IEEE Transactions on Biomedical Engineering 51, 890–894.
Gaihong, L., Yong, L., Xupeng, C., Xiaoyu, M., Xiaogu, Z., 2009. Side Insulation of Tool Electrode and Application in Micro ECM. Electromach. Mold 4, 28–31.
Ghoshal, B., Bhattacharyya, B., 2013. Influence of vibration on micro-tool fabrication by electrochemical machining. Int. J. Mach. Tools Manuf. 64, 49–59.
Goiogana, M., Elkaseer, A., 2019. Self-Flushing in EDM Drilling of Ti6Al4V Using Rotating Shaped Electrodes. Materials 12.
Guo, C., Qian, J., Reynaerts, D., 2017. Electrochemical Machining with Scanning Micro Electrochemical Flow Cell (SMEFC). J. Mater. Process. Technol. 247, 171–183.
Hackert-Oschätzchen, M., Meichsner, G., Zinecker, M., Martin, A., Schubert, A., 2012. Micro machining with continuous electrolytic free jet. Precis. Eng. 36, 612–619.
Han, M. S., Chae, K.W., Min, B. K., 2017. Fabrication of high-aspect-ratio microgrooves using an electrochemical discharge micromilling process. J. Micromech. Microeng. 27, 055004.
Han, M. S., Min, B. K., Lee, S.J., 2008. Modeling gas film formation in electrochemical discharge machining processes using a side-insulated electrode. J. Micromech. Microeng. 18, 045019.
Han, W., Kunieda, M., 2017. Fabrication of tungsten micro-rods by ECM using ultra-short-pulse bipolar current. CIRP Annals 66, 193–196.
Han, W., Kunieda, M., 2018. Wire electrochemical grinding of tungsten micro-rods using neutral electrolyte. Precis. Eng. 52, 458–468.
Han, W., Kunieda, M., 2020. Precision electrochemical machining of tungsten micro-rods using wire electrochemical

turning method. Int. J. Adv. Manuf. Technol. 111, 295–307.

Han, W., Mathew, P.T., Kolagatla, S., Rodriguez, B.J., Fang, F., 2022. Toward Single-Atomic-Layer Lithography on Highly Oriented Pyrolytic Graphite Surfaces Using AFM-Based Electrochemical Etching. Nanomanufacturing and metrology 5, 32–38.

Hansen, H.N., Hocken, R.J., Tosello, G., 2011. Replication of micro and nano surface geometries. CIRP Annals Manufacturing Technology 60, 695–714.

He, S., Tian, R., Wu, W., Li, W., Wang, D., 2021. Helium-ion-beam nanofabrication: extreme processes and applications. International Journal of Extreme Manufacturing 3, 012001.

Hinduja, S and Kunieda, M., 2013. Modelling of ECM and EDM processes. CIRP Annals Manufacturing Technology 62, 775–797.

Hirt, L., Grüter, R.R., Berthelot, T., Cornut, R., Vörös, J., Zambelli, T., 2015. Local surface modification via confined electrochemical deposition with FluidFM. RSC Adv. 5, 84517–84522.

Hu, M., Li, Y., Zhang, Y., Wang, J., Zhu, X., 2013. Experimental Study on Micro Electrochemical Machining with Hydrophobic Side Insulation Electrode. Nanotechnology and precision engineering 11, 348–353.

Hu, Y. Y., Zhu, D., Qu, N.S., Zeng, Y.B., Ming, P.M., 2008. Fabrication of high-aspect-ratio electrode array by combining UV-LIGA with micro electro-discharge machining. Microsyst. Technol. 15, 519–525.

Huh, T.W., Han, G., Ban, W.J., Ahn, H. S., 2017. Efficient fabrication of gold tips by electrochemical etching for tip-enhanced Raman spectroscopy. Int. J. Precis. Eng. Manuf. 18, 221–226.

Hung, J. C., Liu, H. K., Chang, Y. S., Hung, K. E., Liu, S. J., Chen, H. Y., Chen, P. Y., 2014. Development of Electrode Insulation Layer by Using Oxygen Plasma Surface Treatment for Electrochemical Microdrilling. Procedia CIRP 14, 345–348.

Hung, J. C., Liu, Y. R., Tsui, H. P., Fan, Z. W., 2019. Electrode insulation layer for electrochemical machining fabricated through hot-dip aluminizing and microarc oxidation on a stainless-steel substrate. Surf. Coat. Tech. 378, 124995.

Hung, J. C., Tsui, H. P., Chen, P. C., Yang, P. J., 2021. Using a nickel electroplating deposition for strengthening microelectrochemical machining electrode insulation. J. Manuf. Processes 67, 77–90.

Hung, J., Liu, H., Chang, Y., Hung, K., Liu, S., 2013. Development of Helical Electrode Insulation Layer for Electrochemical Microdrilling. Procedia CIRP 6, 373–377.

Hwang, T.W., Kang, N., VanTyne, C.J., Kim, Y. T., Lee, T., Moon, Y.H., 2020. Microforming of fine metallic rods by the selective laser melting of powder. Add. Manuf. 36, 101612.

Ivan Bisterov, Sidahmed Abayzeed, Alistair Speidel, Adam T. Clare, 2022. On-machine measurement with an electrochemical jet machine tool. Int. J. Mach. Tools Manuf. 174, 103859.

Ippolito R, Fasalio G, 1976. The Workpiece Shape in the Electrochemical Machining of External Profiles Using Coated Electrodes. International Journal of Machine Tool Design and Research 16, 129–136.

Jahan, M.P., Rahman, M., Wong, Y.S., Fuhua, L., 2009. On-machine fabrication of high-aspect-ratio micro-electrodes and application in vibration-assisted micro-electrodischarge drilling of tungsten carbide. Proceedings of the Institution of Mechanical Engineers, Part B: Journal of Engineering Manufacture 224, 795–814.

Jain V. K. and Rajurkar K. P., 1991. An integrated approach for tool design in ECM. Precis. Eng. 13, 111-124.

Ji, L., Zhang, Y., Wang, G., Zhang, J., Yang, W., 2021. Performance improvement of high-speed EDM and ECM combined process by using a helical tube electrode with matched internal and external flushing. Int. J. Adv. Manuf. Technol. 117, 1243–1262.

Jo, C.H., Kim, B.H., Chu, C.N., 2009. Micro electrochemical machining for complex internal micro features. CIRP Annals 58, 181–184.

Ju, B. F., Chen, Y. L., Fu, M., Chen, Y., Yang, Y., 2009. Systematic study of electropolishing technique for improving the quality and production reproducibility of tungsten STM probe. Sensor. Act. A Phys. 155, 136–144.

Ju, B.F., Chen, Y.L., Ge, Y., 2011. The art of electrochemical etching for preparing tungsten probes with controllable tip profile and characteristic parameters. Rev. Sci. Instrum. 82, 013707.

Kamaraj, A.B., Sundaram, M.M., 2013. Mathematical modeling and verification of pulse electrochemical micromachining of microtools. Int. J. Adv. Manuf. Technol. 68, 1055–1061.

Kamaraj, A.B., Sundaram, M.M., Mathew, R., 2012. Ultra high aspect ratio penetrating metal microelectrodes for biomedical applications. Microsyst. Technol. 19, 179–186.

Kawafune K, Mikoshiba T, Noto K, Hirata K, 1967. Accuracy in Cavity Sinking by ECM. Annals of CIRP 15, 443–455.

Kim, B.H., Na, C.W., Lee, Y.S., Choi, D.K., Chu, C.N., 2005. Micro Electrochemical Machining of 3D Micro Structure Using Dilute Sulfuric Acid. CIRP Annals 54, 191–194.

Kim, B.H., Park, B.J., Chu, C.N., 2006. Fabrication of multiple electrodes by reverse EDM and their application in micro ECM. J. Micromech. Microeng. 16, 843–850.

Kirchner, V., Cagnon, L., Schuster, R., Ertl, G., 2001. Electrochemical machining of stainless steel microelements with ultrashort voltage pulses. Appl. Phys. Lett. 79, 1721–1723.

Klocke, F., Zeis, M., Klink, A., Veselovac, D., 2013. Technological and economical comparison of roughing strategies via milling, sinking-EDM, wire-EDM and ECM for titanium- and nickel-based blisks. CIRP Journal of Manufacturing Science and Technology 6, 198–203.

Kock, M., Kirchner, V., Schuster, R., 2003. Electrochemical micromachining with ultrashort voltage pulses–a versatile method with lithographical precision. Electrochim. Acta 48, 3213–3219.

Kolhekar, K.R., Sundaram, M., 2018. Study of gas film characterization and its effect in electrochemical discharge machining. Precis. Eng. 53, 203–211.

Kong, Q., LIu, G., Li, Y., Zhou, K., 2015. Preparation of hollow electrode used for micro ECM. Optics and Precision Engineering 23, 2810–2818.

Kong, Q.C., Li, Y., Liu, G.D., Li, C.J., Tong, H., Gan, W.M., 2017. Electrochemical machining for micro holes with high aspect ratio on metal alloys using three-electrode PPS in neutral salt solution. Int. J. Adv. Manuf. Technol. 93, 1903–1913.

Kong, Q.C., Liu, G.L., Song, J.L., Tan, Q.F., Liu, G.Z., Zhao, S.Q., 2021. Preparation of sidewall-insulation layer on micro-hollow electrodes for ECM by asymmetric-timed bipolar electrophoretic coating method and its application. Precis. Eng. 67, 24–35.

Koyano, T., Hosokawa, A., Igusa, R., Ueda, T., 2017. Electrochemical machining using porous electrodes fabricated by powder bed fusion additive manufacturing process. CIRP Annals 66, 213–216.

Koyano, T., Yoshida, J., Hosokawa, A., Furumoto, T., Hashimoto, Y., 2022. Surface quality improvement of electrochemical machining using porous electrodes by mixing bubbles into electrolyte, In: T. Koyano, M.U. (Ed.), Proceedings of INSECT 2022 conference, 2022, pp. 151–156.

Kozak, J., 1998. Mathematical models for computer simulation of electrochemical machining processes. J. Mater. Process. Technol. 76, 1–3.

Kuhn, D., Martin, A., Eckart, C., Sieber, M., Morgenstern, R., Hackert-Oschätzchen, M., Lampke, T., Schubert, A., 2017. Localised anodic oxidation of aluminium material using a continuous electrolyte jet. IOP Conference Series: Materials Science and Engineering 181, 012042.

Kumar, R., Singh, I., 2018. Productivity improvement of micro EDM process by improvised tool. Precis. Eng. 51, 529–535.

Kumar, R., Singh, I., 2019. A modified electrode design for improving process performance of electric discharge drilling. J. Mater. Process. Technol. 264, 211–219.

Kunieda, M., Mizugai, K., Watanabe, S., Shibuya, N., Iwamoto, N., 2011. Electrochemical micromachining using flat electrolyte jet. CIRP Annals 60, 251–254.

Lee, E.S., Baek, S.Y., Cho, C.R., 2005. A study of the characteristics for electrochemical micromachining with ultrashort

voltage pulses. Int. J. Adv. Manuf. Technol. 31, 762–769.
Lee, G., Jung, H., Son, J., Nam, K., Kwon, T., Lim, G., Kim, Y.H., Seo, J., Lee, S.W., Yoon, D.S., 2010. Experimental and numerical study of electrochemical nanomachining using an AFM cantilever tip. Nanotechnology 21, 185301.
Leo Kumar, S.P., Jerald, J., Kumanan, S., Prabakaran, R., 2014. A Review on Current Research Aspects in Tool-Based Micromachining Processes. Mater. Manuf. Process 29, 1291–1337.
Li, G., Natsu, W., Yu, Z., 2021a. Elucidation of the mechanism of the deteriorating interelectrode environment in micro EDM drilling. Int. J. Mach. Tools Manuf. 167, 103747.
Li, T., Bai, Q., Gianchandani, Y.B., 2013. High precision batch mode micro-electro-discharge machining of metal alloys using DRIE silicon as a cutting tool. J. Micromech. Microeng. 23, 095026.
Li, X., Ming, P., Ao, S., Wang, W., 2022. Review of additive electrochemical micro-manufacturing technology. Int. J. Mach. Tools Manuf. 173, 103848.
Li, Y., Hu, R., 2013. Micro Electrochemical Machining for Tapered Holes of Fuel Jet Nozzles. Procedia CIRP 6, 395–400.
Li, Y., Liu, G., Zhong, H., Tong, H., Tan, Q., 2020. Processing and testing integrated silicon electrode and preparation method, Chinese Patents.
Li, Y., Zheng, Y., Yang, G., Peng, L., 2003. Localized electrochemical micromachining with gap control. Sensor. Act. A Phys. 108, 144–148.
Li, Z., Bai, J., Cao, Y., Wang, Y., Zhu, G., 2019. Fabrication of microelectrode with large aspect ratio and precision machining of micro-hole array by micro-EDM. J. Mater. Process. Technol. 268, 70–79.
Li, Z., Cao, B., Dai, Y., 2021b. Research on Multi-Physics Coupling Simulation for the Pulse Electrochemical Machining of Holes with Tube Electrodes. Micromachines 12, 950.
Lim, H.S., Wong, Y.S., Rahman, M., Edwin Lee, M.K., 2003a. A study on the machining of high-aspect ratio micro-structures using micro-EDM. J. Mater. Process. Technol. 140, 318–325.
Lim, Y. M., Kim, S. H., 2001. An electrochemical fabrication method for extremely thin cylindrical micropin. Int. J. Mach. Tools Manuf. 41, 10.
Lim, Y. M., Lim, H. J., Liu, J.R., Kim, S.H., 2003b. Fabrication of cylindrical micropins with various diameters using DC current density control. J. Mater. Process. Technol. 141, 251–255.
Liu, B., Zou, H., Luo, H., Yue, A.X., 2020a. Investigation on the Electrochemical Micromachining of Micro Through-Hole by Using Micro Helical Electrode. Micromachines 11.
Liu, G., Li, Y., Kong, Q., Tong, H., 2017a. Research on ECM process of micro holes with internal features. Precis. Eng. 47, 508–515.
Liu, G., Li, Y., Kong, Q., Tong, H., Zhong, H., 2018a. Silicon-based tool electrodes for micro electrochemical machining. Precis. Eng. 52, 425–433.
Liu, G., Li, Y., Tong, H., 2020b. Fabrication of silicon electrodes used for micro electrochemical machining. J. Micromech. Microeng. 30, 065005.
Liu, G., Li, Y., Tong, H., Zhong, H., 2020c. Effect of Anisotropically-etched Silicon Electrode on Electrolytic Products Flow in Micro ECM. Procedia CIRP 95, 782–786.
Liu, G., Tong, H., Li, Y., Zhong, H., 2021a. Novel structure of a sidewall-insulated hollow electrode for micro electrochemical machining. Precis. Eng. 72, 356–369.
Liu, G., Tong, H., Li, Y., Zhong, H., Tan, Q., 2021b. A profile shaping and surface finishing process of micro electrochemical machining for microstructures on microfluidic chip molds. Int. J. Adv. Manuf. Technol. 115, 1621–1636.
Liu, G., Tong, H., Shi, H., Li, Y., Li, J., 2022a. Fabrication of a Tool Electrode with Hydrophobic Features and Its Stray-Corrosion Suppression Performance for Micro-electrochemical Machining. Langmuir 38, 2711–2719.
Liu, G., Zhu, Y., Liu, S., Li, C., 2022b. Research on conductive-material-filled electrodes for sidewall insulation performance in micro electrochemical machining. Adv. Manuf. https://doi.org/10.1007/s40436-022-00429-7

Liu, J., Huang, Q., Wu, M., Zou, Z., Lin, Z., Guo, Z., He, J., Chen, X., 2020d. Electrochemical Discharge Grinding of Metal Matrix Composites Using Shaped Abrasive Tools Formed by Sintered Bronze/diamond. Sci. Eng. Compos. Mater. 27, 346–358.

Liu, J., Lin, Z., Yue, T., Guo, Z., Jiang, S., 2018b. An analysis of the tool electrode working mechanism of grinding-aided electrochemical discharge machining of MMCs. Int. J. Adv. Manuf. Technol. 99, 1369–1378.

Liu, J.W., Yue, T.M., Guo, Z.N., 2013. Grinding-aided electrochemical discharge machining of particulate reinforced metal matrix composites. Int. J. Adv. Manuf. Technol. 68, 2349–2357.

Liu, W., Ao, S., Li, Y., Liu, Z., Luo, Z., Wang, Z., Song, R., 2017b. Modeling and fabrication of microhole by electrochemical micromachining using retracted tip tool. Precis. Eng. 50, 77–84.

Liu, W., Ao, S., Li, Y., Liu, Z., Zhang, H., Luo, Z., Yu, H., 2016. Investigation on the profile of microhole generated by electrochemical micromachining using retracted tip tool. Int. J. Adv. Manuf. Technol. 87, 877–889.

Liu, W., Luo, Z., Yuan, T., Li, Y., Zhang, H., Ao, S., 2017c. The multi-physics analysis for a novel tool structure to improve the accuracy in electrochemical micro-machining. Int. J. Adv. Manuf. Technol. 94, 1991–2001.

Liu, Y., Cai, H., Li, H., 2015. Fabrication of micro spherical electrode by one pulse EDM and their application in electrochemical micromachining. J. Manuf. Processes 17, 162–170.

Liu, Y., Li, M., Niu, J., Lu, S., Jiang, Y., 2019a. Fabrication of Taper Free Micro-Holes Utilizing a Combined Rotating Helical Electrode and Short Voltage Pulse by ECM. Micromachines 10.

Liu, Y., Xu, X., Guo, C., Kong, H., 2019b. Analysis on Machining Performance of Nickel-Base Superalloy by Electrochemical Micro-milling with High-Speed Spiral Electrode. Micromachines 10.

Liu, Y., Zhu, D., Zeng, Y., Yu, H., 2010. Development of microelectrodes for electrochemical micromachining. Int. J. Adv. Manuf. Technol. 55, 195–203.

Liu, Y., Zhu, D., Zhu, L., 2011. Micro electrochemical milling of complex structures by using in situ fabricated cylindrical electrode. Int. J. Adv. Manuf. Technol. 60, 977–984.

Lohrengel, M.M., Rosenkranz, C., Rohrbeck, D., 2007. The iron-electrolyte interface at extremely large current densities. Microchim Acta 156, 163–166.

Lohrengel, M.M., Rosenkranz, C., Klüppel, I., Moehring, A., Bettermann, H., Bossche, B.V.d., Deconinck, J., 2004. A new microcell or microreactor for material surface investigations at large current densities. Electrochimica Acta 49, 2863–2870.

Lu, J., Zhan, S., Liu, B., Zhao, Y., 2022. Plasma-enabled electrochemical jet micromachining of chemically inert and passivating material. International Journal of Extreme Manufacturing 4, 045101.

Lutey, A.H.A., Jing, H., Romoli, L., Kunieda, M., 2021. Electrolyte Jet Machining (EJM) of antibacterial surfaces. Precis. Eng. 70, 145–154.

Lyubimov, V.V., Volgin, V.M., Mescheder, U., Gnidina, I.V., Ivanov, A.S., 2017. Investigation of plastic electrode tools for electrochemical machining of silicon. Precis. Eng. 47, 546–556.

Ma, X., 2010. Research on Fundamental Techniques of Micro ECM for Array Hole Fabrication. Tsinghua University.

Ma, X., Schuster, R., 2011. Locally enhanced cathodoluminescence of electrochemically fabricated gold nanostructures. J. Electroanal. Chem. 662, 12–16.

Malshe, A.P., Rajurkar, K.P., Virwani, K.R., Taylor, C.R., Bourell, D.L., Levy, G., Sundaram, M.M., McGeough, J.A., Kalyanasundaram, V., Samant, A.N., 2010. Tip-based nanomanufacturing by electrical, chemical, mechanical and thermal processes. CIRP Annals 59, 628–651.

Masuzawa, T., Fujino, M., Kobayashi, K., Suzuki, T., Kinoshita, N., 1985. Wire Electro-Discharge Grinding for Micro-Machining. CIRP Annals 34, 431–434.

Masuzawa, T., Tönshoff, H.K., 1997. Three-Dimensional Micromachining by Machine Tools. CIRP Annals 46, 621–628.

Mathew, R., Sundaram, M.M., 2012. Modeling and fabrication of micro tools by pulsed electrochemical machining. J. Mater. Process. Technol. 212, 1567–1572.

Matsumoto, F., Yamada, M., Tsuta, M., Nakamura, S., Ando, N., Soma, N., 2023. Review of the structure and performance of through-holed anodes and cathodes prepared with a picosecond pulsed laser for lithium-ion batteries. International Journal of Extreme Manufacturing 5, 012001.

McKelvey, K., O'Connell, M.A., Unwin, P.R., 2013. Meniscus confined fabrication of multidimensional conducting polymer nanostructures with scanning electrochemical cell microscopy (SECCM). Chem. Commun. 49, 2986–2988.

Meng, L., Yongbin, Z., Qu, N., Zhu, D., 2014. Electrical conductivity of carbon nanotube tool electrodes. Optics and precision engineering 22, 8.

Meng, L., Zeng, Y., Zhu, D., 2020. Dynamic Liquid Membrane Electrochemical Modification of Carbon Nanotube Fiber for Electrochemical Microfabrication. ACS appl. material interfaces. 12, 6183–6192.

Mi, D., Natsu, W., 2015. Proposal of ECM method for holes with complex internal features by controlling conductive area ratio along tool electrode. Precis. Eng. 42, 179–186.

Mi, D., Natsu, W., 2017. Design of ECM tool electrode with controlled conductive area ratio for holes with complex internal features. Precis. Eng. 47, 54–61.

Mitchell-Smith, J., Bisterov, I., Speidel, A., Ashcroft, I., Clare, A.T., 2019. Direct-writing by active tooling in electrochemical jet processing. Manufacturing Letters 19, 15–20.

Mitchell-Smith, J., Speidel, A., Gaskell, J., Clare, A.T., 2017. Energy distribution modulation by mechanical design for electrochemical jet processing techniques. Int. J. Mach. Tools Manuf. 122, 32–46.

Mohri, N., Tani, T., 2006. Micro-pin Electrodes Formation by Micro-Scanning EDM Process. CIRP Annals 55, 175–178.

Momotenko, D., Page, A., Adobes-Vidal, M., Unwin, P.R., 2016. Write-Read 3D Patterning with a Dual-Channel Nanopipette. ACS nano 10, 8871–8878.

Nastasi, R., Koshy, P., 2014. Analysis and performance of slotted tools in electrical discharge drilling. CIRP Annals 63, 205–208.

Natsu, W., Ooshiro, S., Kunieda, M., 2008. Research on generation of three-dimensional surface with micro-electrolyte jet machining. CIRP Journal of Manufacturing Science and Technology 1, 27–34.

Osenbruggen, C.v., Regt, C.d., 1985. Electrocheniical micromachining. Philips Tech. Rev 42, 22–32.

Parandoush, P., Hossain, A., 2014. A review of modeling and simulation of laser beam machining. Int. J. Mach. Tools Manuf. 85, 135–145.

Park, B.J., Kim, B.H., Chu, C.N., 2006. The Effects of Tool Electrode Size on Characteristics of Micro Electrochemical Machining. CIRP Annals 55, 197–200.

Park, M.S., Chu, C.N., 2007. Micro-electrochemical machining using multiple tool electrodes. J. Micromech. Microeng. 17, 1451–1457.

Patro, S.K., Mishra, D.K., Arab, J., Dixit, P., 2019. Numerical and experimental analysis of high-aspect-ratio micro-tool electrode fabrication using controlled electrochemical machining. J. Appl. Electrochem. 50, 169–184.

Pattavanitch, J., Hinduja, S., 2012. Machining of turbulated cooling channel holes in turbine blades. CIRP Annals 61, 199–202.

Pradeep, N., Sundaram, K.S., Pradeep Kumar, M., 2019. Performance investigation of variant polymer graphite electrodes used in electrochemical micromachining of ASTM A240 grade 304. Mater. Manuf. Process 35, 72–85.

Pu, Y., Tong, H., Li, J., Li, Y., Ji, B., 2020. Micro-SACE scanning process with different tool-surface roughness. Mater. Manuf. Process 35, 1181–1187.

Puthumana, G., Joshi, S.S., 2011. Investigations into performance of dry EDM using slotted electrodes. Int. J. Precis. Eng. Manuf. 12, 957–963.

Qi, X., Fang, X., Zhu, D., 2018. Investigation of electrochemical micromachining of tungsten microtools. Int. J. Refract. Met. H. 71, 307–314.

Qiao, H., Zhihe, C., Jianfeng, C., Zhao, J., 2021. Experimental study on water jet guided laser micro-machining of mono-

crystalline silicon. Opt. Laser Technol. 140, 107057.
Qingfeng, Y., Xingqiao, W., Ping, W., Zhiqiang, Q., Lin, Z., Yongbin, Z., 2016. Fabrication of micro rod electrode by electrical discharge grinding using two block electrodes. J. Mater. Process. Technol. 234, 143–149.
Quitzke, S., Kröning, O., Safranchik, D., Zeidler, H., Danilov, I., Martin, A., Böttger-Hiller, F., Essel, S., Schubert, A., 2022. Design and setup of a jet-based technology for localized small scale Plasma electrolytic Polishing. J. Manuf. Processes 75, 1123–1133.
Rahman, M., Asad, A.B.M.A., Masaki, T., Saleh, T., Wong, Y.S., Senthil Kumar, A., 2010. A multiprocess machine tool for compound micromachining. Int. J. Mach. Tools Manuf. 50, 344–356.
Rajurkar, K.P., Levy, G., Malshe, A., Sundaram, M.M., McGeough, J., Hu, X., Resnick, R., DeSilva, A., 2006a. Micro and Nano Machining by Electro-Physical and Chemical Processes. CIRP Annals 55, 643–666.
Rajurkar, K.P., Levy, G., Malshe, A., Sundaram, M.M., McGeough, J., Hu, X., Resnick, R., DeSilva, A., 2006b. Micro and Nano Machining by Electro-Physical and Chemical Processes. Annals of the CIRP 55, 24.
Rajurkar, K.P., Sundaram, M.M., Malshe, A.P., 2013. Review of Electrochemical and Electrodischarge Machining. Procedia CIRP 6, 13–26.
Rajurkar, K.P., Zhu, D., Wei, B., 1998. Minimization of Machining Allowance in Electrochemical Machining. CIRP Annals 47, 165–168.
Rakwal, D., Heamawatanachai, S., Tathireddy, P., Solzbacher, F., Bamberg, E., 2009. Fabrication of compliant high aspect ratio silicon microelectrode arrays using micro-wire electrical discharge machining. Microsyst. Technol. 15, 789–797.
Rashedul, I.M., Zhang, Y., Zhou, K., Wang, G., Xi, T., Ji, L., 2021. Influence of Different Tool Electrode Materials on Electrochemical Discharge Machining Performances. Micromachines 12.
Rathod, V., Doloi, B., Bhattacharyya, B., 2013. Parametric Investigation Into the Fabrication of Disk Microelectrodes by Electrochemical Micromachining. Journal of Micro and Nano-Manufacturing 1.
Rathod, V., Doloi, B., Bhattacharyya, B., 2014. Sidewall Insulation of Microtool for Electrochemical Micromachining to Enhance the Machining Accuracy. Mater. Manuf. Process 29, 305–313.
Ravi, N., Chuan, S., 2002. The effects of electro-discharge machining block electrode method for microelectrode machining. J. Micromech. Microeng. 12, 532–540.
Saxena, K.K., Chen, X., Qian, J., Reynaerts, D., 2020a. A Tool-Based Precision Hybrid Laser-Electrochemical Micromachining Process: Process Analysis by Multidisciplinary Simulations and Experiments. J. Electrochem. Soc. 167, 143502.
Saxena, K.K., Qian, J., Reynaerts, D., 2018. A review on process capabilities of electrochemical micromachining and its hybrid variants. Int. J. Mach. Tools Manuf. 127, 28–56.
Saxena, K.K., Qian, J., Reynaerts, D., 2020b. Development and investigations on a hybrid tooling concept for coaxial and concurrent application of electrochemical and laser micromachining processes. Precis. Eng. 65, 171–184.
Saxena, K.K., Qian, J., Reynaerts, D., 2020c. A tool-based hybrid laser-electrochemical micromachining process: Experimental investigations and synergistic effects. Int. J. Mach. Tools Manuf. 155, 103569.
Schuster, R., Kirchner, V., Allongue, P., Ertl, G., 2000. Electrochemical Micromachining. Science 289, 98–101.
Sharma, V., Patel, D.S., Jain, V.K., Ramkumar, J., 2020. Wire electrochemical micromachining: An overview. Int. J. Mach. Tools Manuf. 155, 103579.
Sharstnioua, A., Niauzoraua, S., Ferreirab, P.M., Azeredo, B.P., 2018. Electrochemical nanoimprinting of silicon. PNAS 116, 10264–10269.
Sheu, D. Y., 2008. High-speed micro electrode tool fabrication by a twin-wire EDM system. J. Micromech. Microeng. 18, 105014.
Sheu, D. Y., 2014. Manufacturing tactile spherical stylus tips by combination process of micro electro chemical and one-pulse electro discharge technology. Int. J. Adv. Manuf. Technol. 74, 741–747.

Silva, A. K. M., Altena, H. S. J., McGeough, J. A., 2000. Precision ECM by Process Characteristic Modelling. CIRP Annals 49, 151–155.

Song, K.Y., Chung, D.K., Park, M.S., Chu, C.N., 2013. EDM turning using a strip electrode. J. Mater. Process. Technol. 213, 1495–1500.

Speidel, A., Bisterov, I., Saxena, K.K., Zubayr, M., Reynaerts, D., Natsu, W., Clare, A.T., 2022. Electrochemical jet manufacturing technology: From fundamentals to application. Int. J. Mach. Tools Manuf. 180, 103931.

Speidel, A., Xu, D., Bisterov, I., Mitchell-Smith, J., Clare, A.T., 2021. Unveiling surfaces for advanced materials characterisation with large-area electrochemical jet machining. Mater. Design 2022, 109539.

Spieser, A., Ivanov, A., 2013. Recent developments and research challenges in electrochemical micromachining (μECM). Int. J. Adv. Manuf. Technol. 69, 19.

Sugita, T., Hiramatsu, K., Ikeda, S., Matsumura, M., 2013a. Fabrication of pores in a silicon carbide wafer by electrochemical etching with a glassy-carbon needle electrode. ACS Appl. Mater. interfaces 5, 2580–2584.

Sugita, T., Hiramatsu, K., Ikeda, S., Matsumura, M., 2013b. Pore formation in a p-type silicon wafer using a platinum needle electrode with application of square-wave potential pulses in HF solution. ACS Appl. Mater. interfaces 5, 1262–1268.

Sun, C. H., Zhu, D., Li, Z. Y., Wang, L., 2006. Application of FEM to tool design for electrochemical machining freeform surface. Finite Elements in Analysis and Design 43, 168 – 172.

Takahata, K., Shibaike, N., Guckel, H., 2000. High-aspect-ratio WC-Co microstructure produced by the combination of LIGA and micro-EDM. Microsyst. Technol. 6, 175–178.

Tang, W., Kang, X., Zhao, W., 2017. Enhancement of electrochemical discharge machining accuracy and surface integrity using side-insulated tool electrode with diamond coating. J. Micromech. Microeng. 27, 065013.

Tsui, H. P., Hung, J. C., Wu, K. L., You, J. C., Yan, B. H., 2011. Fabrication of a Microtool in Electrophoretic Deposition for Electrochemical Microdrilling and in Situ Micropolishing. Mater. Manuf. Process 26, 740–745.

Tsui, H. P., Hung, J. C., You, J. C., Yan, B. H., 2008. Improvement of Electrochemical Microdrilling Accuracy Using Helical Tool. Mater. Manuf. Process 23, 499–505.

Tzu WeiHuang, Dong YeaSheu, 2020. High aspect ratio of micro hole drilling by Micro-EDM with different cross-section shape micro tools for flushing process. Procedia CIRP 95, 550–553.

Uchiyama, M., Kunieda, M., 2013. Application of large deflection analysis for tool design optimization in an electrochemical curved hole machining method. Precis. Eng. 37, 765–770.

Van Camp, D., Bouquet, J., Qian, J., Vleugels, J., Lauwers, B., 2018. Investigation on Hybrid Mechano-electrochemical Milling of Ti6Al4V. Procedia CIRP 68, 156–161.

Wüthrich, R., Hof, L.A., Lal, A., Fujisaki, K., Bleuler, H., Mandin, P., Picard, G., 2005. Physical principles and miniaturization of spark assisted chemical engraving (SACE). J. Micromech. Microeng. 15, S268–S275.

Wang, J., Chen, W., Gao, F., Han, F., 2014. A new electrode sidewall insulation method in electrochemical drilling. Int. J. Adv. Manuf. Technol. 75, 21–32.

Wang, J., Natsu, W., 2022. Mechanism and characteristics of electrochemical machining using electrolyte absorbed in solid porous ball. Precis. Eng. 77, 307–319.

Wang, M., Bao, Z., Wang, X., Xu, X., 2016a. Fabrication of disk microelectrode arrays and their application to micro-hole drilling using electrochemical micromachining. Precis. Eng. 46, 184–192.

Wang, M., Peng, W., Yao, C., Zhang, Q., 2009. Electrochemical machining of the spiral internal turbulator. Int. J. Adv. Manuf. Technol. 49, 969–973.

Wang, M., Qu, N., 2021. Investigation on material removal mechanism in mechano-electrochemical milling of TC4 titanium alloy. J. Mater. Process. Technol. 295, 117206.

Wang, M., Zhang, Y., He, Z., Peng, W., 2016b. Deep micro-hole fabrication in EMM on stainless steel using disk micro-

tool assisted by ultrasonic vibration. J. Mater. Process. Technol. 229, 475–483.
Wang, M., Zhu, D., Xu, H., 2006. Use of Micro-helix Electrodes in Improving Performance of Micro-ECM. Mechanical science and technology 25, 4.
Wang, M.H., Zhu, D., 2008. Fabrication of multiple electrodes and their application for micro-holes array in ECM. Int. J. Adv. Manuf. Technol. 41, 42–47.
Wang, M.H., Zhu, D., 2009. Simulation of fabrication for gas turbine blade turbulated cooling hole in ECM based on FEM. J. Mater. Process. Technol. 209, 1747–1751.
Wang, W., Zhu, D., Qu, N.S., Huang, S.F., Fang, X.L., 2010. Electrochemical drilling with vacuum extraction of electrolyte. J. Mater. Process. Technol. 210, 238–244.
Wang, Y. Q., Bai, J. C., 2014. Diameter control of microshafts in wire electrical discharge grinding. Int. J. Adv. Manuf. Technol. 72, 1747–1757.
Wang, Y., Qu, N., Zeng, Y., Wu, X., Zhu, D., 2013. The fabrication of high-aspect-ratio cylindrical nano tool using ECM. Int. J. Precis. Eng. Manuf. 14, 2179–2186.
Wang, Y., Yang, F., Zhang, W., 2019. Development of Laser and Electrochemical Machining Based on Internal Total Reflection. J. Electrochem. Soc. 166, E481–E488.
Wang, Y., Zeng, Y., Qu, N., Zhu, D., 2015. Electrochemical micromachining of small tapered microstructures with sub-micro spherical tool. Int. J. Adv. Manuf. Technol. 84, 851–859.
Wang, Y., Zeng, Y., Qu, N., Zhu, D., 2016c. Fabrication of sub-micro spherical probes by liquid membrane pulsed electrochemical etching. J. Mater. Process. Technol. 231, 171–178.
Wang, Y., Zhang, W., 2021. Theoretical and experimental study on hybrid laser and shaped tube electrochemical machining (Laser-STEM) process. Int. J. Adv. Manuf. Technol. 112, 1601–1615.
Wu, M., Liu, J., He, J., Chen, X., Guo, Z., 2020a. Fabrication of surface microstructures by mask electrolyte jet machining. Int. J. Mach. Tools Manuf. 148, 103471.
Wu, X., Qu, N., Zeng, Y., Wang, Y., Zhu, D., 2013. Experimental study on submicron electrochemical machining. Journal of Southeast University (Natural Science Edition) 43, 5.
Wu, X., Sang, Y., Yang, T., Zeng, Y., 2020b. Fabrication of Fe-based metal glass microelectrodes by a vertical liquid membrane electrochemical etching method. Rev. Sci. Instrum. 91, 035109.
Yamazaki, M., Suzuki, T., Mori, N., Kunieda, M., 2004. EDM of micro-rods by self-drilled holes. J. Mater. Process. Technol. 149, 134–138.
Yang, C. K., Cheng, C. P., Mai, C. C., Cheng Wang, A., Hung, J. C., Yan, B. H., 2010. Effect of surface roughness of tool electrode materials in ECDM performance. Int. J. Mach. Tools Manuf. 50, 1088–1096.
Yang, C. K., Wu, K. L., Hung, J. C., Lee, S. M., Lin, J. C., Yan, B. H., 2011. Enhancement of ECDM efficiency and accuracy by spherical tool electrode. Int. J. Mach. Tools Manuf. 51, 528–535.
Yang, I., Park, M.S., Chu, C.N., 2009. Micro ECM with ultrasonic vibrations using a semi-cylindrical tool. Int. J. Precis. Eng. Manuf. 10, 5–10.
Yao, J., Chen, Z.T., Nie, Y.J., Li, Q., 2016. Investigation on the electrochemical machining by using metal reinforced double insulating layer cathode. Int. J. Adv. Manuf. Technol. 89, 2031–2040.
Yi, Z., Zhang, M., 2015. Fabrication of high-aspect-ratio platinum probes by two-step electrochemical etching. Rev. Sci. Instrum. 86, 085105.
Yin, Q., Wang, B., Zhang, Y., Ji, F., Liu, G., 2014. Research of lower tool electrode wear in simultaneous EDM and ECM. J. Mater. Process. Technol. 214, 1759–1768.
Zeng, Y., Wang, Y., Qu, N., Zhu, D., 2013. Fabrication of a high-aspect-ratio sub-micron tool using a cathode coated with stretched-out insulating layers. Rev. Sci. Instrum. 84, 095006.
Zhan, D., Han, L., Zhang, J., He, Q., Tian, Z.W., Tian, Z.Q., 2017. Electrochemical micro/nano-machining: principles and

practices. Chem. Soc. Rev. 46, 1526–1544.
Zhan, S., Zhao, Y., 2020. Plasma-assisted electrochemical machining of microtools and microstructures. Int. J. Mach. Tools Manuf. 156, 103596.
Zhan, S., Zhao, Y., 2021. Intentionally-induced dynamic gas film enhances the precision of electrochemical micromachining. J. Mater. Process. Technol. 291, 117049.
Zhang, C., Xu, Z., Lu, J., Geng, T., 2021. An electrochemical discharge drilling method utilising a compound flow field of different fluids. J. Mater. Process. Technol. 298, 117306.
Zhang, C., Xu, Z., Zhang, X., Zhang, J., 2020a. Surface integrity of holes machined by electrochemical discharge drilling method. CIRP Journal of Manufacturing Science and Technology 31, 643–651.
Zhang, C., Yao, J., Zhang, C., Chen, X., Liu, J., Zhang, Y., 2020b. Electrochemical milling of narrow grooves with high aspect ratio using a tube electrode. J. Mater. Process. Technol. 282, 116695.
Zhang, H., Ao, S., Liu, W., Luo, Z., Niu, W., Guo, K., 2017. Electrochemical micro-machining of high aspect ratio micro-tools using quasi-solid electrolyte. Int. J. Adv. Manuf. Technol. 91, 2965–2973.
Zhang, L., Tong, H., Li, Y., 2015a. Precision machining of micro tool electrodes in micro EDM for drilling array micro holes. Precis. Eng. 39, 100–106.
Zhang, S., Zhou, Y., Zhang, H., Xiong, Z., To, S., 2019a. Advances in ultra-precision machining of micro-structured functional surfaces and their typical applications. Int. J. Mach. Tools Manuf. 142, 16–41.
Zhang, W., Kitamura, T., Kunieda, M., Abe, K., 2014. Observation of ECM Gap Phenomena through Transparent Electrode. International Journal of Electrical Machining 19, 40–44.
Zhang, Y., Wang, C., Wang, Y., Ji, L., Tang, J., Ni, Q., 2019b. Effects of Helical Tube Electrode Structure on Mixed Machining Product Transfer in Micro-Machining Channel during Tube Electrode High-Speed Electrochemical Discharge Machining. Micromachines 10.
Zhang, Y., Wang, C., Wang, Y., Ni, Q., Ji, L., 2019c. Geometric Accuracy Improvement by Using Electrochemical Reaming with a Helical Tube Electrode as Post-Processing for EDM. Materials 12.
Zhang, Y., Xu, Z., Xing, J., Zhu, D., 2016a. Effect of tube-electrode inner diameter on electrochemical discharge machining of nickel-based superalloy. Chinese J. Aeronaut. 29, 1103–1110.
Zhang, Y., Xu, Z., Zhu, D., Xing, J., 2015b. Tube electrode high-speed electrochemical discharge drilling using low-conductivity salt solution. Int. J. Mach. Tools Manuf. 92, 10–18.
Zhang, Y., Xu, Z., Zhu, Y., Zhu, D., 2016b. Effect of tube-electrode inner structure on machining performance in tube-electrode high-speed electrochemical discharge drilling. J. Mater. Process. Technol. 231, 38–49.
Zhao, W. S., Jia, B. X., Wang, Z. L., Hu, F. Q., 2006. Study on Block Electrode Discharge Grinding of Micro Rods. Key Engineering Materials 304–305.
Zhao, Y., Kunieda, M., 2019. Investigation on electrolyte jet machining of three-dimensional freeform surfaces. Precis. Eng. 60, 42–53.
Zhao, Y., Zhao, C., Wang, S., Kakudo, S., Kunieda, M., 2020. Selective and localized embrittlement of metal by cathodic hydrogenation utilizing electrochemical jet. Precis. Eng. 65, 259–268.
Zheng, Z. P., Su, H. C., Huang, F. Y., Yan, B. H., 2007. The tool geometrical shape and pulse-off time of pulse voltage effects in a Pyrex glass electrochemical discharge microdrilling process. J. Micromech. Microeng. 17, 265–272.
Zhu, D., Xu, H., 2002. Improvement of electrochemical machining accuracy by using dual pole tool. J. Mater. Process. Technol. 129, 15–18.
Zhu, D., Zeng, Y.B., Xu, Z.Y., Zhang, X.Y., 2011. Precision machining of small holes by the hybrid process of electrochemical removal and grinding. CIRP Annals 60, 247–250.
Zou, H., Yue, X., Luo, H., Liu, B., Zhang, S., 2020. Electrochemical micromachining of micro hole using micro drill with non-conductive mask on the machined surface. J. Manuf. Processes 59, 366–377.

Zou, Z., Liu, J., Xiao, Y., Deng, Y., Guo, Z., 2021. Study on the influence of dynamic characteristics of bubbles on electrochemical discharge machining conductive materials. Procedia CIRP 65, 5.